FINAL REPORT
FOR RESEARCH STUDY ENTITLED
"PERFORMANCE EVALUATION OF THE GRAVITY PROBE B DESIGN"

Submitted To:

National Aeronautics and Space Administration
George C. Marshall Space Flight Center
Marshall Space Flight Center, Alabama 35812

Contract Number:
NAS8-40618

Submitted by:

bd Systems, Inc.
385 Van Ness Avenue, Suite 200
Torrance, California

5 April 1996

TABLE OF CONTENTS

TABLE OF FIGURES

TABLE OF TABLES

TABLE OF ACRONYMS

Acronym	Definition
DOF	Degrees-of-Freedom
GPB	Gravity Probe B
GSI	Guide Star Invalid
GSV	Guide Star Valid
m	Meter
mas	Milliarcsec
mn	Millinewton
nm	Nanometer

GPB SIMULATION DEVELOPMENT FINAL REPORT

1. Introduction

This report documents the simulation of the Lockheed Martin designed Gravity Probe B (GPB) spacecraft developed tool by bd Systems Inc using the TREETOPS simulation. This study quantifies the effects of flexibility and liquid helium slosh on GPB spacecraft control performance. The TREETOPS simulation tool permits the simulation of flexible structures given that a flexible body model of the structure is available. For purposes of this study, a flexible model of the GPB spacecraft was obtained from Lockheed Martin. To model the liquid helium slosh effects, computational fluid dynamics (CFD) results[1] were obtained from Dr. R. J. Hung at the University of Alabama in Huntsville (UAH), and used to develop a dynamic model of the slosh effects. The flexible body and slosh effects were incorporated separately into the TREETOPS simulation, which places the vehicle in a 650 km circular polar orbit and subjects the spacecraft to realistic environmental disturbances and sensor error quantities. In all of the analysis conducted in this study the spacecraft is pointed at an inertially fixed guide star (GS) and is rotating at a constant rate about this line of sight.

2. GPB Simulation Components

The GPB TREETOPS simulation is made up of the spacecraft control sensors and actuators, the attitude and translation controllers, environmental disturbances, a slosh model of the liquid Helium, a flexible body spacecraft dynamics model, and a science gyro model. Each of these models is discussed in the following subsections.

2.1. Spacecraft Configuration

2.1.1. Sensors

The spacecraft sensors modeled in this simulation are the science telescope, drag free sensor, control gyros, and the roll star trackers. The sensor errors specified in this section were taken from Lockheed Martin[2].

The science telescope is modeled using the TREETOPS star tracker sensor. This sensor provides a line of sight error about the spacecraft pitch and yaw axes during guide star valid (GSV) phases. The science telescope model for each axis is shown in Figure 2.1.1-1. Science telescope error is modeled by a zero mean gaussian noise with a standard deviation of 22.36 milliarcseconds that is added to the true pointing error. The resulting signals are then quantized using a least significant bit weight of 0.25 milliarcseconds.

Figure 2.1.1-1 Science Telescope Model

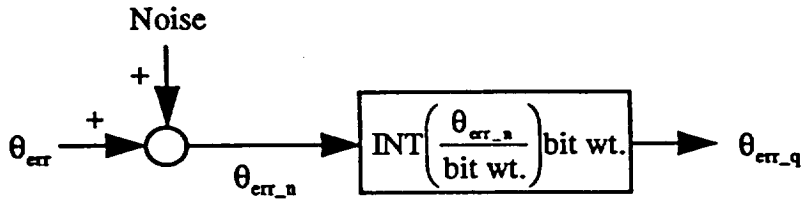

The control gyros are modeled using the TREETOPS rate gyro sensor. These sensors provide the angular rate with respect to inertial space about each of the three body axes. The control gyro model for each axis is shown in Figure 2.1.1-2. For the pitch and yaw axes, a gaussian noise with a mean drift of 0.003 arcsec/second and a standard deviation of 0.002236 arcsec/second is added to the true rate, then the signals are quantized using a least significant bit weight of 1.3 milliarcseconds. For the roll axis, a gaussian noise with a mean drift of 0.003 arcsec/second and a standard deviation of 0.002236 arcsec/second is added to the true rate, after which the signals are quantized using a least significant bit weight of 37.5 milliarcseconds in low range mode or 375 milliarcseconds in high range mode. During the guide star invalid (GSI) phase, the control gyro derived rates are propagated using quaternions to produce the pitch and yaw line of sight errors. At the end of each guide star valid (GSV) phase, the science telescope signal is used to update the initial attitude to be used in the attitude propagation during the guide star invalid phase.

Figure 2.1.1-2 Control Gyro Model

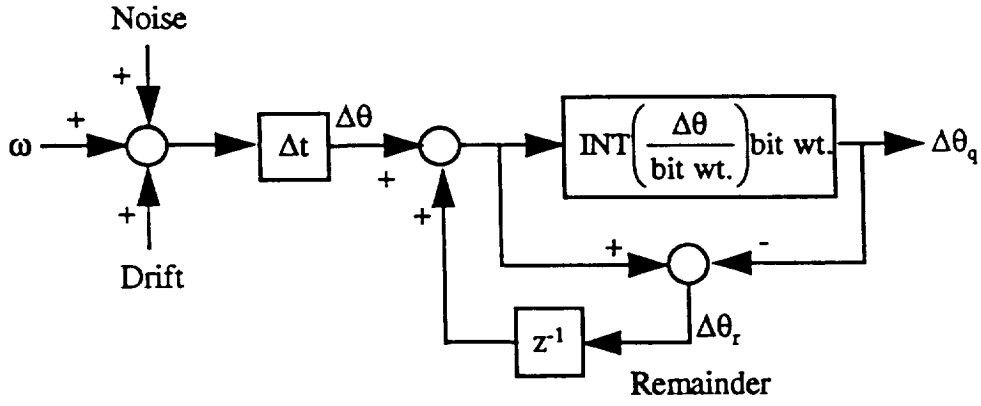

The roll star tracker is modeled using the TREETOPS integrating rate gyro sensor. This provides the roll angle. The roll star tracker model is shown in Figure 2.1.1-3. A zero mean gaussian noise with a standard deviation of 5.0 arcseconds is added to the true roll angle. The resulting signal is then quantized using a least significant bit weight of 0.5 arcseconds. The roll error is computed by subtracting this signal from the commanded roll angle.

Figure 2.1.1-3 Roll Star Tracker Model

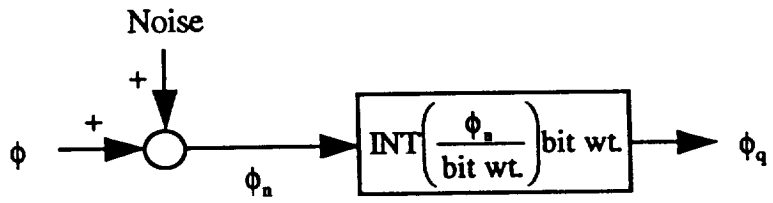

The drag free sensor is modeled using the TREETOPS position vector sensor. This provides a relative position vector from the spacecraft to the drag free proof mass in the inertial frame. The inertial frame relative position vector is converted to the body frame. For each translational body axis, a zero mean gaussian noise with a standard deviation of 3.354 nanometers is added to the true displacement, then the signals are quantized using a least significant bit weight of 1 nanometer.

Figure 2.1.1-4 Drag Free Sensor Model

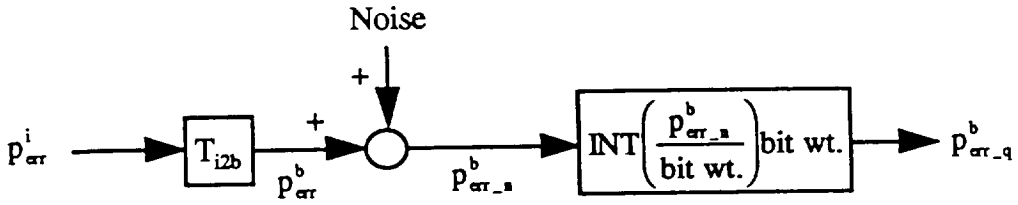

2.1.2. Actuators

The 16 thrusters are modeled using 16 of the TREETOPS reaction jet actuators. Each thruster is modeled as shown in Figure 2.1.2-1. The commanded thrust for each thruster is quantized using a least significant bit weight of 0.0025 milliNewtons. Then each thrust signal is delayed one control cycle (0.1 seconds) and a hysteresis of 0.005 milliNewtons is applied[3]. Finally, a separate zero mean gaussian noise with a standard deviation of 0.0559 milliNewtons is added to each thruster.

Figure 2.1.2-1 Thruster Model

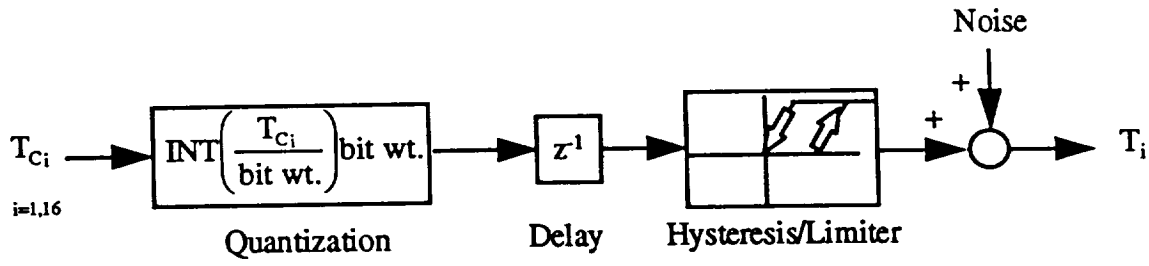

2.2. Environmental Disturbances

The environmental disturbances implemented in the GPB TREETOPS simulation include the cryoperm shield magnetic torque, the aerodynamic force and torque, and the gravity gradient force and torque.

2.2.1. Magnetic Disturbance

The cryoperm shield magnetic moment is calculated as

$$M_{mag} = \begin{bmatrix} 176320 & 0 & 0 \\ 0 & 160320 & 0 \\ 0 & 0 & 2160000 \end{bmatrix} B_b$$

where B_b is the Earth's magnetic field vector in the spacecraft body frame. The cryoperm shield magnetic torque vector is calculated as

$$T_{cryo} = M_{mag} \times B_b .$$

The cryoperm shield magnetic torque for one orbit is shown in Figure 2.2-1 and is applied at the spacecraft center of mass.

2.2.2. Aerodynamic Disturbance

The aerodynamic force and torque vectors in the spacecraft body frame are calculated as follows

$$F_{aero} = \begin{bmatrix} 0.0025\sin(\omega_o t + \pi/2)\sin(\omega_r t - \pi/2) \\ 0.0025\sin(\omega_o t + \pi/2)\sin(\omega_r t) \\ 0.0035\sin(\omega_o t + \pi) \end{bmatrix}$$

$$T_{aero} = \begin{bmatrix} 0.002\sin(\omega_o t)\sin(2\omega_o t)\sin(\omega_r t + \pi) \\ 0.002\sin(\omega_o t)\sin(2\omega_o t)\sin(\omega_r t + \pi/2) \\ 0.0024\sin(\omega_o t + \pi/2)\sin(2\omega_o t)\{1 + 0.06\sin(4\omega_r t)\} \end{bmatrix}$$

where ω_o is the orbit rate and ω_r is the roll rate. The aerodynamic force and torque for one orbit are shown in Figures 2.2-2 and 2.2-3, respectively, and are applied at the spacecraft center of mass.

2.2.3. Gravity Gradient Disturbance

The gravity gradient force and torque vectors are computed as

$$F_{ss} = \frac{\mu m_{sc}}{R_0^3}\left[r_{pm} - 3\left(\hat{R}_0 \cdot r_{pm}\right)\hat{R}_0\right]$$

$$T_{ss} = \frac{3\mu}{R_0^3}\left[\begin{array}{l} \hat{R}_0 \times I \cdot \hat{R}_0 + \\ 5J_2\left(\frac{R_e}{R_0}\right)^2\left(-\hat{N}\cdot\hat{R}_0\left(\hat{R}_0 \times I \cdot \hat{N} + \hat{N} \times I \cdot \hat{R}_0\right) + \frac{1}{2}\left(7\left(\hat{N}\cdot\hat{R}_0\right)^2 - 1\right)\hat{R}_0 \times I \cdot \hat{R}_0\right) \end{array}\right]$$

where μ is the gravitational constant, m_{sc} is the spacecraft mass, r_{pm} is the vector from the center of mass to the proof mass, R_0 is the vector from the center of the Earth to the spacecraft center of mass and I is the spacecraft inertia dyadic, N is the north vector, and J_2 is the gravitational coefficient 0.00108263. The gravity gradient force and torque vectors are shown in Figures 2.2-4 and 2.2-5, respectively, and are applied at the spacecraft center of mass.

Figure 2.2-1 Cryoperm Shield Magnetic Disturbance Torque

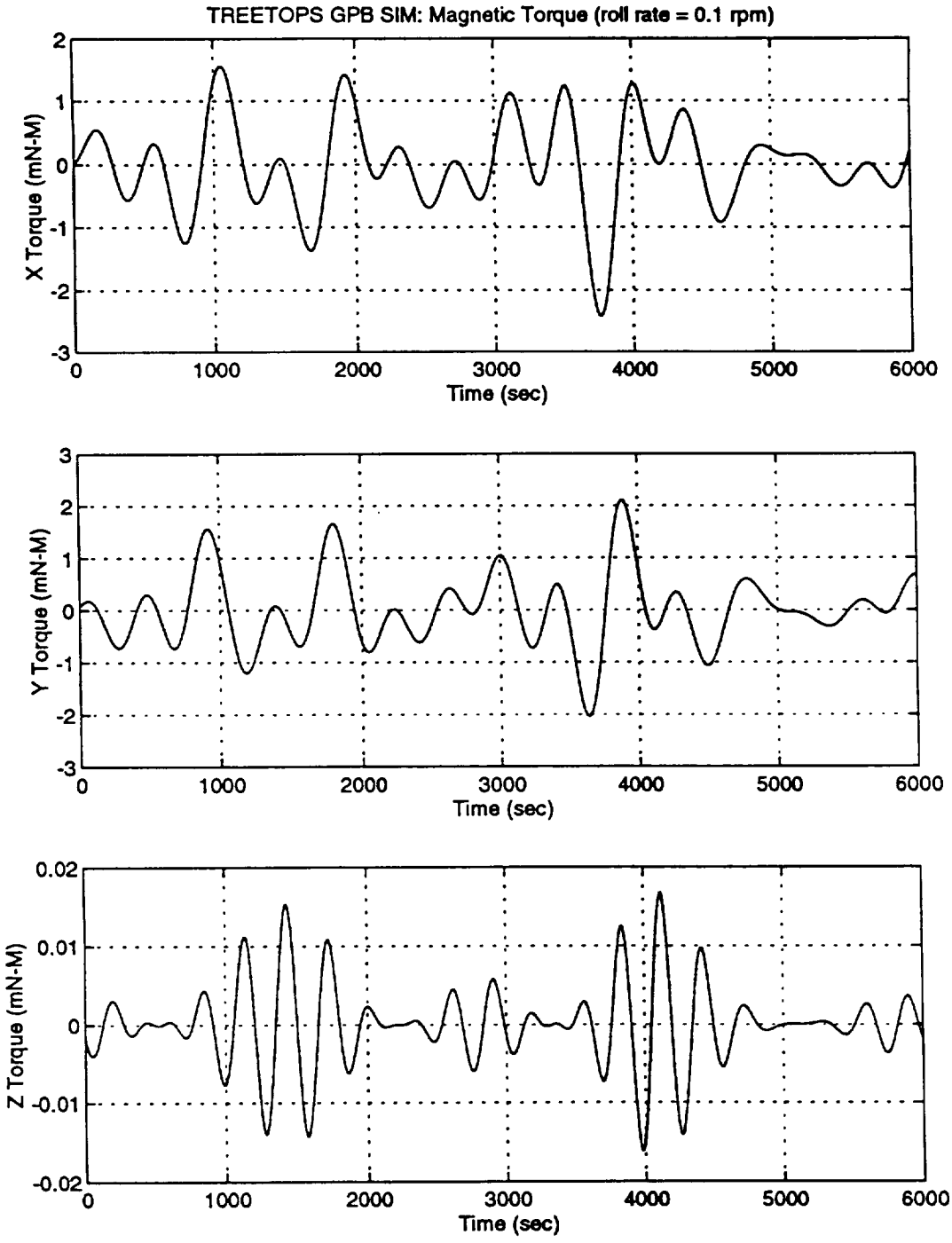

Figure 2.2-2 Aerodynamic Disturbance Force

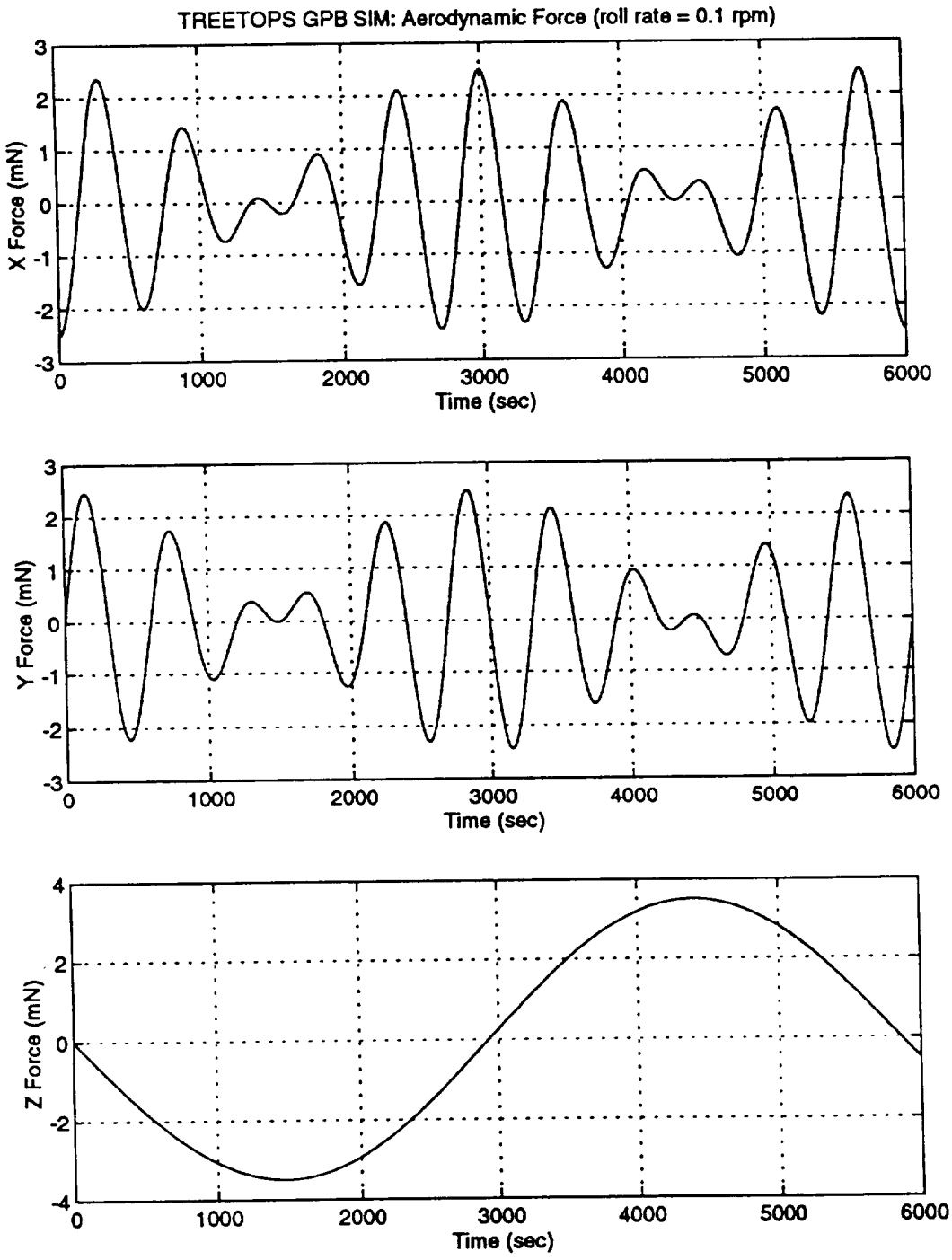

Figure 2.2-3 Aerodynamic Disturbance Torque

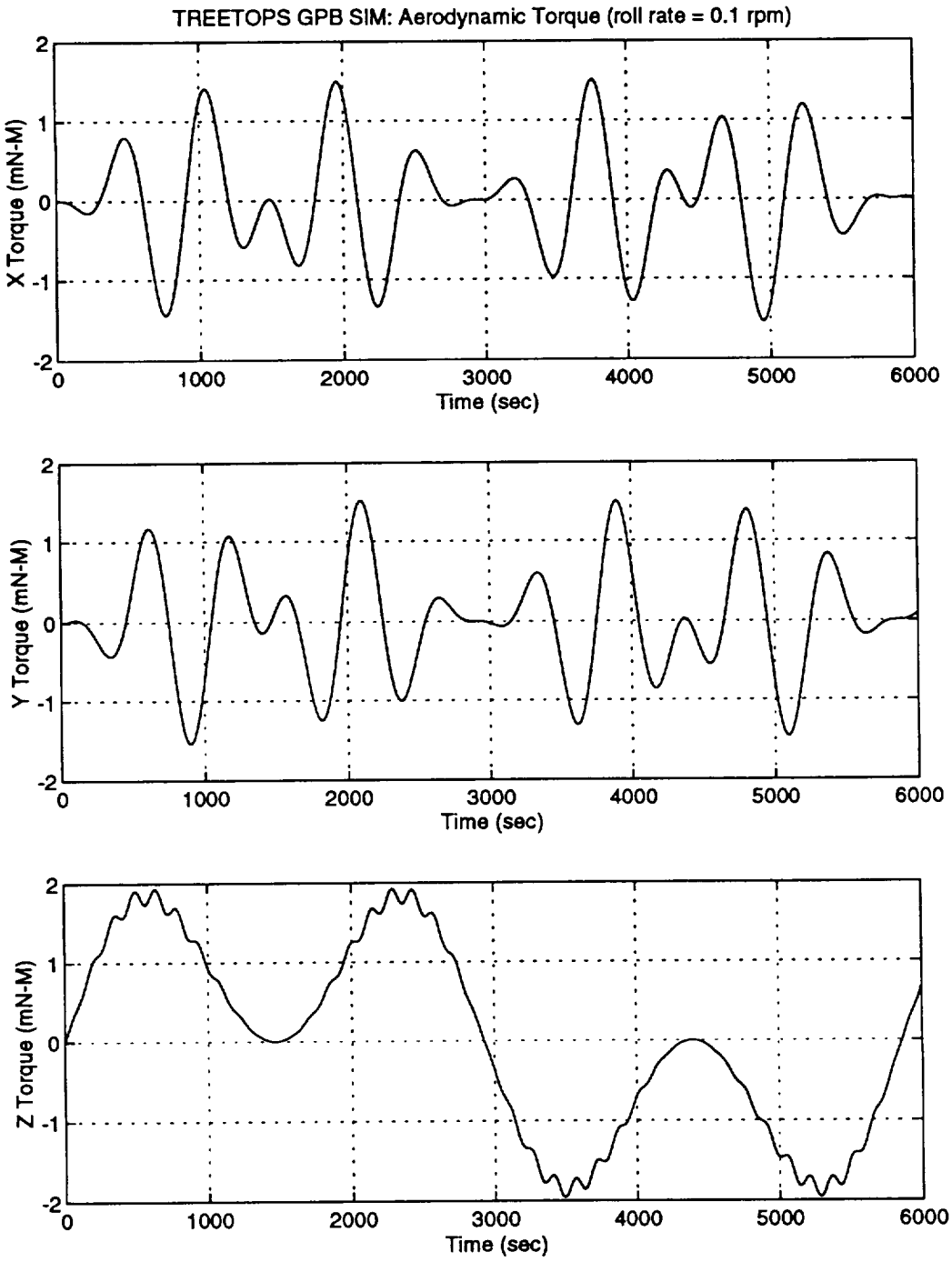

Figure 2.2-4 Gravity Gradient Disturbance Force

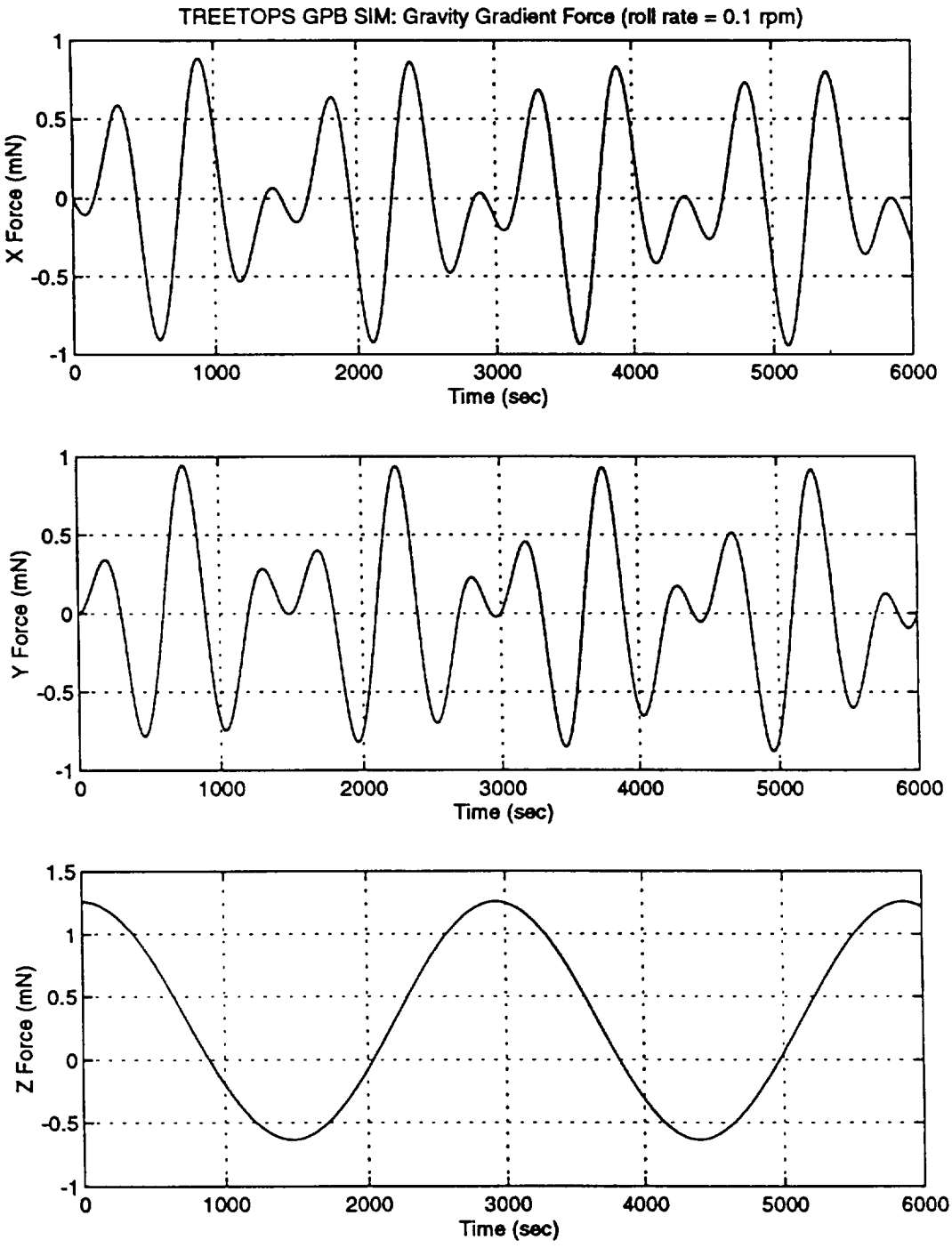

Figure 2.2-5 Gravity Gradient Disturbance Torque

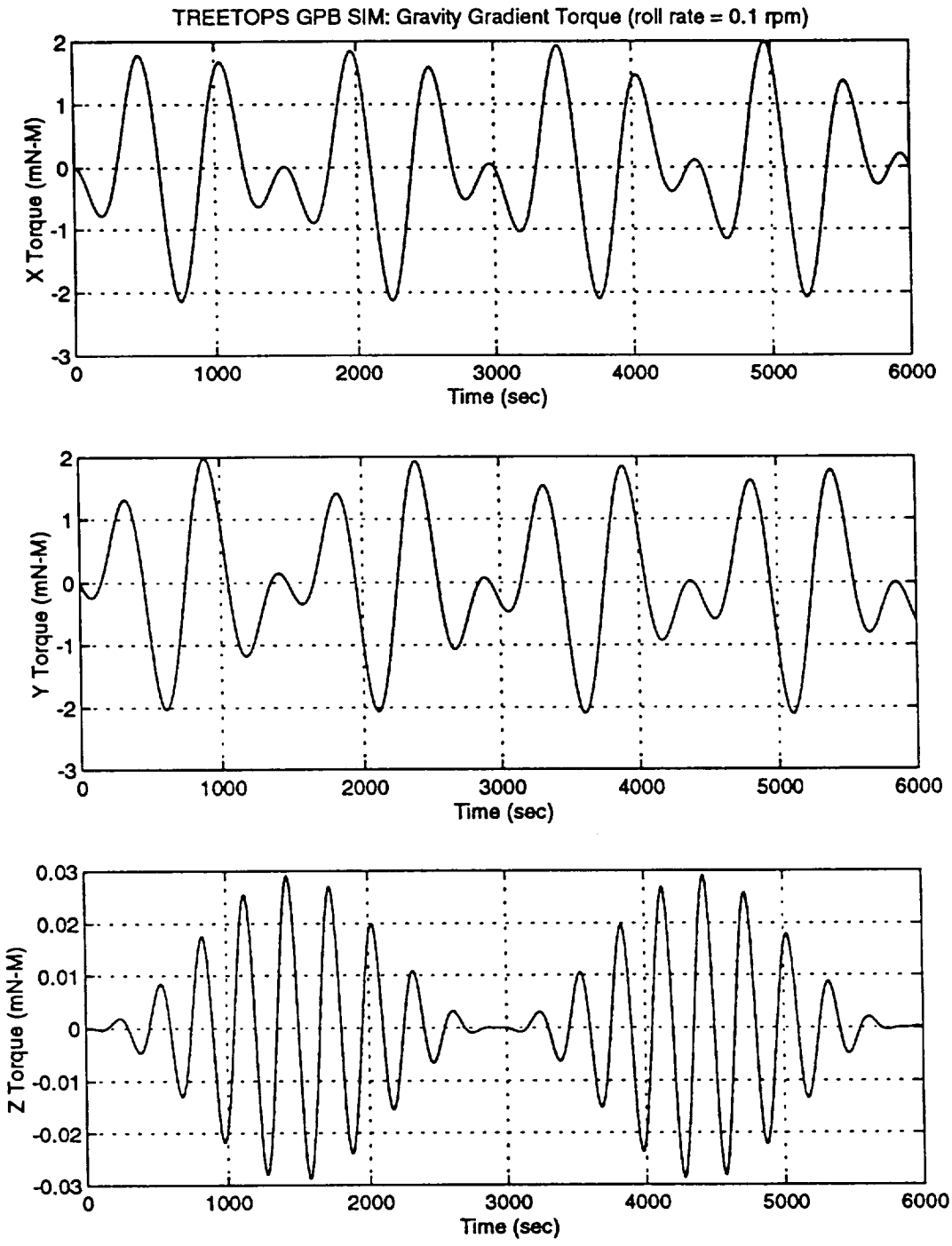

2.3. Control System Operation

2.3.1. Translational Control

The GPB translational controller[4] used in the TREETOPS simulation is shown in Figure 2.3.1-1. This same controller is used for all three axes. The translational position error (i.e. the distance between the spacecraft and proof mass along each body axis) comes from the drag free sensor. This error is converted from the body frame to the nadir frame for control computations. A PID controller is used with a limiter on the integral loop to produce a force command. This command is filtered by a second order filter which has a peak at the roll frequency to attenuate disturbances at the roll frequency. The output of the filter is transformed back to the body frame and then limited before being sent to the thruster selection logic. The translational controller gains and limits are shown in Table 2.3.1-1.

Table 2.3.1-1 Translational Controller Gains and Limits

LIMITS	
1 (micrometers)	0.5
2 (milliNewtons)	5.0
GAINS	
K_p (1 / sec^2)	2.44
K_r (sec)	1.2435
K_i (1 / sec)	0.605
Bandwidth (Hz)	0.5

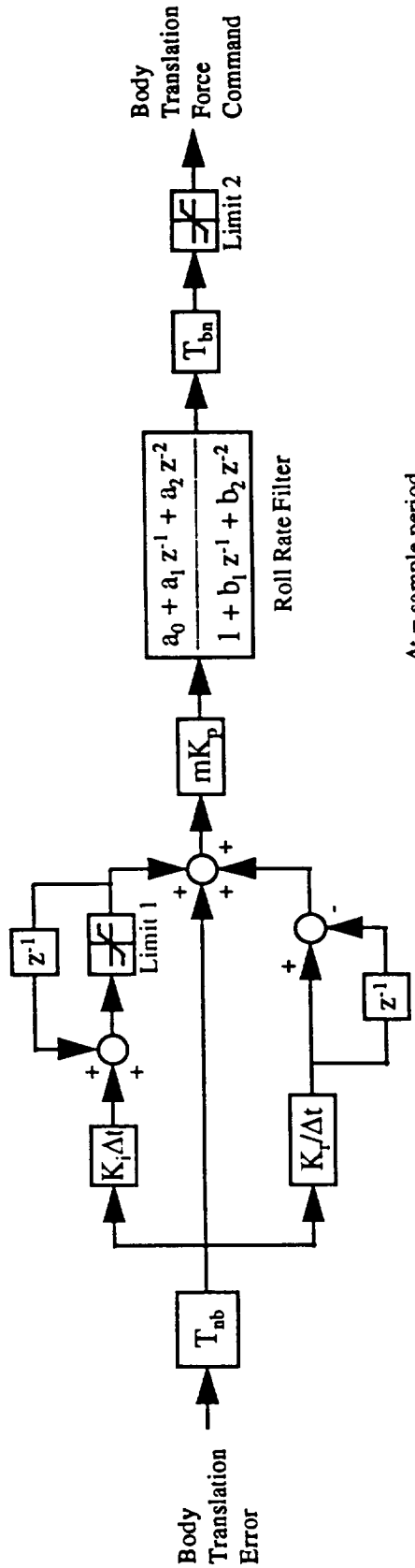

Δt = sample period

$Z_a = 3.0$ $Z_b = 0.003$

$W_a = W_b$ = roll rate (r/s)

$b_0 = (4 + 4*\Delta t*Z_b*W_b + W_b^2*\Delta t^2)$

$a_0 = \{ (4 + 4*\Delta t*Z_a*W_a + W_a^2*\Delta t^2) * W_b^2/W_a^2 \} / b_0$

$a_1 = \{ (2*W_a^2*\Delta t^2 - 8) * W_b^2/W_a^2 \} / b_0$

$a_2 = \{ (W_a^2*\Delta t^2 - 4*\Delta t*Z_a*W_a + 4) * W_b^2/W_a^2 \} / b_0$

$b_1 = \{ 2*W_b^2*\Delta t^2 - 8 \} / b_0$

$b_2 = \{ W_b^2*\Delta t^2 - 4*\Delta t*Z_b*W_b + 4 \} / b_0$

T_{nb} - Transformation from body to nadir frame

T_{bn} - Transformation from nadir to body frame

K_p - Position Gain

K_r - Rate Gain

K_i - Integral Gain

m - Mass of spacecraft

FIGURE 2.3.1-1 Translational Controller

2.3.2. Attitude Control

The GPB attitude controller[4] used in the TREETOPS simulation is shown in Figure 2.3.2-1. This same controller is used for all three axes. The attitude error for pitch and yaw comes from the science telescope during Guide Star Valid phases and from the propagated control gyro rates during Guide Star Invalid phases. The attitude error for roll comes from the roll star trackers. The attitude rate errors for the three axes come from the control gyros. A PID controller is used with a limiter on the proportional, integral, and derivative loops, as well as on the filtered sum. The control command is filtered by a second order filter which has a peak at the roll frequency to attenuate disturbances at the roll frequency. The output of the attitude controller is a torque command for each axis which is sent to the thruster selection logic. The attitude controller gains and limits are shown in Table 2.3.2-1.

Table 2.3.2-1 Attitude Controller Gains and Limits

LIMITS	Pitch/Yaw	Roll
1 (arcsec)	1.0	60.0
4 (arcsec)	0.25	20.0
5 (arcsec)	0.05	4.0
6 (arcsec)	0.25	20.0
7 (arcsec)	0.25	20.0
GAINS		
K_p (1 / sec^2)	0.482	0.054
K_r (sec)	1.98	7.26
K_i (1 / sec)	0.25	0.0023
Bandwidth (Hz)	0.15	0.06

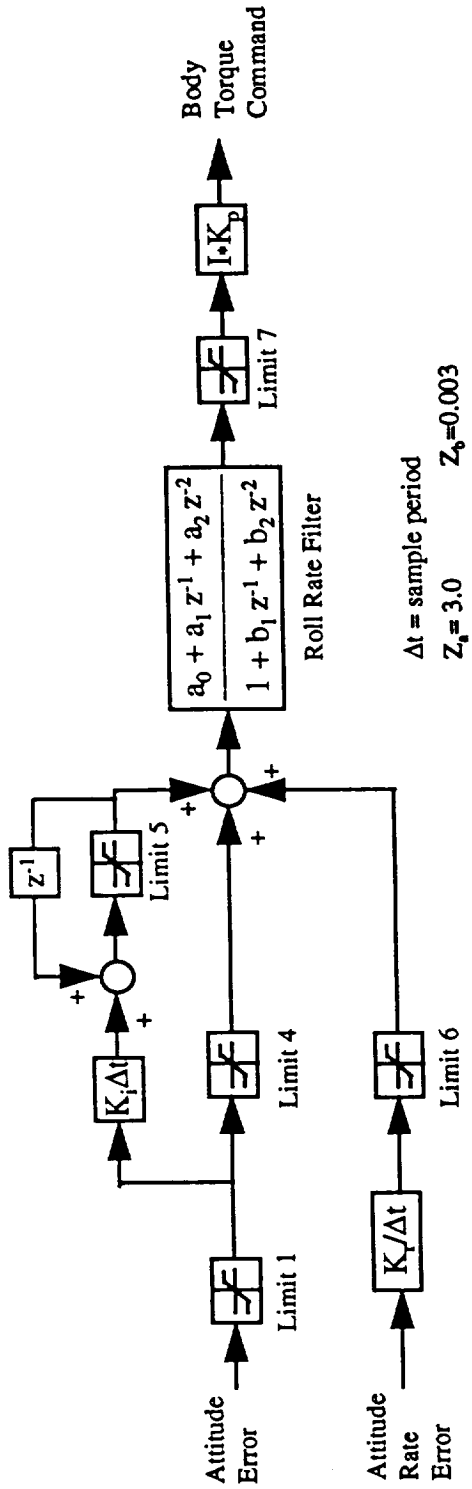

FIGURE 2.3.2-1 Attitude Controller

2.3.3. Thruster Selection Logic

The thruster selection logic determines the thrust command to each of the sixteen thrusters based on the commanded force vector from the translation controller, the commanded torque vector from the attitude controller, and the helium flow command. The flow diagram of the thruster selection logic is shown in Figure 2.3.3-1.

Figure 2.3.3-1 Thruster Selection Logic

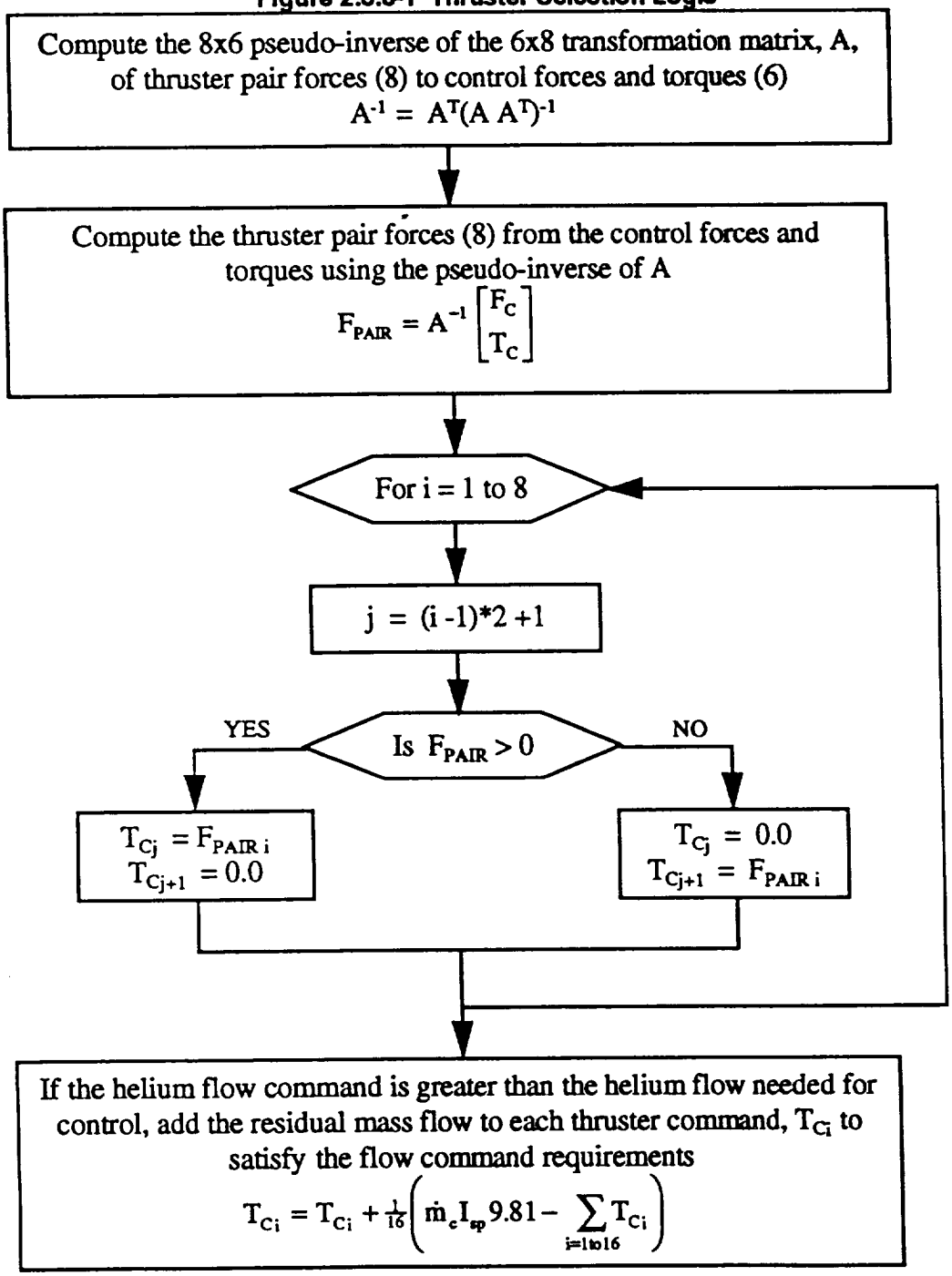

2.4. GPB Helium Slosh Model

The slosh of the Helium in the dewar of the GPB spacecraft is modeled in the TREETOPS simulation as shown in Figure 2.4-1. Four slosh masses are placed symmetrically about the dewar center of mass, two on the x axis and two on the y axis. Each of these masses is free to move in all three coordinate directions. The distance from the vehicle centerline (z axis) to the connect point of each mass is determined by the spin rate of the spacecraft and the stiffness of the spring connecting each slosh mass to the main body. The initial displacement of the springs between the main body and slosh masses are set to start the simulation in an equilibrium condition. Table 2.4-1 shows the slosh input data that was chosen to match the results of Dr. Hung[1].

Table 2.4-1 Helium Slosh Model Input Data

Mass of each slosh body	71.9 kg
Number of slosh masses	4
Dewar tank fill level	80%
Distance from centerline to slosh mass	0.35 m
Initial spring displacement	0.22778264 m
Spring Stiffness (x, y, z)	0.02, 0.02, 0.04 N/m
Spring Damping (x, y, z)	0.5, 0.5, 0.01 N/(m/s)
Spacecraft spin rate	0.1 rpm
Distance from spacecraft cm to slosh cm (z)	-0.1 m

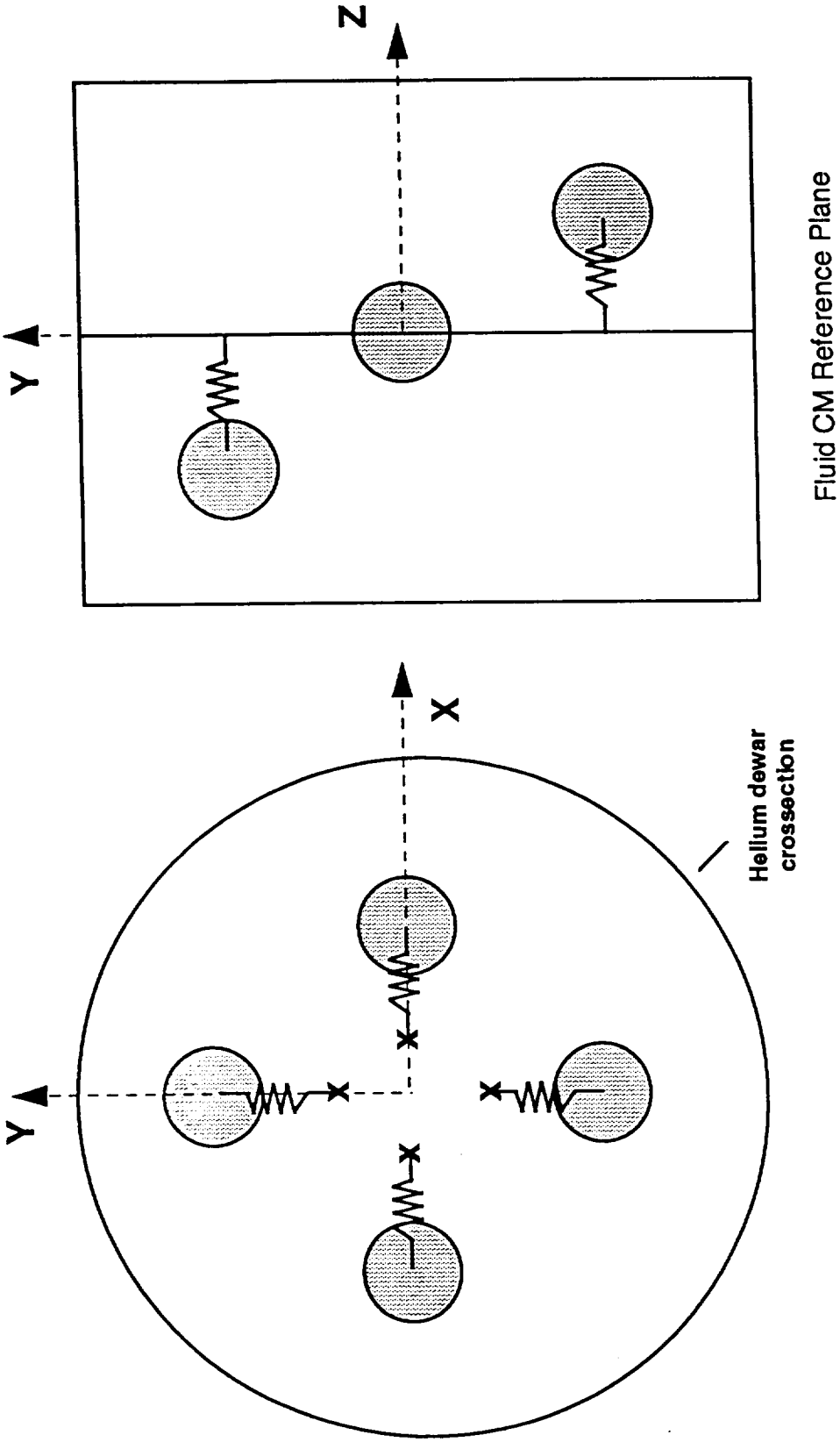

FIGURE 2.4-1 Helium Slosh Model

2.4.1. GPB Helium Slosh Model Comparison Results

The slosh model results from the simulation were compared to the results from Dr. Hung of the University of Alabama at Huntsville (UAH)[1]. Figure 2.4.1-1 shows the comparison of the helium fluid center of mass motion due to the aerodynamic force/torque disturbances for one orbit. Figure 2.4.1-2 shows the comparison of the helium fluid center of mass motion due to the gravity gradient force/torque disturbances for one orbit. Figure 2.4.1-3 shows the comparison of the helium fluid center of mass motion due to the cryoperm shield magnetic torque disturbance for one orbit. The GPB TREETOPS simulation (bd Systems) results of fluid center of mass motion compare well with Hung's results for the aerodynamic and gravity gradient disturbances, with the only significant difference being a different high frequency component in the z axis (roll) results. The comparison of fluid center of mass motion due to cryoperm shield magnetic torque was not as close as with the other disturbances. Retuning of the model was not accomplished, however, because it was deemed most important to match the fluid motion caused by the largest disturbances i.e. aerodynamic and gravity gradient effects.

Figure 2.4.1-1 Helium Fluid Center of Mass Motion Due To The Aerodynamic Force/Torque Disturbances

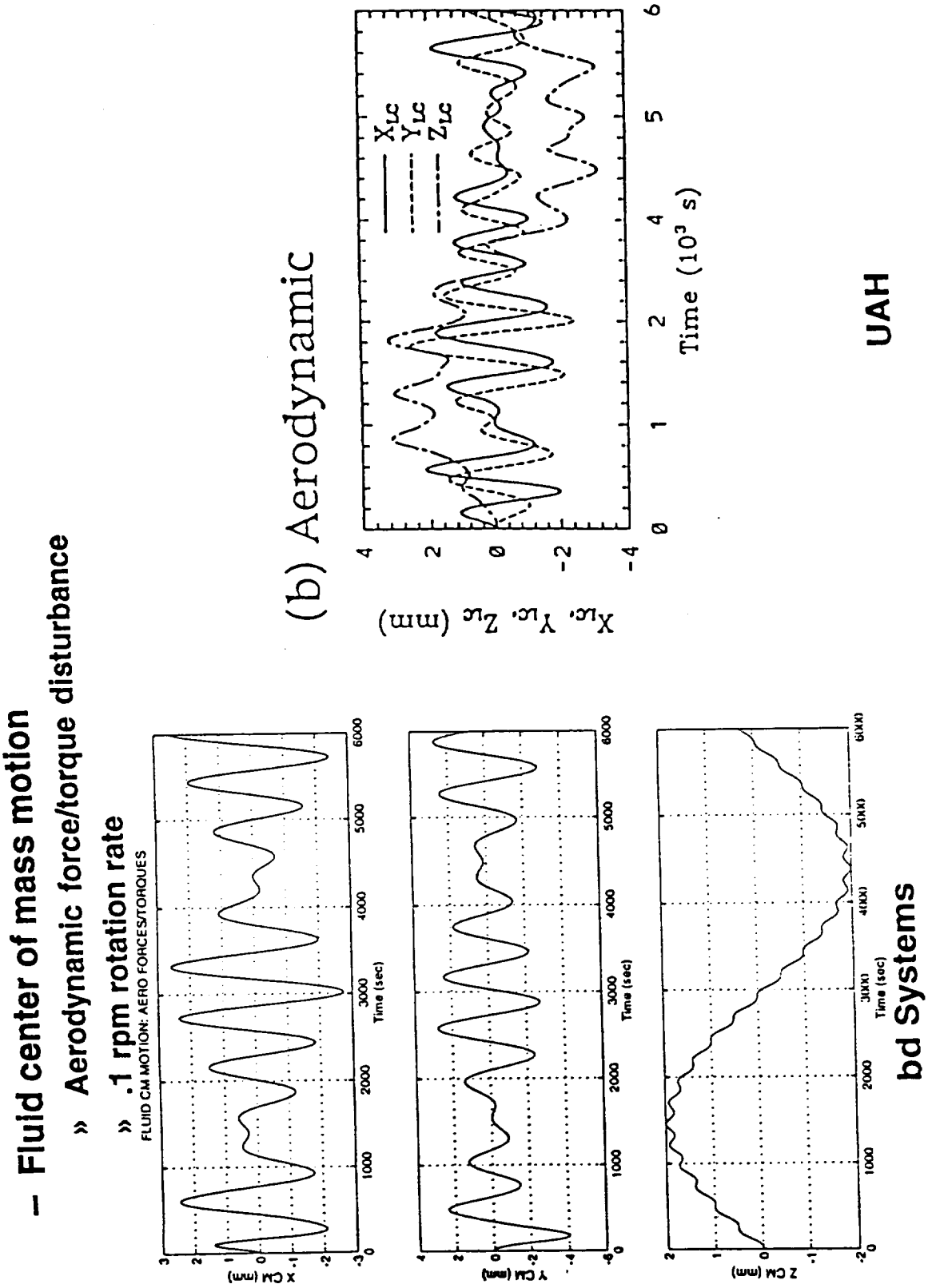

Figure 2.4.1-2 Helium Fluid Center of Mass Motion Due To The Gravity Gradient Force/Torque Disturbances

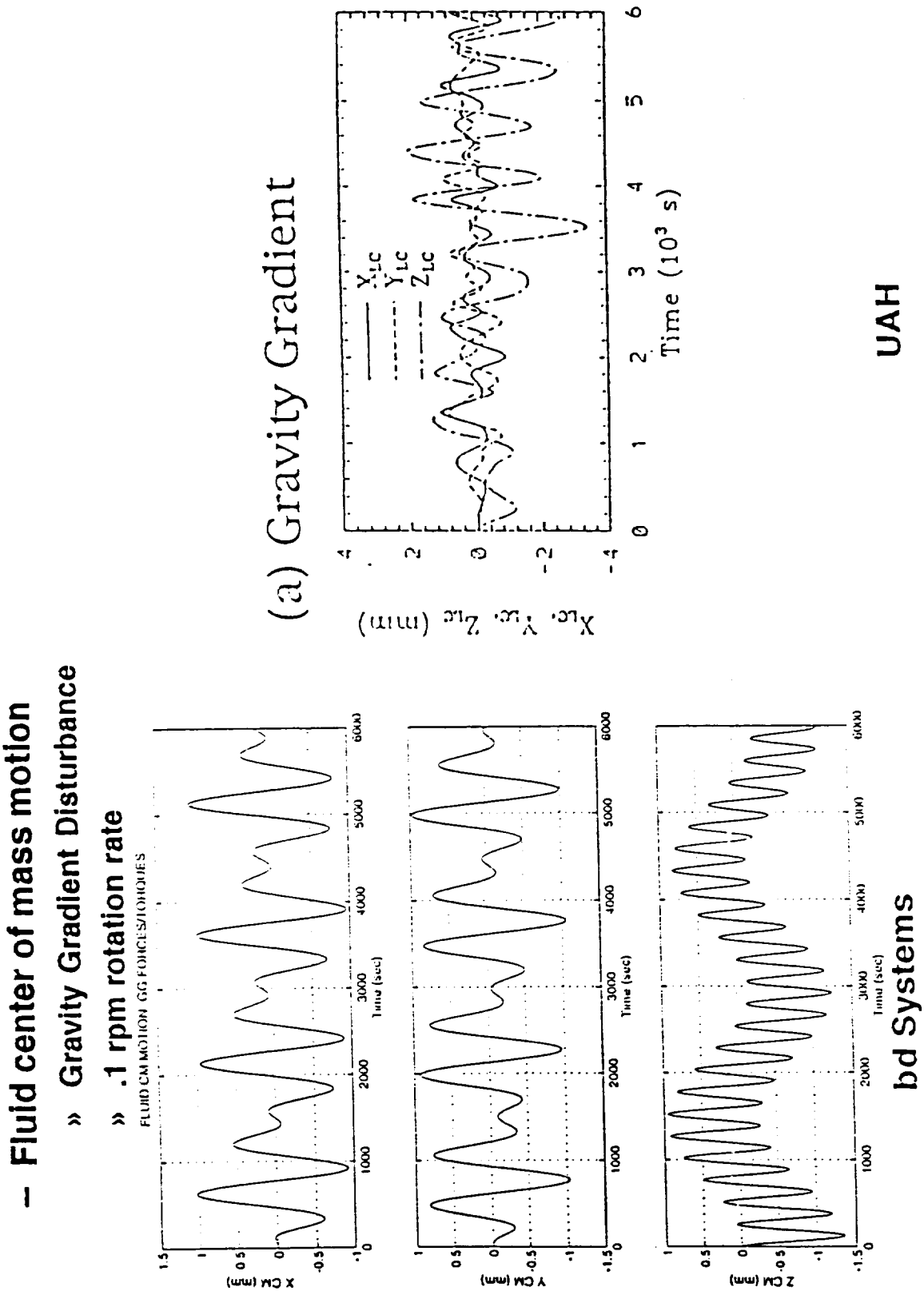

Figure 2.4.1-3 Helium Fluid Center of Mass Motion Due To The Cryoperm Shield Magnetic Torque Disturbance

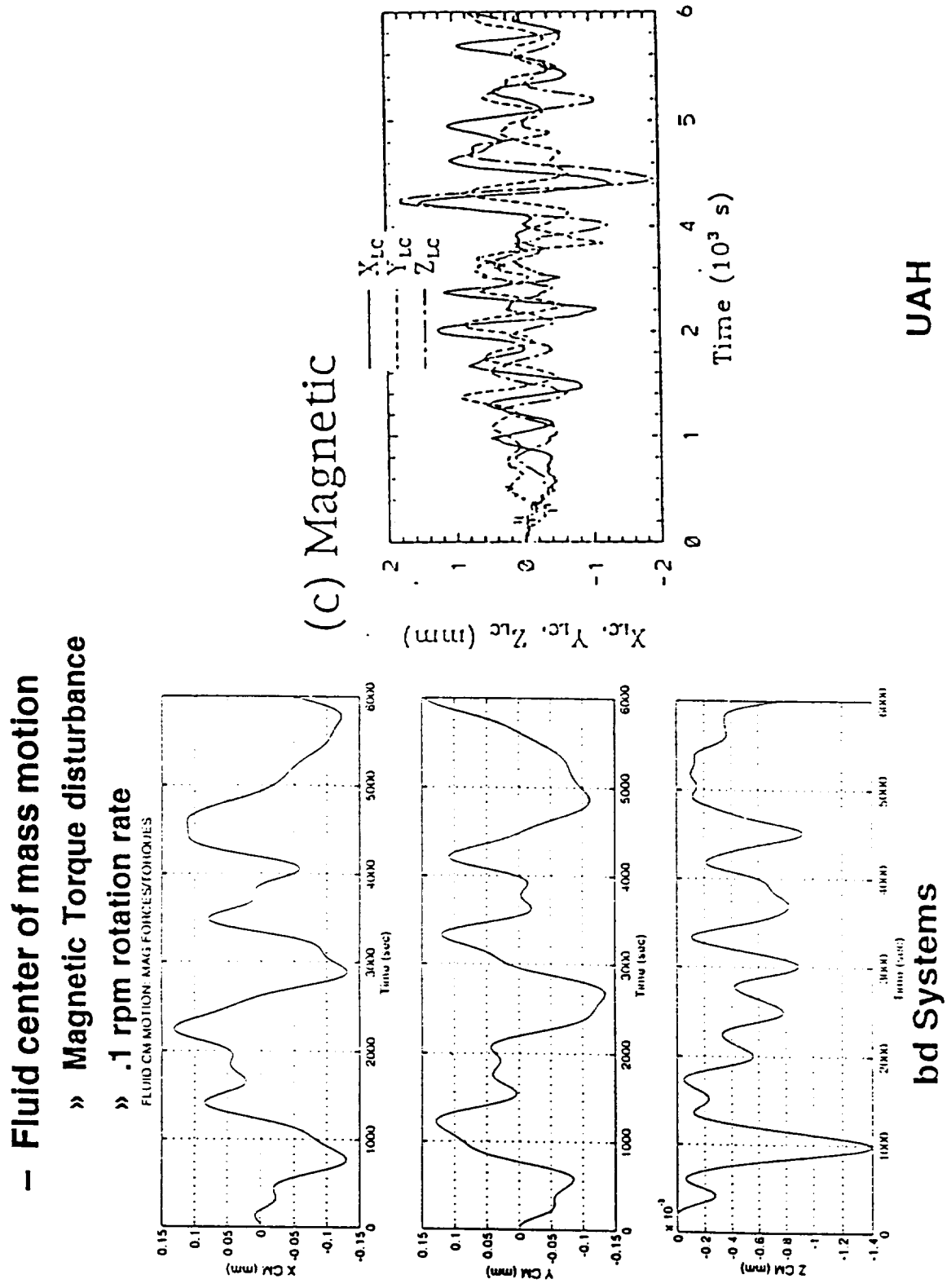

2.5. GPB Flexible Body Model

The TREETOPS GPB flexible body spacecraft model was generated from an on-orbit structural dynamics model[5] supplied by Lockheed Martin. A graphical representation of this model is shown in Figure 2.5-1. This model was supplied to MSFC in an I-DEAS Master Series 2.1 format. It was converted by MSFC to a MSC Nastran universal input format and given to bd Systems for processing. The model represents the beginning of mission deployed configuration. The mass properties are shown in Table 2.5-1 and the node locations used in the TREETOPS model are shown in Table 2.5-2. The closest node in the model to any of the science gyro locations was at grid 10950, whose location was between science gyros 2 and 3. The modal frequencies are shown in Table 2.5-3. These first eight flexible body modes were used in the TREETOPS simulation and are all the flexible body modes below 13 Hz.

Figure 2.5-1 GPB Flexible Body Spacecraft FEM Drawing

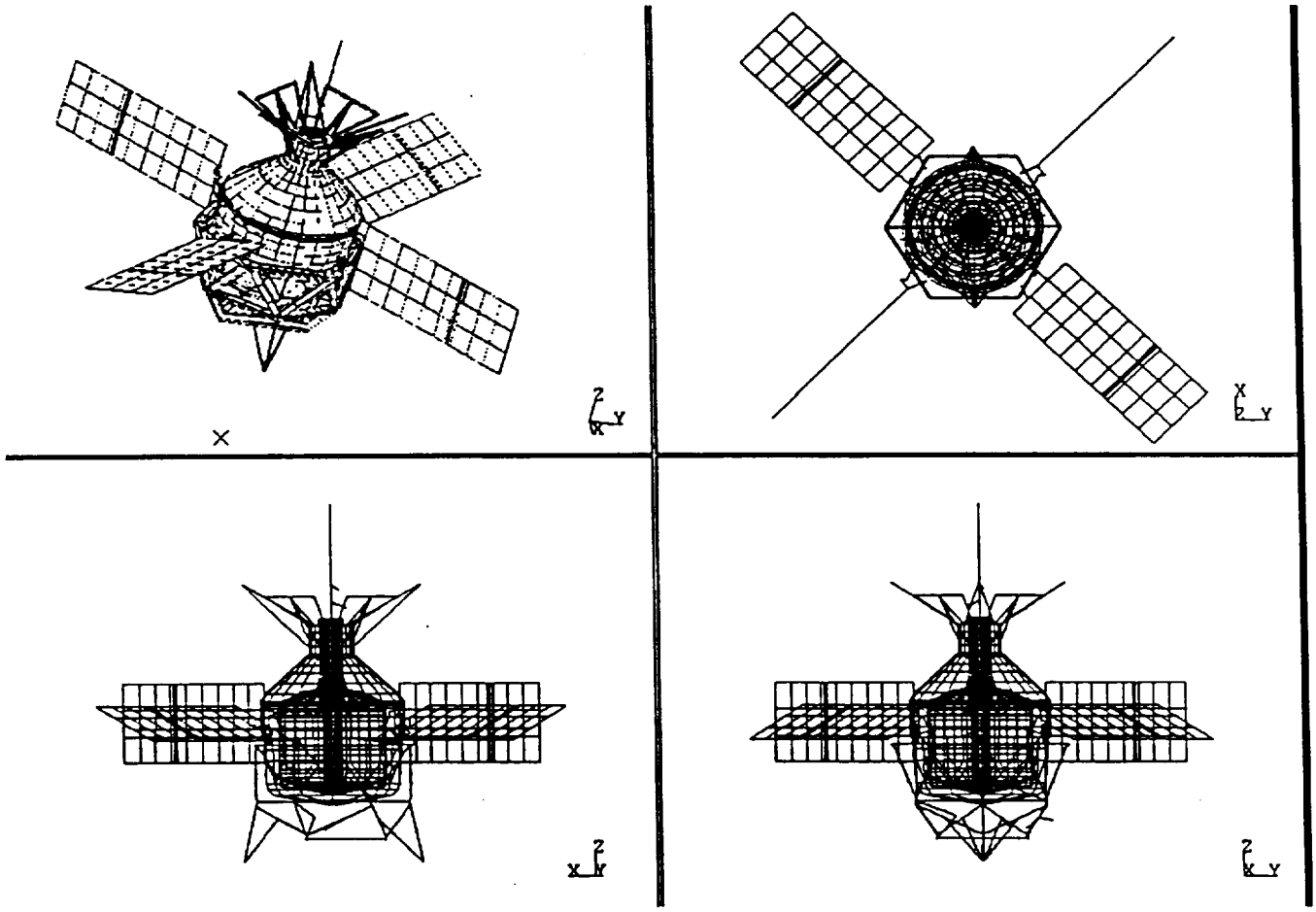

Table 2.5-1 GPB Finite Element Model (FEM) Mass Properties

	FEM
Mass (kg)	3190
Ixx (kg-m^2)	4320
Iyy (kg-m^2)	4418
Izz (kg-m^2)	2760
Cgx (m)	0
Cgy (m)	0
Cgz (m)	0

Table 2.5-2 GPB Flexible Body Model Node Locations

Node	Node No.	X(m)	Y(m)	Z(m)
Center of Mass	13001	0.0	0.0	0.0
Control Gyro	40002	0.19050	1.08457	0.60196
Proof Mass	10949	0.0	0.0	-0.04810
Thruster Pod 1	921230	-1.28651	0.0	2.547830
Thruster Pod 2	921231	1.28651	0.0	2.547830
Thruster Pod 3	921229	-1.28651	0.0	-1.86217
Thruster Pod 4	921228	1.28651	0.0	-1.86217
Science Gyro	10950	0.0	0.0	-0.37873

Table 2.5-3 GPB Flexible Body Model Modal Frequencies

Mode No.	Frequency (Hz)
1-6	0.0
7	1.32
8	1.63
9	1.93
10	2.09
11	2.28
12	2.72
13	3.78
14	4.57

2.6. GPB Science Gyro Model

A simple science gyro model was developed to compute the north-south and east-west Newtonian drifts in the science gyro. A graphical depiction of the science gyro model is shown in Figure 2.6-1. According to Kasdin and Gauthier[8], the Newtonian drifts are caused by two sources, electrostatic support dependent torques and electrostatic support independent torques. The dependent torques include the earth's gravity gradient force acting on rotor mass unbalance and on rotor oblateness (not modeled). The independent torque is that produced by earth's gravity gradient acting directly on the oblate science gyro rotor. The science gyro center of gravity is assumed to be displaced from its center of geometry by 2 μin. The electrostatic forces are applied at the science gyro center of geometry. Only forces perpendicular to the angular momentum vector are assumed to produce noncyclic gyro drift

2.6.1. GPB Science Gyro Comparison Results

The science gyro drift angles due to spherical earth gravity gradient force acting through the rotor mass unbalance are shown in Figure 2.6.1-1, with a negligible east-west drift of -2.6×10^{-8} macs/year. The science gyro drift angles due to an oblate earth gravity gradient force acting through the rotor mass unbalance are shown in Figure 2.6.1-2, with an east-west drift of -1.77 macs/year. The science gyro drift angles due to an earth gravity gradient torque, including J2 effects, on an oblate rotor are shown in Figure 2.6.1-3, with an east-west drift of 0.013 macs/year.

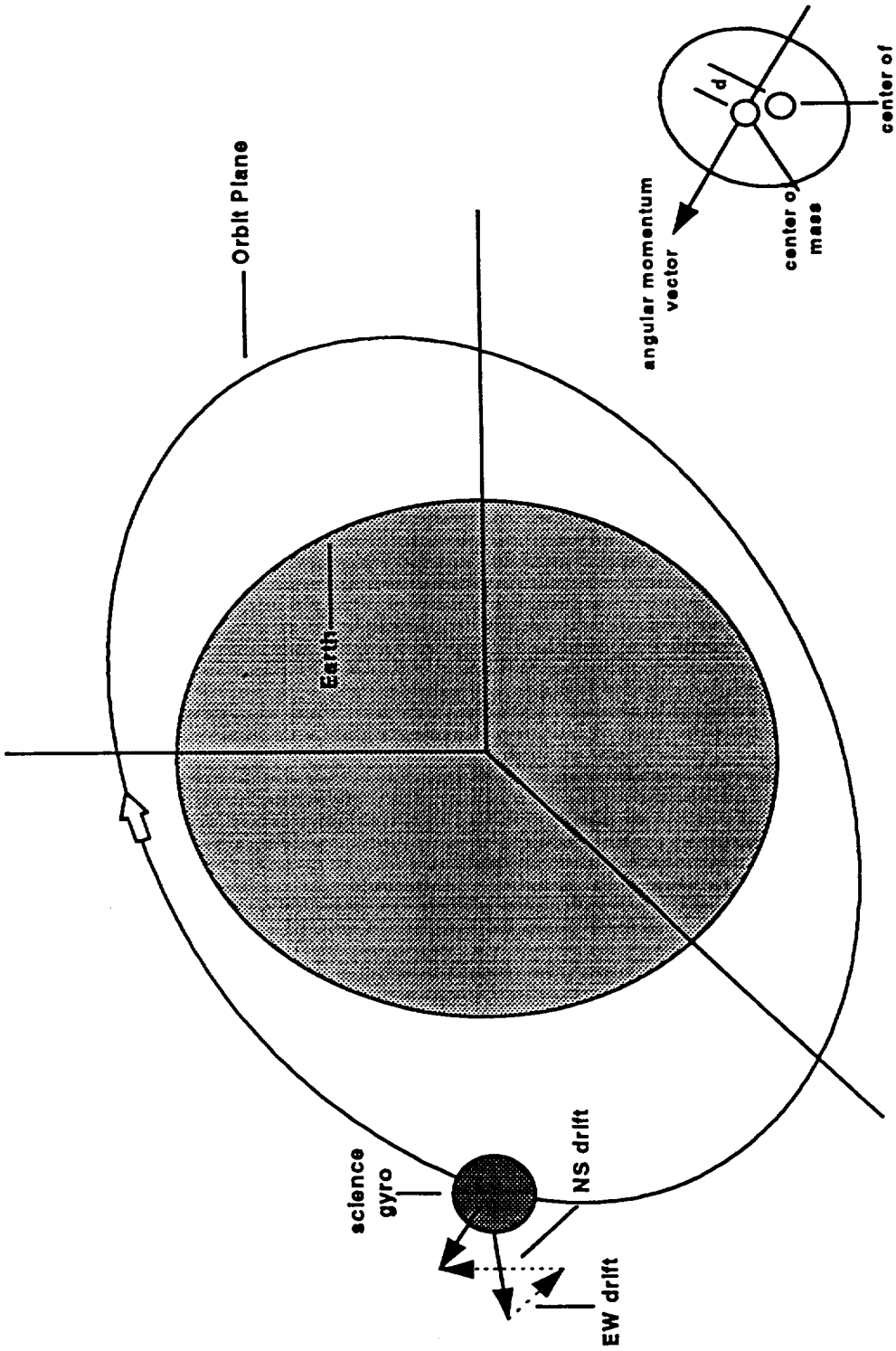

FIGURE 2.6-1 Science Gyro Model

Figure 2.6.1-1 Science Gyro Drift Angles Due To Spherical Earth Gravity Gradient Force Acting On Rotor Mass Unbalance

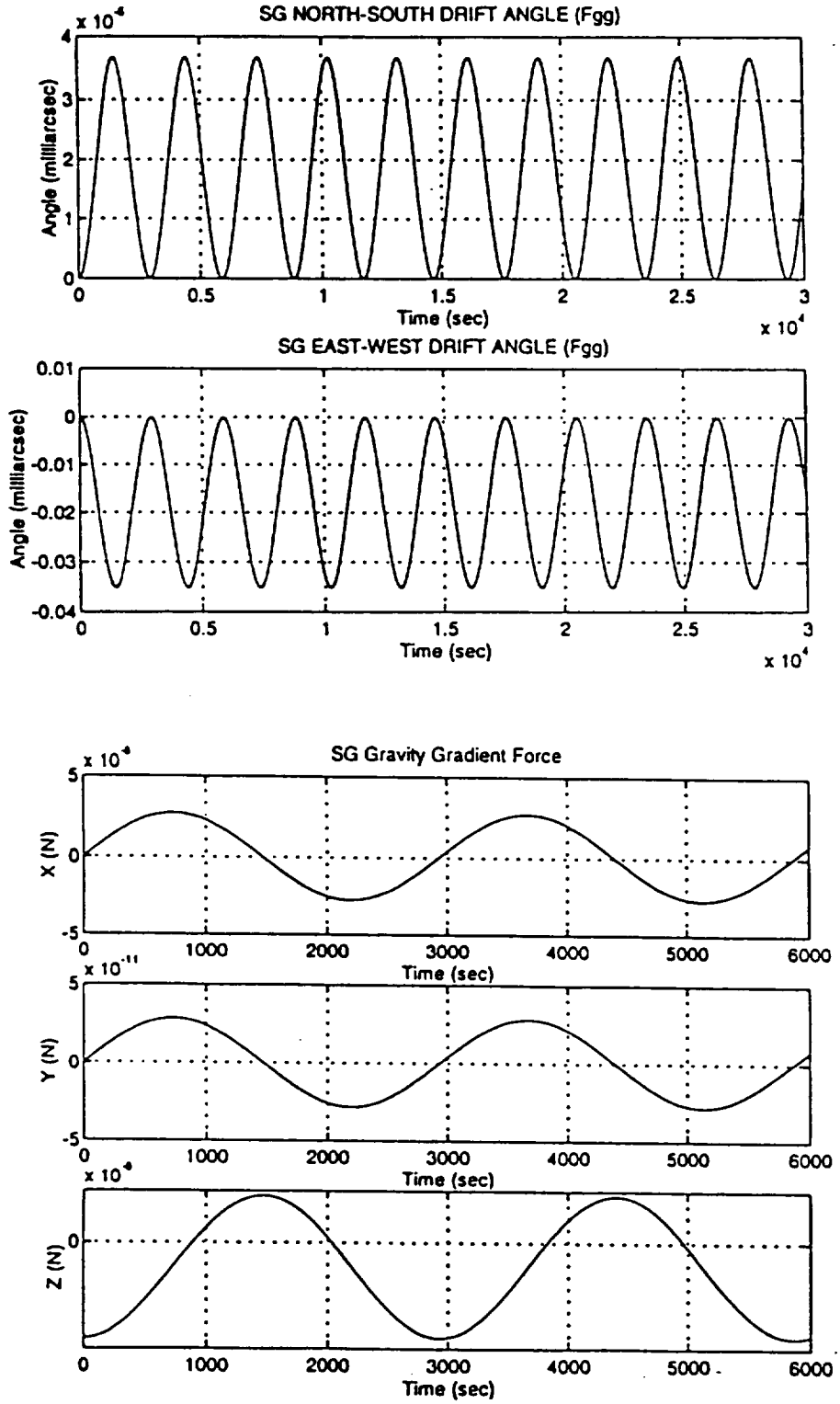

Figure 2.6.1-2 Science Gyro Drift Angles Due To An Oblate Earth Gravity Gradient Force Acting On Rotor Mass Unbalance

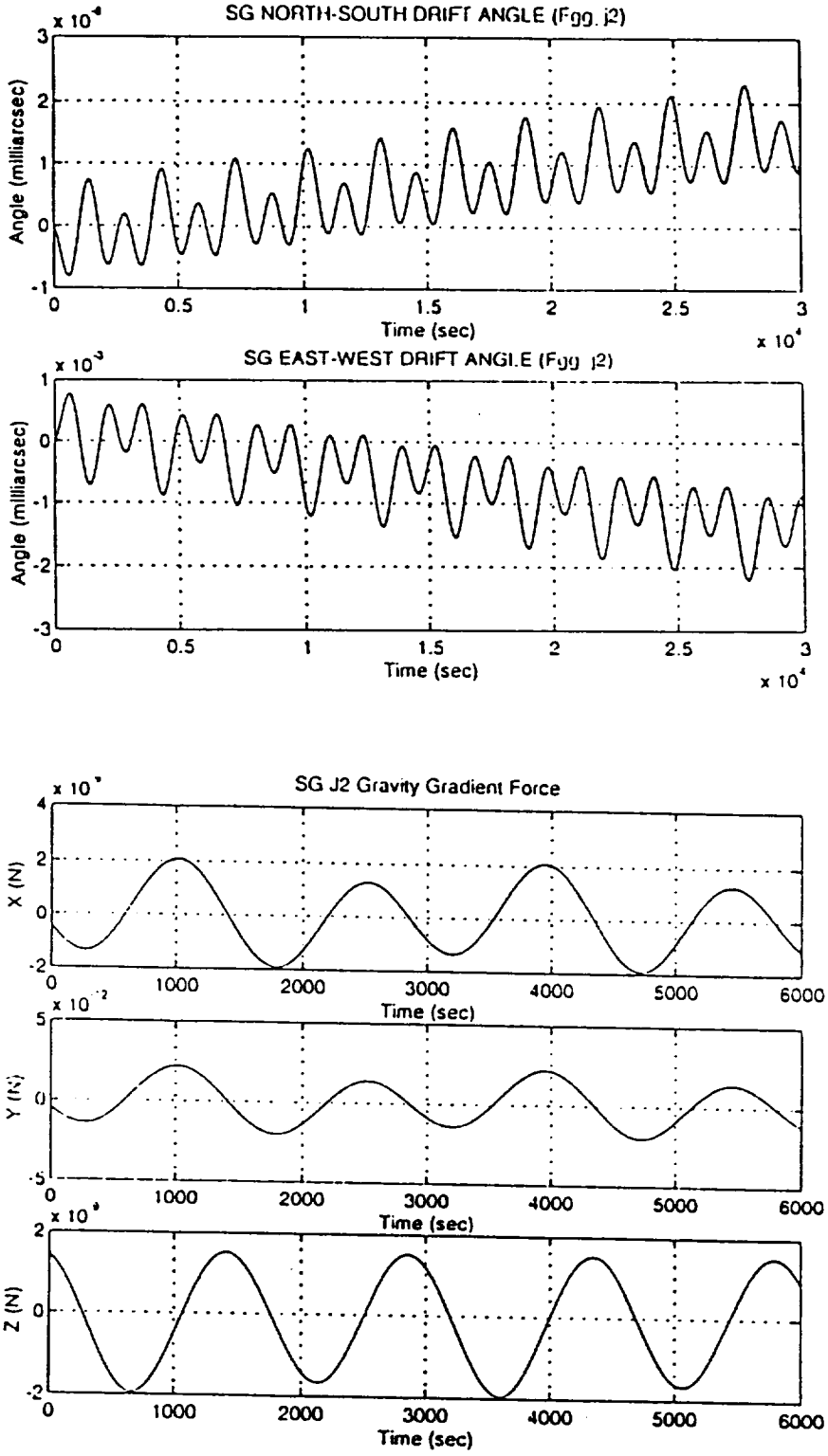

Figure 2.6.1-3 Science Gyro Drift Angles Due To An Earth Gravity Gradient Torque, Including J2 Effects, On An Oblate Rotor

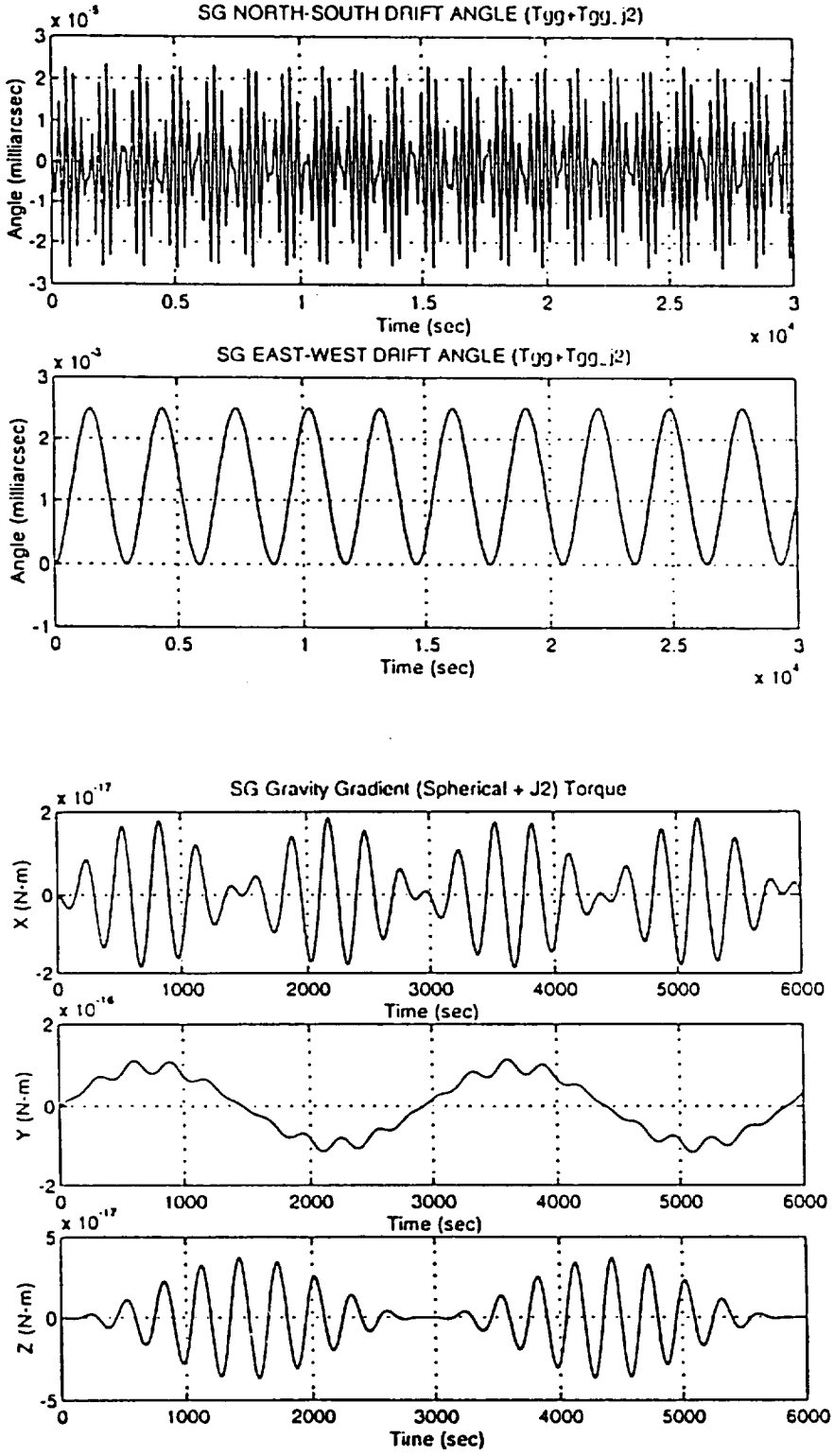

3. GPB Simulation Performance Results

The purpose of the performance evaluation was to determine the spacecraft pointing control response, in both the guide star valid and invalid phases, the roll control response, and the translation control response. All significant disturbances affecting the vehicle were evaluated, including aerodynamic disturbances, gravity gradient disturbances, and cryoperm shield magnetic disturbances. All sensor and actuator error characteristics were included in the performance evaluation. Individual runs were made to evaluate the spacecraft's ability to meet the budgeted control requirements. A summary of the performance runs is shown in Table 3-1. The performance responses for the flexible body runs accomplished at .3 rpm and .5 rpm are shown in Figures 3-1 through 3-38.

Table 3-1 Performance Run Summary

RIGID BODY @ 0.3 rpm ROLL RATE	GSV LOS Error (marcs)	GSI LOS Error (marcs)	Roll Error (arcs)	Translation Error (nm)
ENVIR (AERO+GRAV GRAD+CRYO)	0.33	2.18	0.96	0.36
THRUSTER ERRORS	9.57	8.63	0.018	7.41
ROLL STAR TRACKER NOISE/QUANTIZATION	0.55E-11	1.0E-11	0.028E-6	1.0E-10
SCIENCE TELESCOPE NOISE/QUANTIZATION	7.82	21.37	0.54	0.31
CONTROL GYRO DRIFT	0.0051	191.9	0.047E-3	0.0033
CONTROL GYRO NOISE	1.29	32.93	0.0015	0.079
CONTROL GYRO QUANTIZATION	0.17E-10	0.22E-10	0.002	0.45E-11
DRAG FREE SENSOR NOISE	0.15E-4	0.16E-4	0.28E-6	3.10
DRAG FREE SENSOR QUANTIZATION	0.50E-11	0.60E-11	0.30E-6	0.13E-11

FLEXIBLE BODY @ 0.3 rpm ROLL RATE	GSV LOS Error (marcs)	GSI LOS Error (marcs)	Roll Error (arcs)	Translation Error (nm)
ENVIR. (AERO+GRAV GRAD+CRYO)	0.33	3.66	0.96	0.36
THRUSTER ERRORS	9.64	8.65	0.018	7.37
ROLL STAR TRACKER NOISE/QUANTIZATION	0.28	1.75	0.54	1.30
SCIENCE TELESCOPE NOISE/QUANTIZATION	7.90	22.88	0.13E-4	0.32
CONTROL GYRO DRIFT	0.0054	192.9	0.47E-3	0.0034
CONTROL GYRO NOISE	1.31	33.05	0.0015	0.082
CONTROL GYRO QUANTIZATION	0.77	1.96	0.002	0.61
DRAG FREE SENSOR NOISE	0.03	1.76	0.34E-4	3.10
DRAG FREE SENSOR QUANTIZATION	0.0016	1.77	0.20E-5	1.23

Summary Runs				
CONTROL (ENVIRONMENT & THRUSTERS)	9.52	8.97	0.96	7.24
DETERMINATION (ALL SENSORS)	7.90	215.66	0.70	3.44
TOTAL (ENVIRONMENT&THRUSTERS&SENSORS)	12.05	215.03	1.23	8.39

FLEXIBLE BODY @ 0.5 rpm ROLL RATE	GSV LOS Error (marcs)	GSI LOS Error (marcs)	Roll Error (arcs)	Translation Error (nm)
ENVIR. (AERO+GRAV GRAD+CRYO)	0.33	5.76	1.04	0.37
THRUSTER ERRORS	9.61	9.54	0.016	7.39
ROLL STAR TRACKER NOISE/QUANTIZATION	0.29	4.99	0.55	1.31
SCIENCE TELESCOPE NOISE/QUANTIZATION	8.08	25.91	0.14E-4	0.35
CONTROL GYRO DRIFT	0.0050	115.42	0.47E-3	0.0032
CONTROL GYRO NOISE	1.37	17.62	0.0015	0.090
CONTROL GYRO QUANTIZATION	0.77	6.39	0.002	0.71
DRAG FREE SENSOR NOISE	0.029	5.01	0.35E-4	3.18
DRAG FREE SENSOR QUANTIZATION	0.002	5.03	0.36E-5	1.26

The results summarized in this table indicate that the flexible body effects during periods where the spacecraft is stabilized at a constant roll rate (non transient periods) produce only small differences from the rigid body results. This indicates that the flexible body effects are of minimal importance to spacecraft control during quiescent periods.

Figure 3-1 LOS Error (.3 rpm, GSV and GSI, Environmental Dist Only)

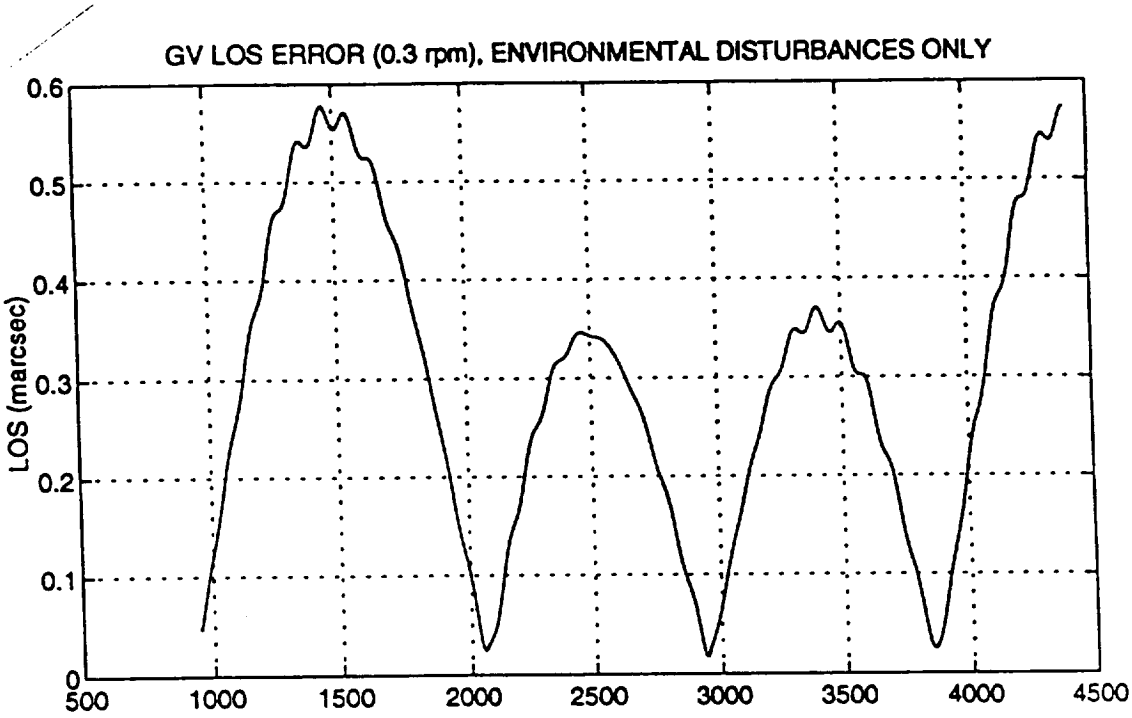

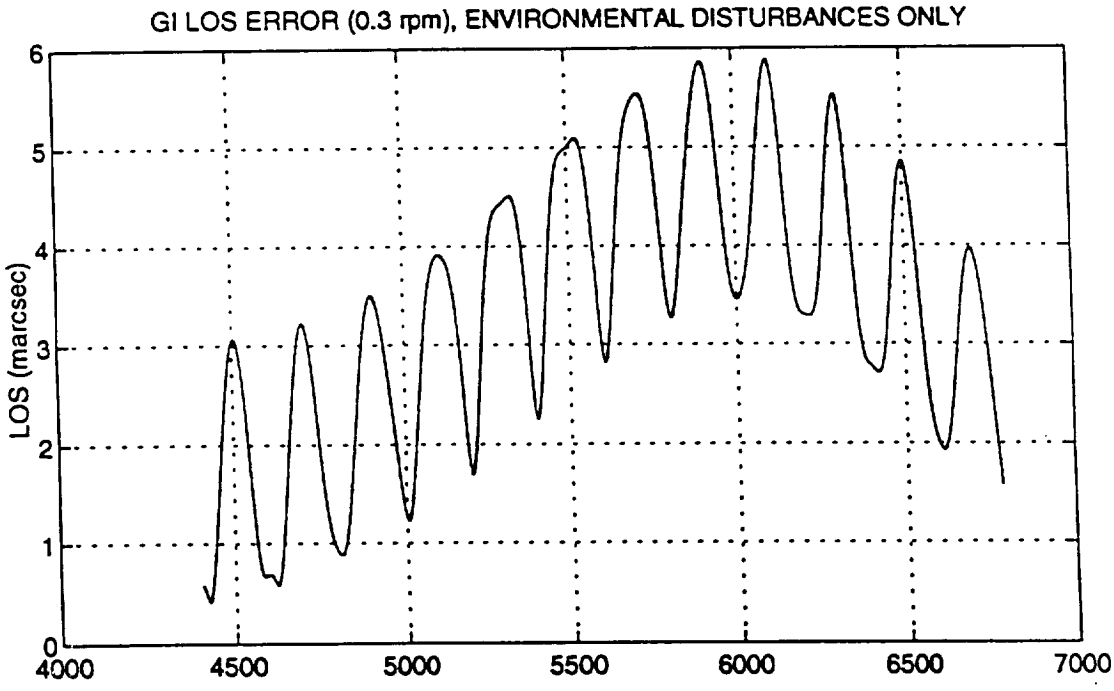

Figure 3-2 Roll and Translational Error (.3 rpm, Environmental Dist Only)

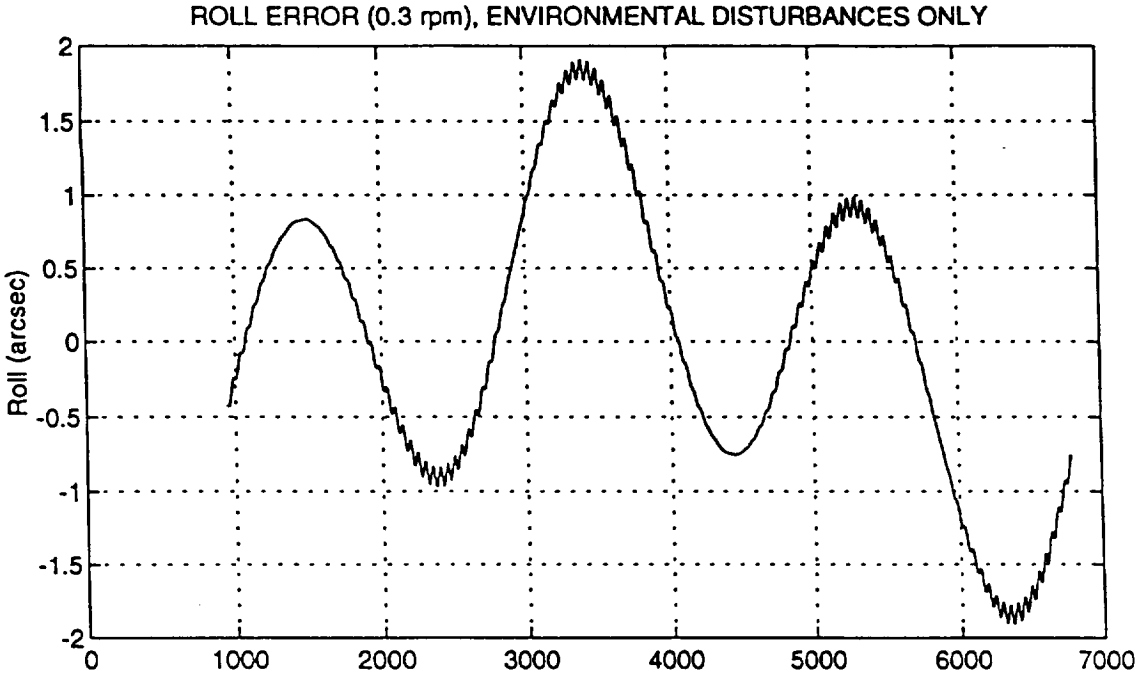

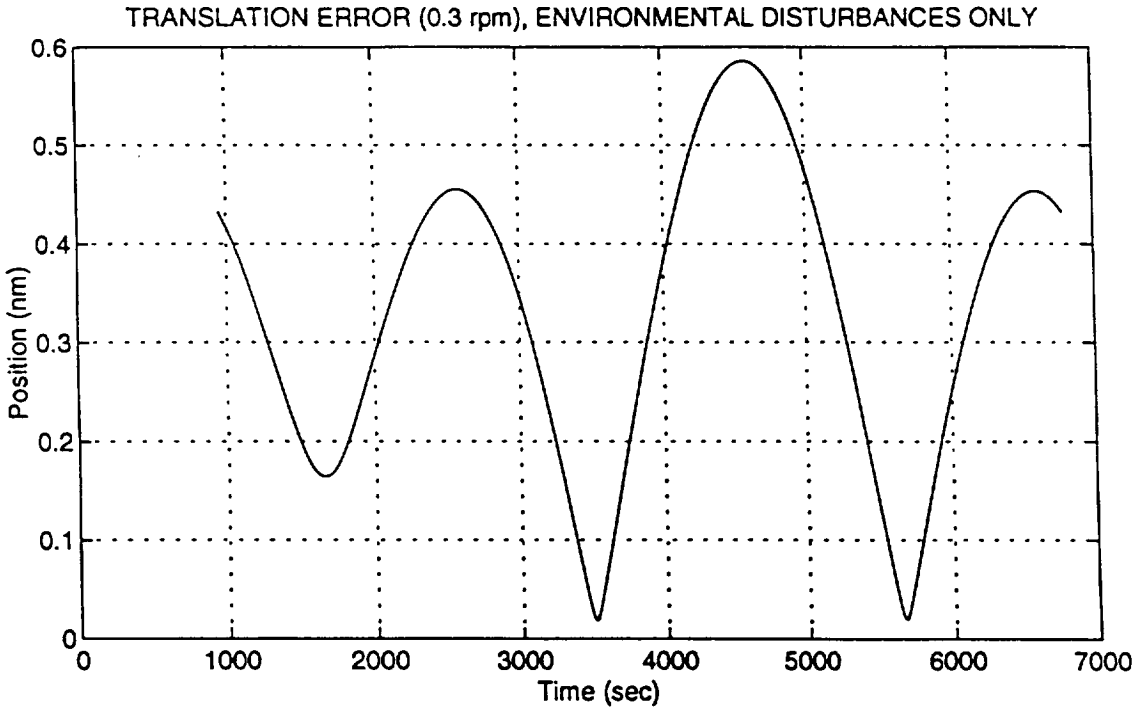

Figure 3-3 LOS Error (.3 rpm, GSV and GSI, Thruster Errors)

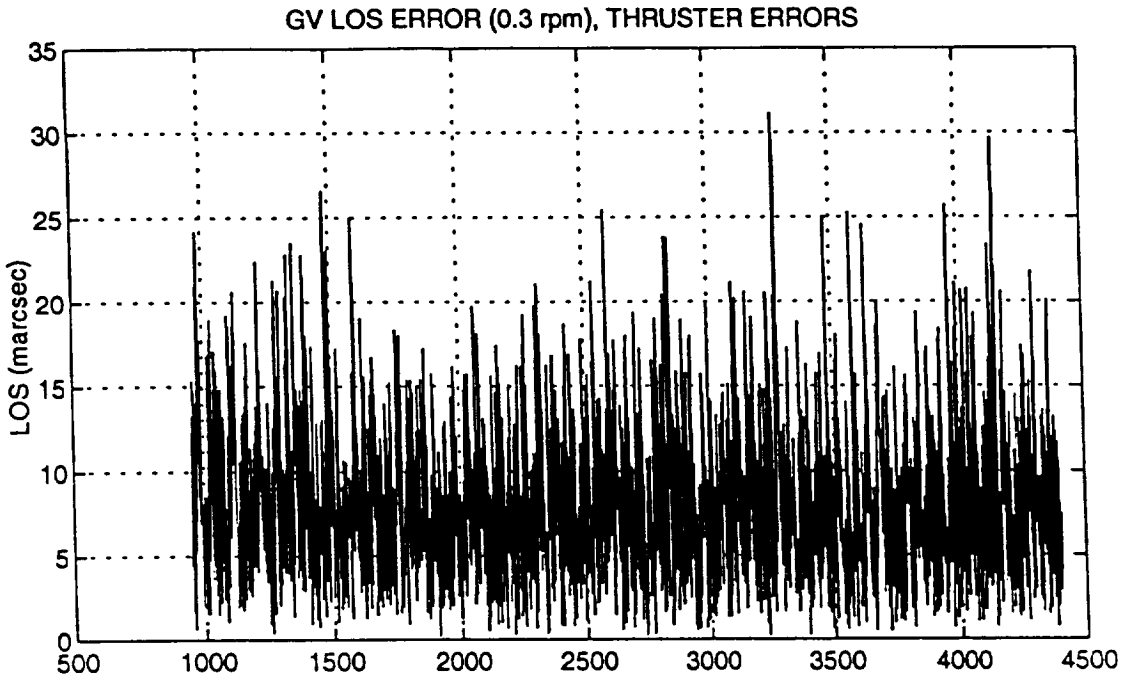

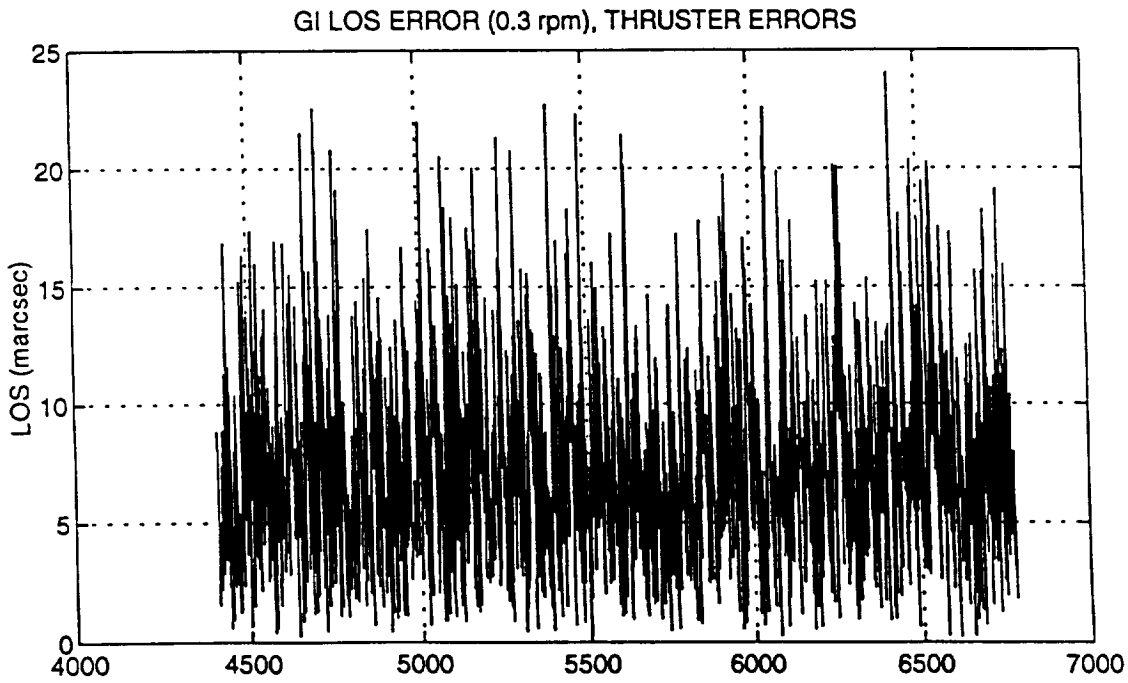

Figure 3-4 Roll and Translational Error (.3 rpm, Thruster Errors)

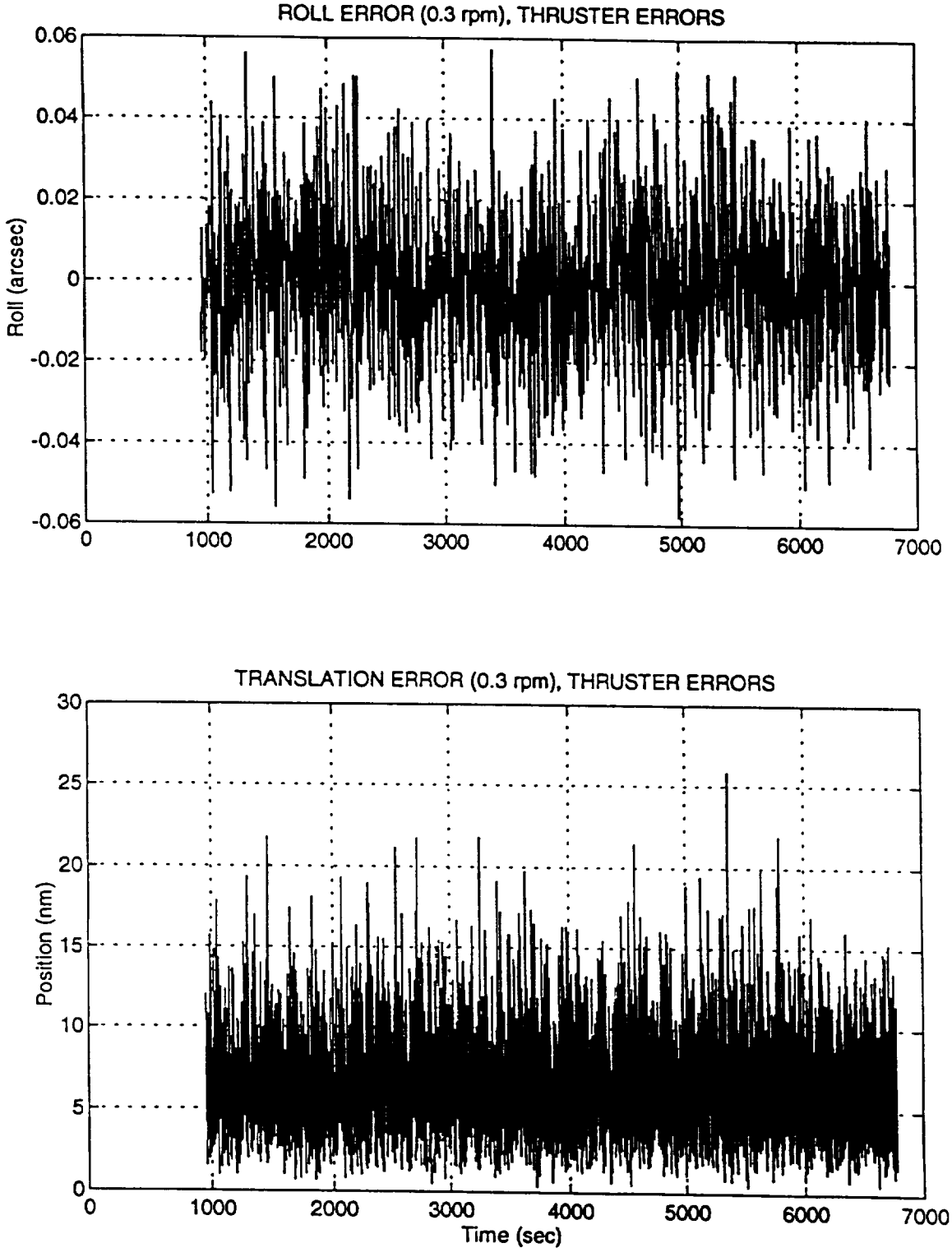

Figure 3-5 LOS Error (.3 rpm, GSV and GSI, Roll Star Tracker Noise/Quantization)

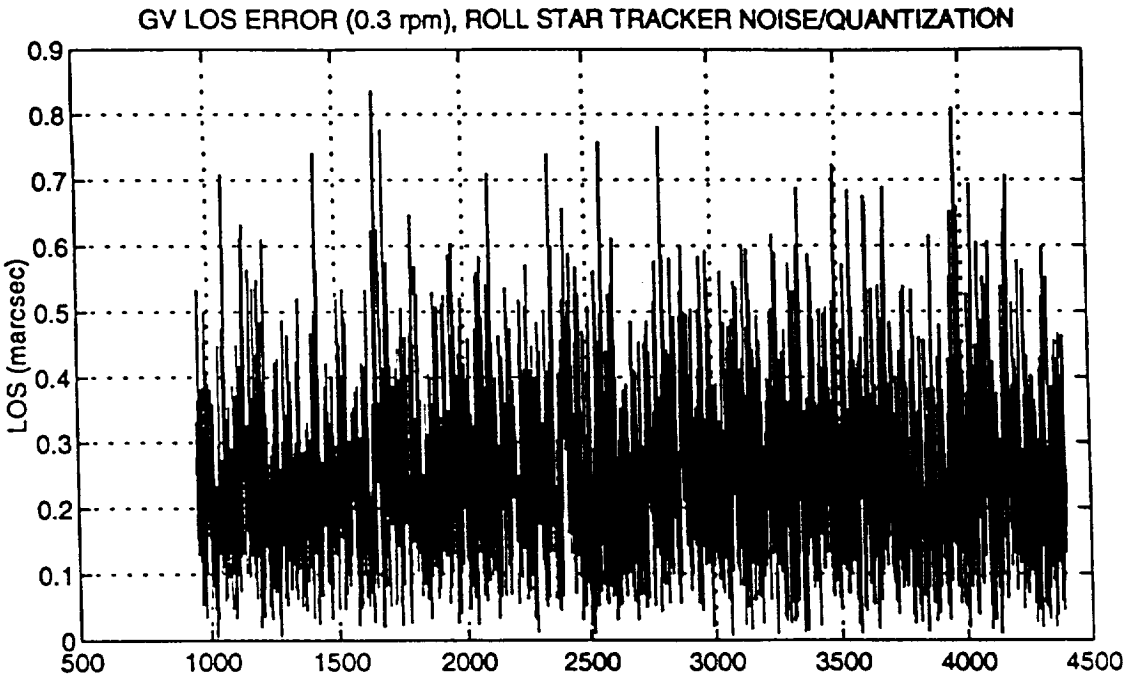

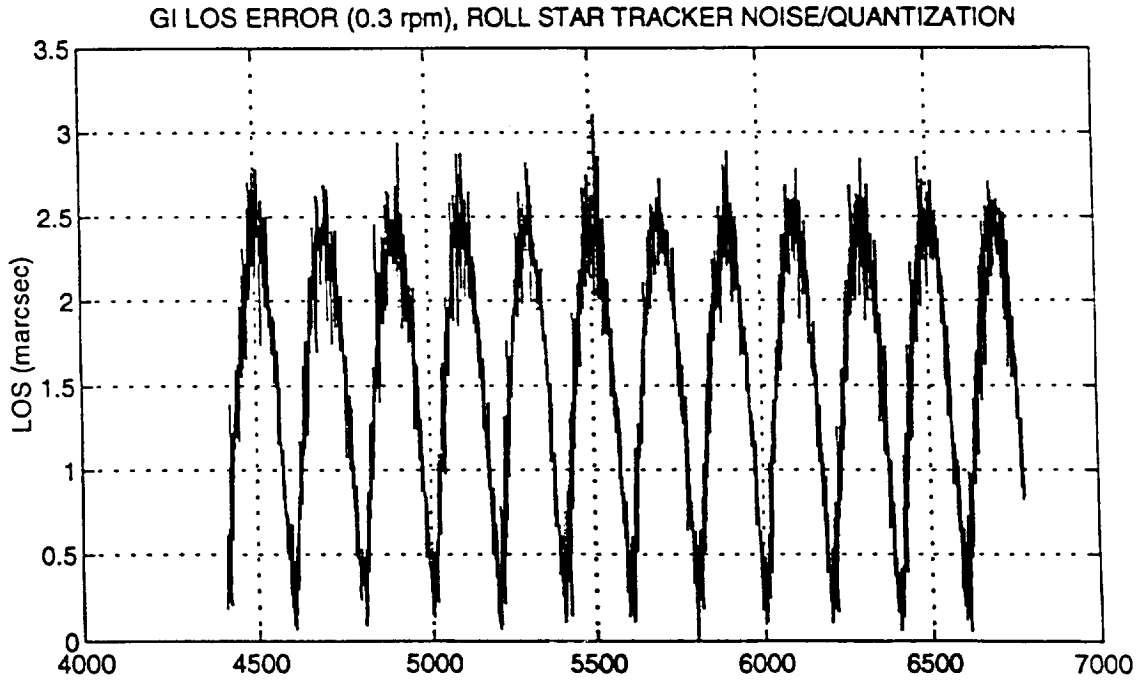

Figure 3-6 Roll and Translational Error (.3 rpm, Roll Star Tracker Noise/Quantization)

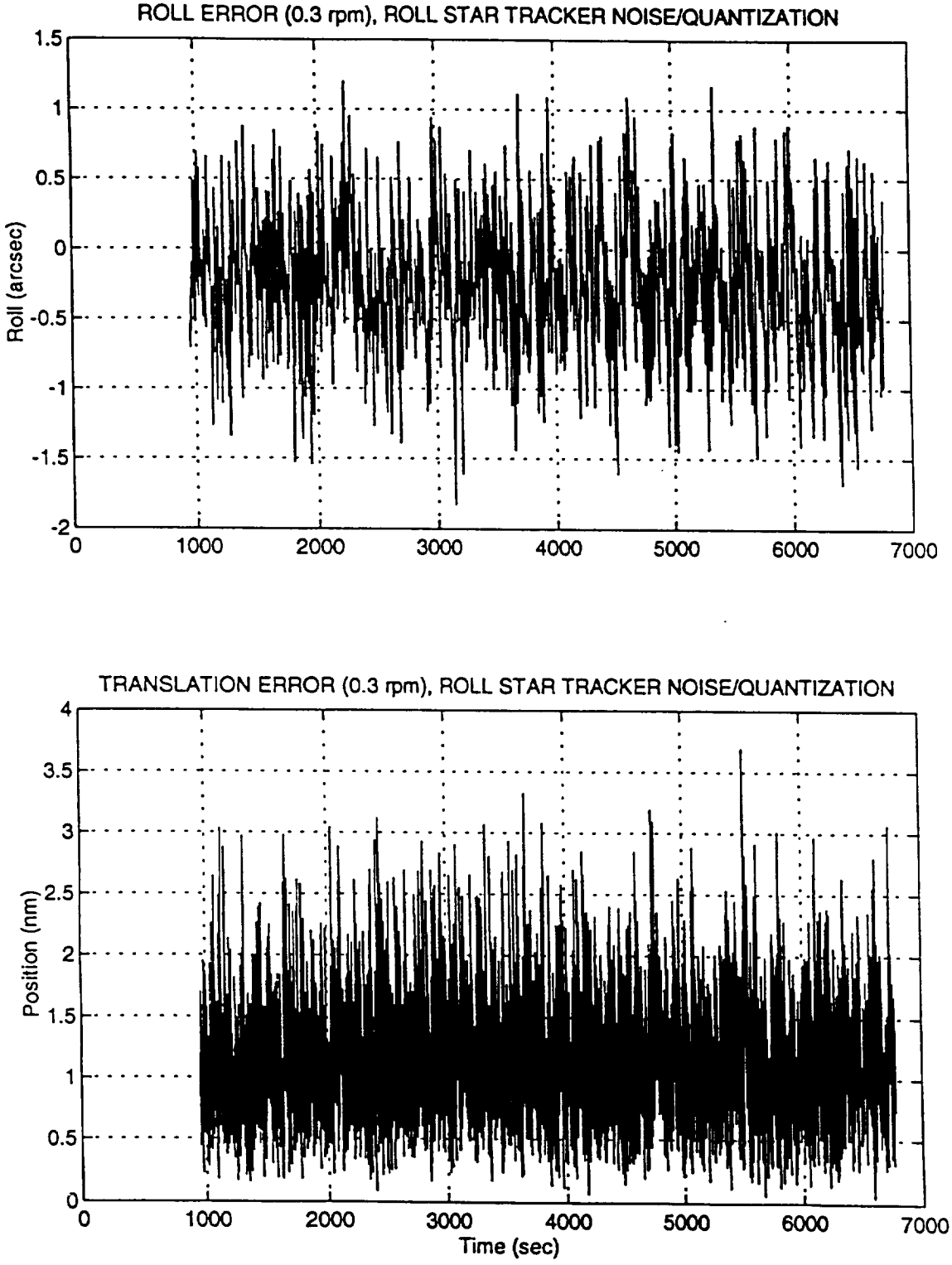

Figure 3-7 LOS Error (.3 rpm, GSV and GSI, Science Telescope Noise/Quantization)

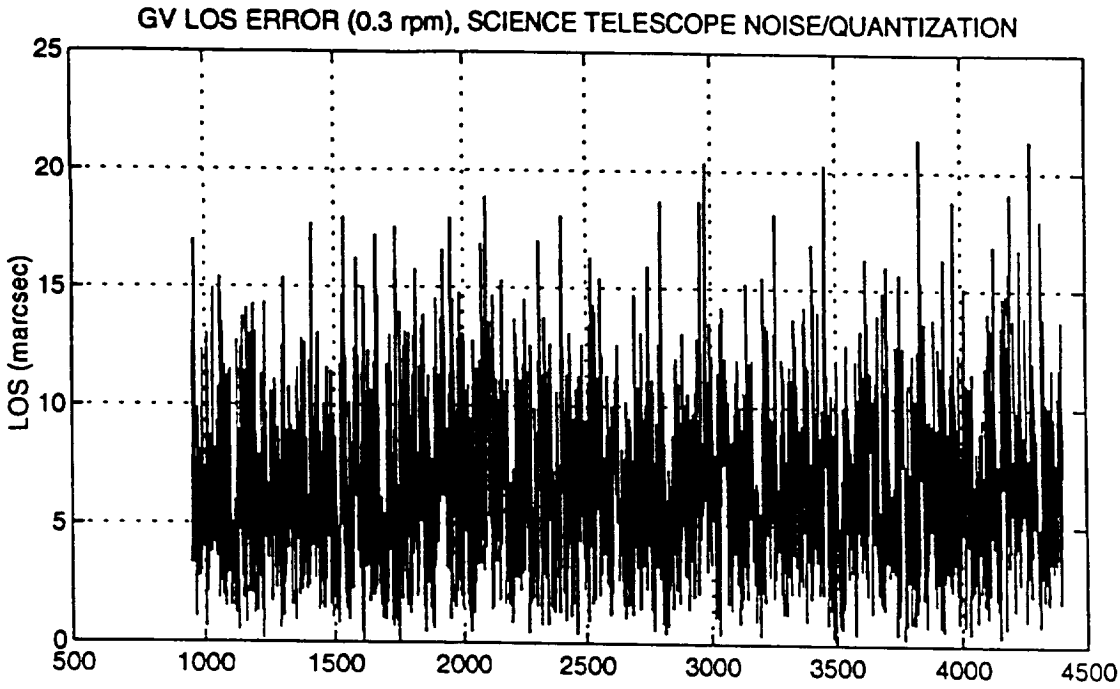

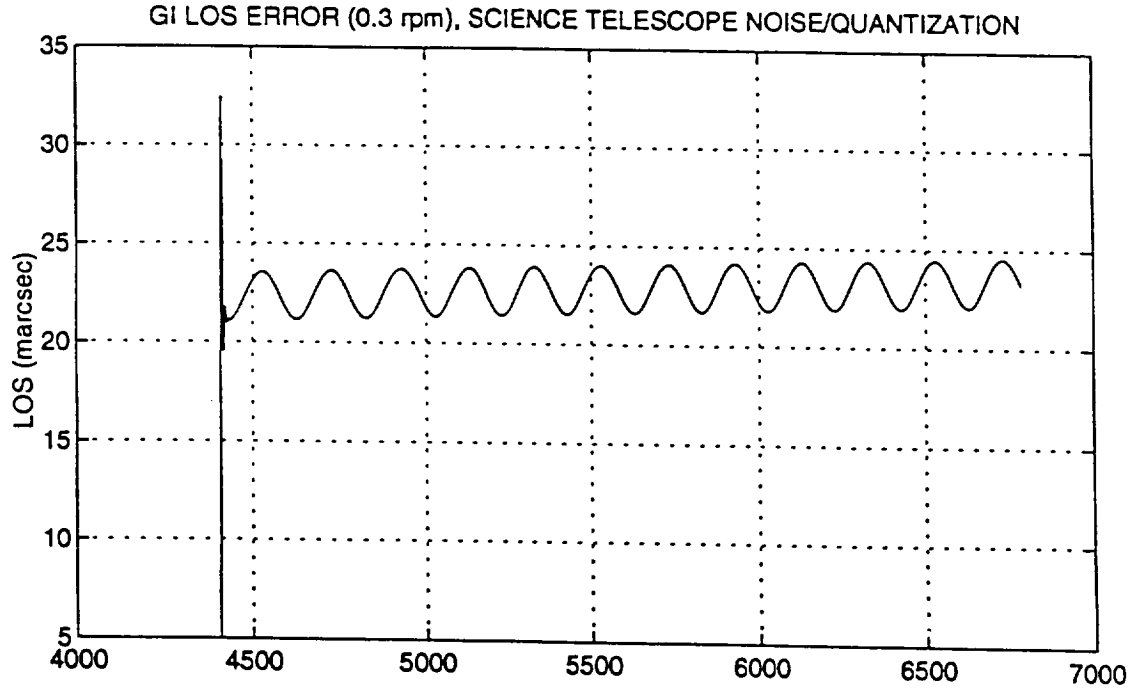

Figure 3-8 Roll and Translational Error (.3 rpm, Science Telescope Noise/Quantization)

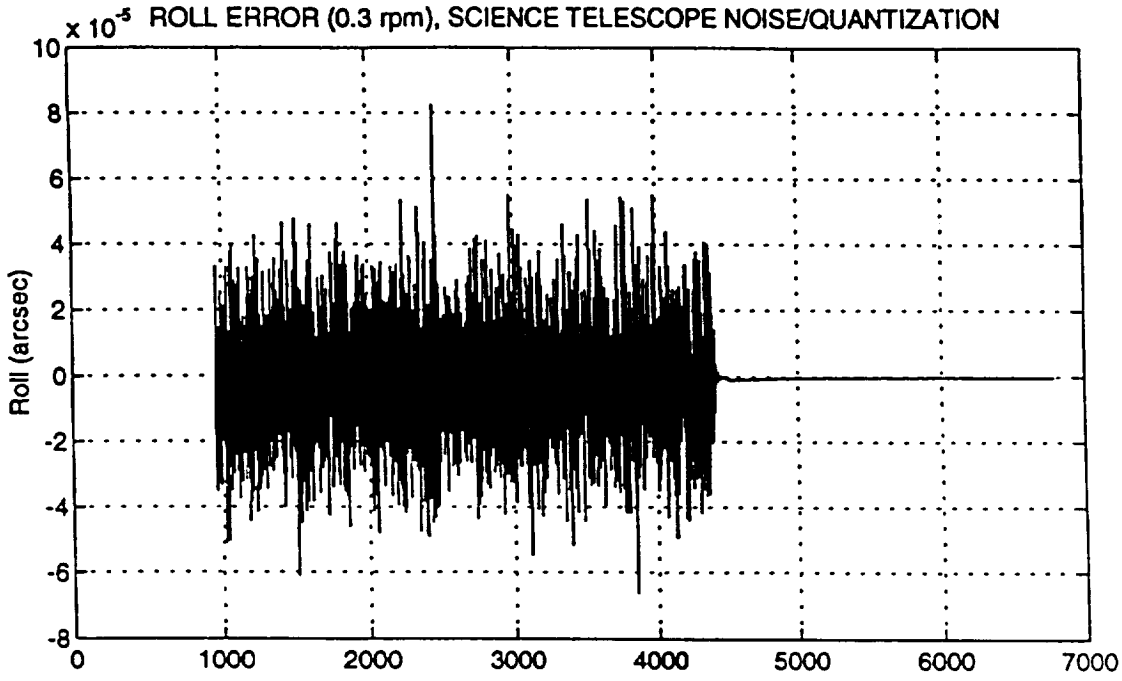

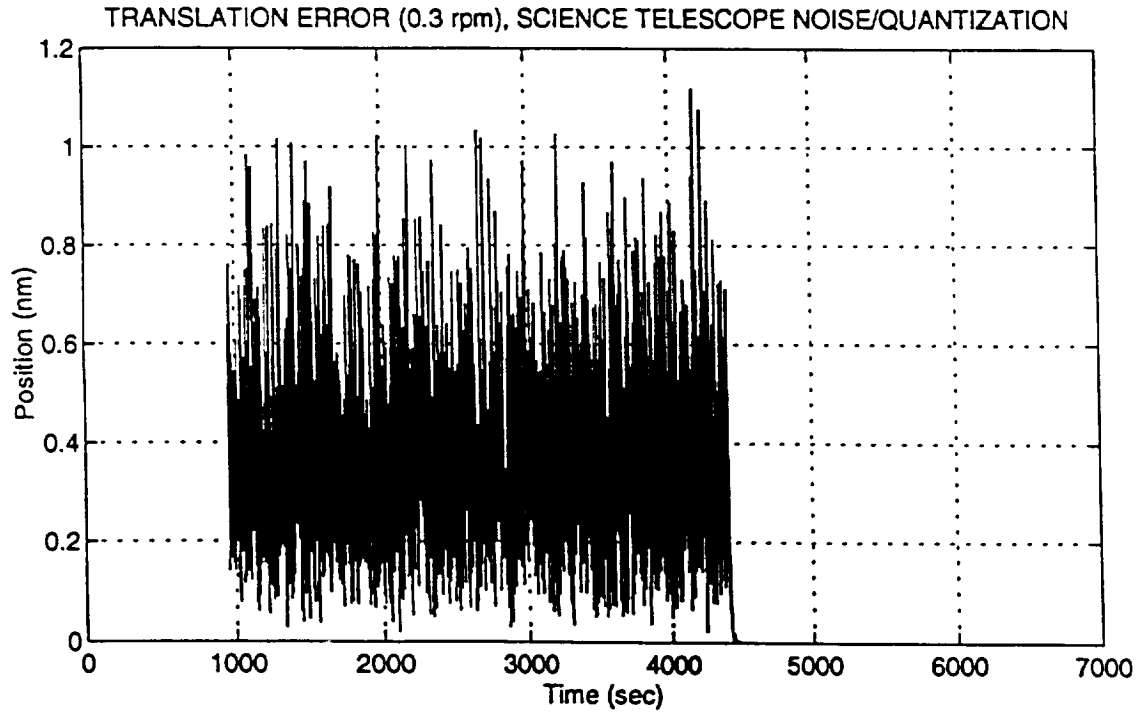

Figure 3-9 LOS Error (.3 rpm, GSV and GSI, Control Gyro Drift)

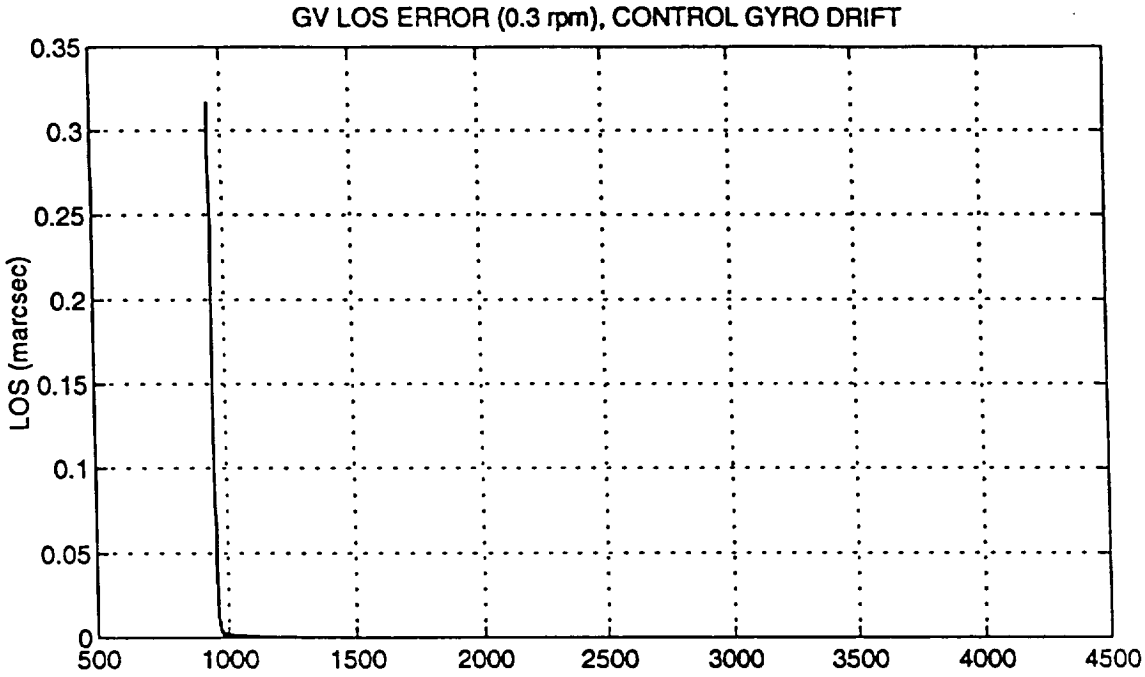

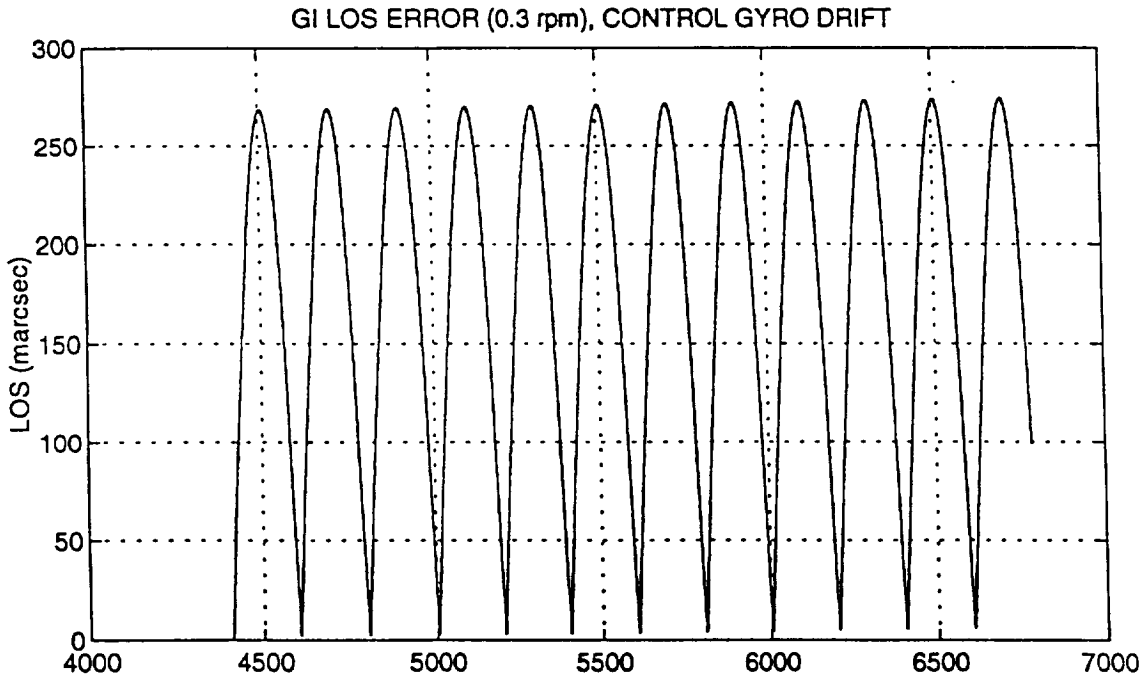

Figure 3-10 Roll and Translational Error (.3 rpm, Control Gyro Drift)

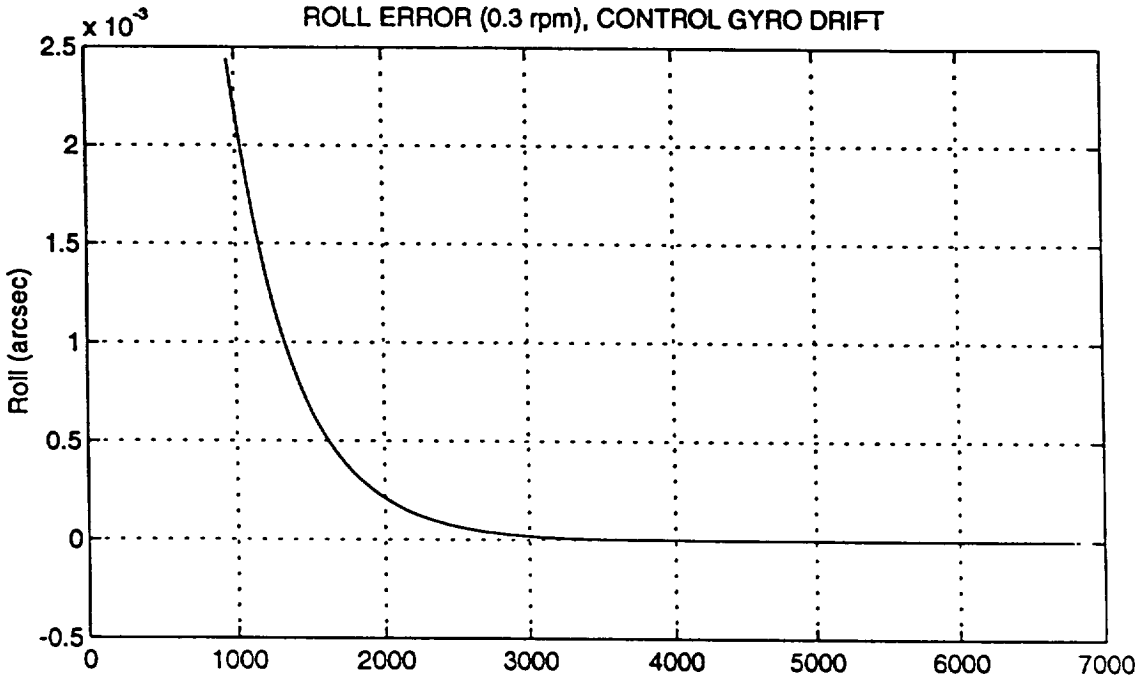

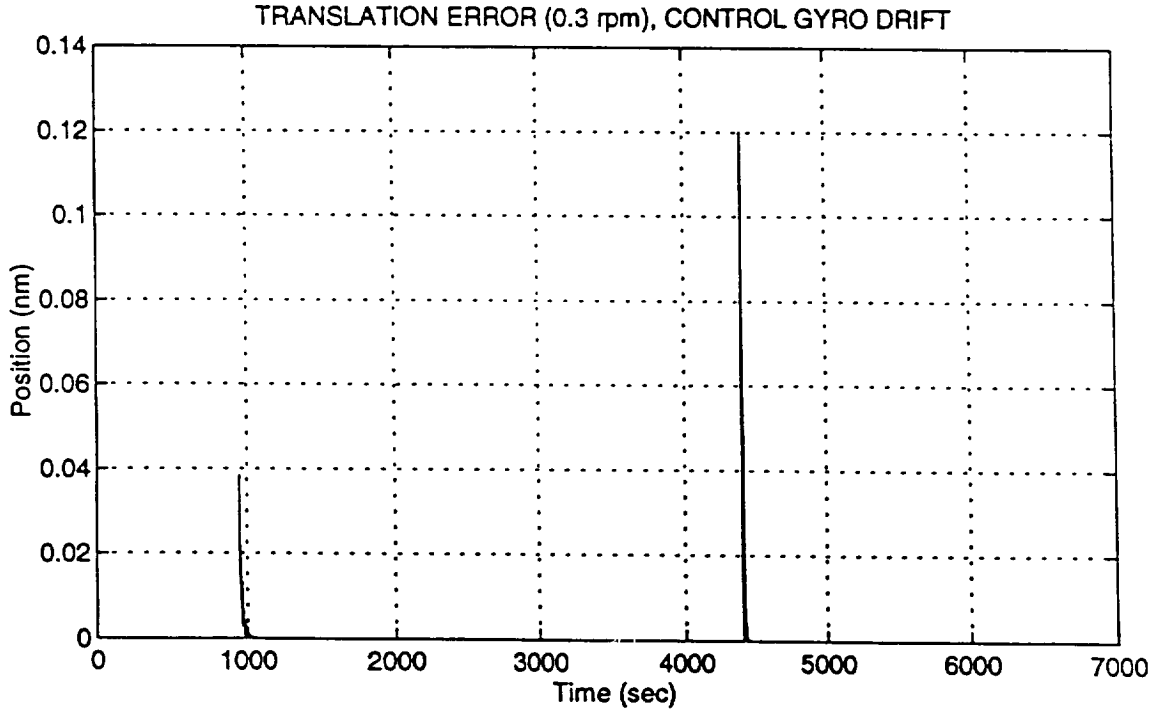

Figure 3-11 LOS Error (.3 rpm, GSV and GSI, Control Gyro Noise)

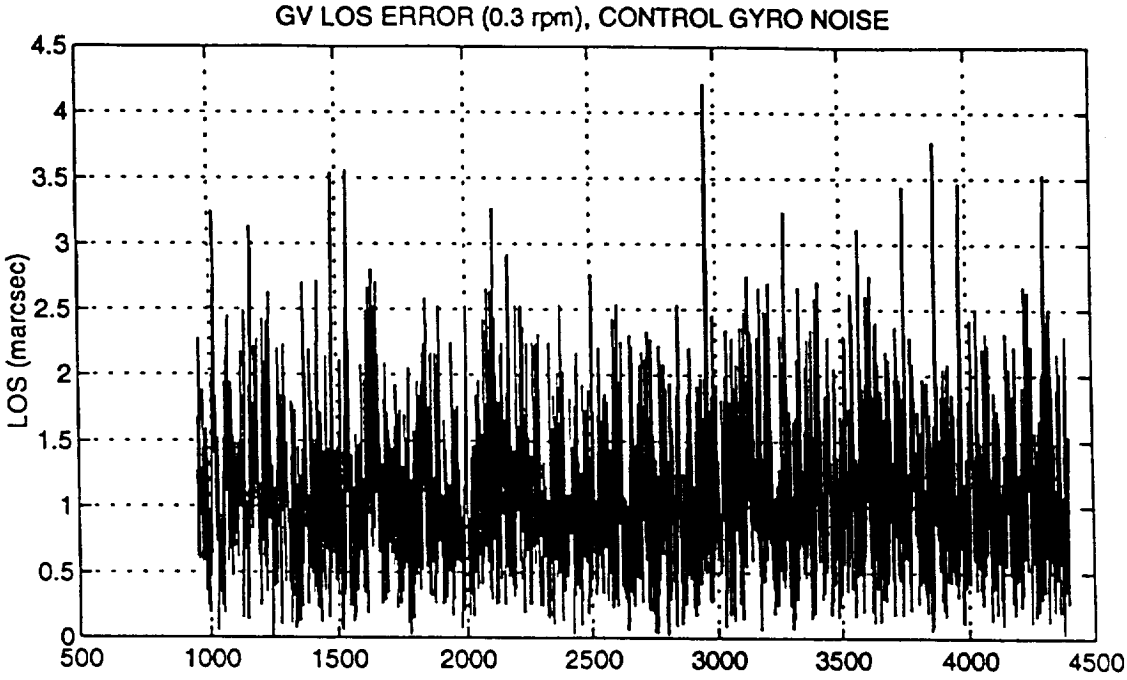

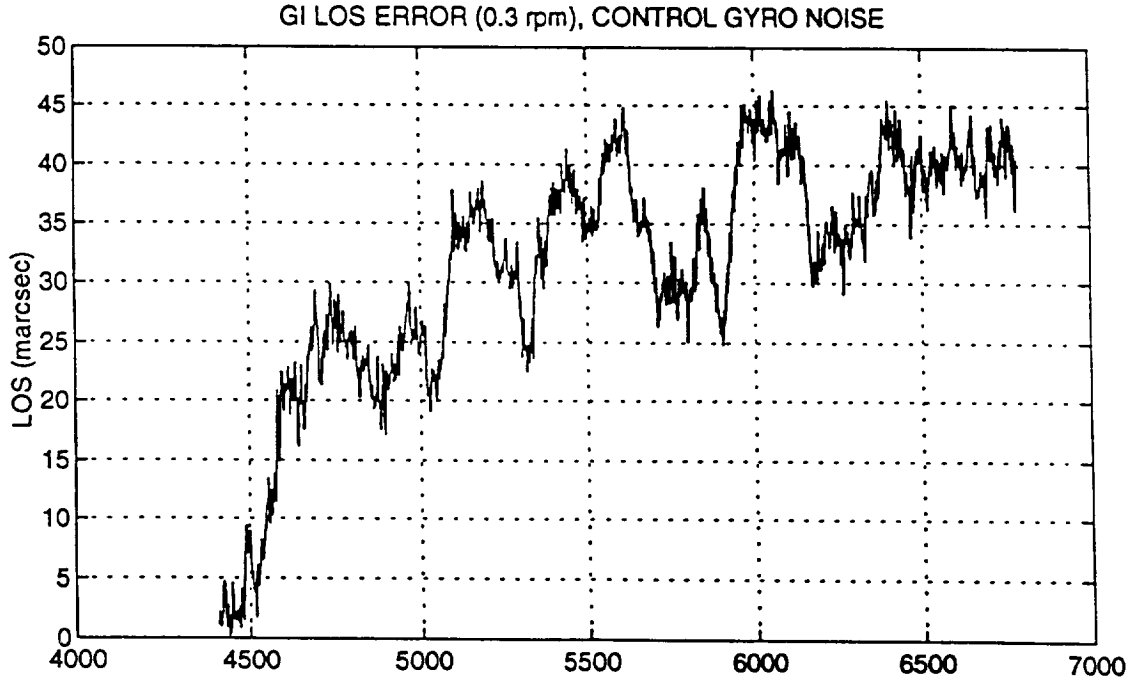

Figure 3-12 Roll and Translational Error (.3 rpm, Control Gyro Noise)

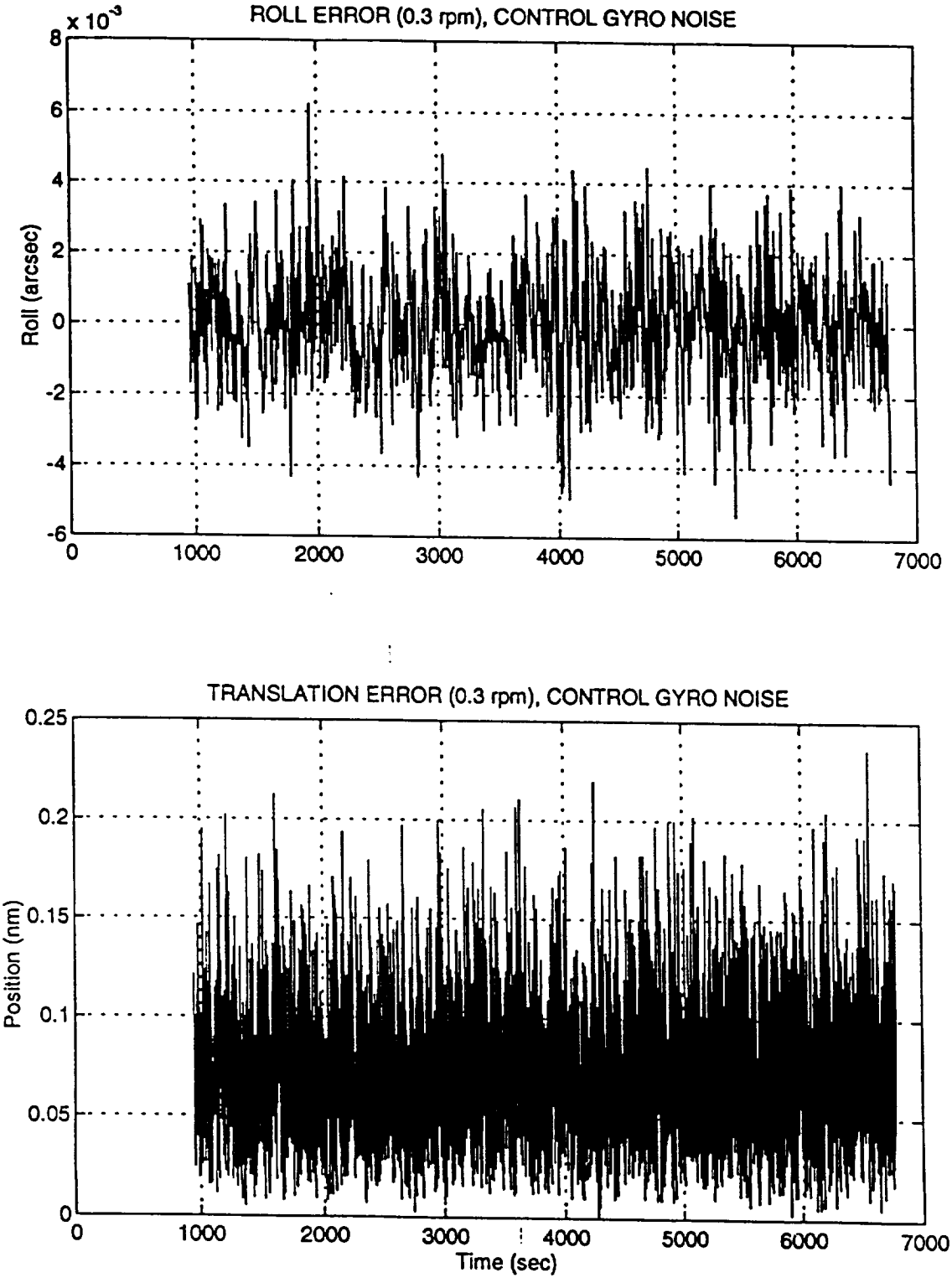

Figure 3-13 LOS Error (.3 rpm, GSV and GSI, Control Gyro Quantization)

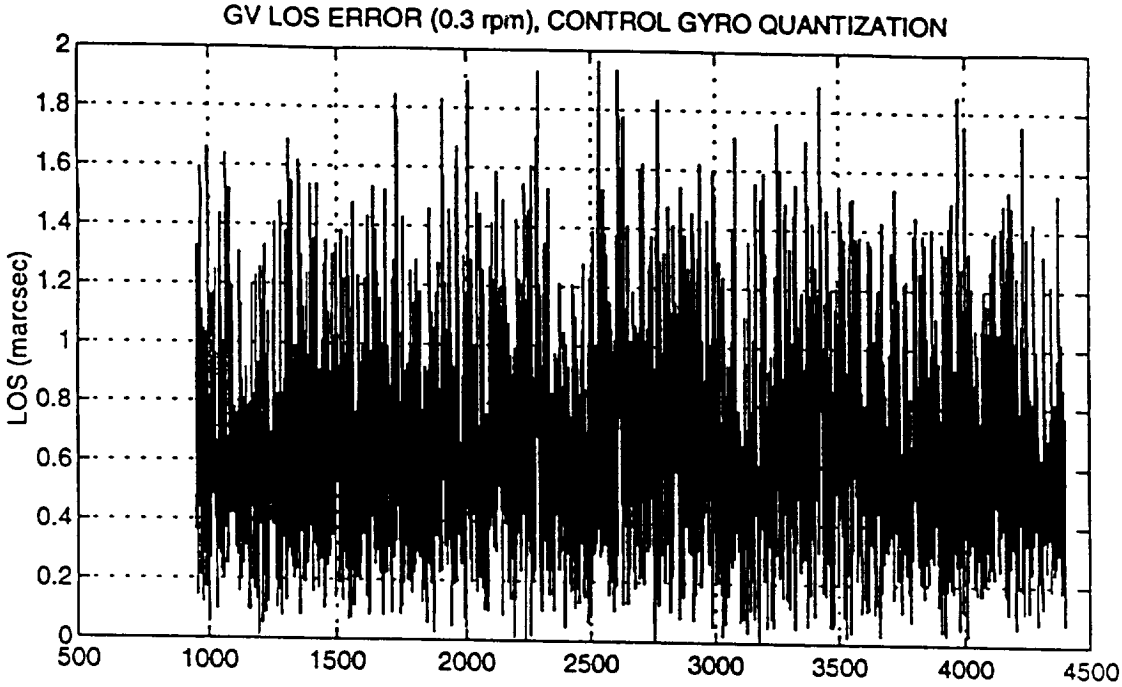

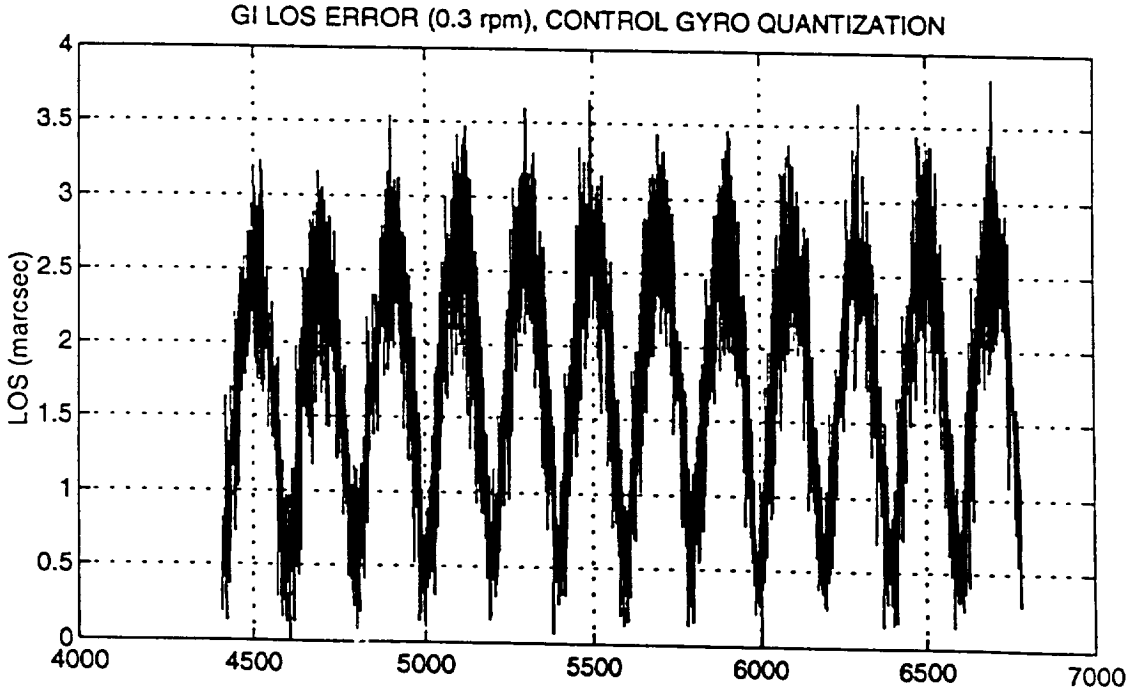

Figure 3-14 Roll and Translational Error (.3 rpm, Control Gyro Quantization)

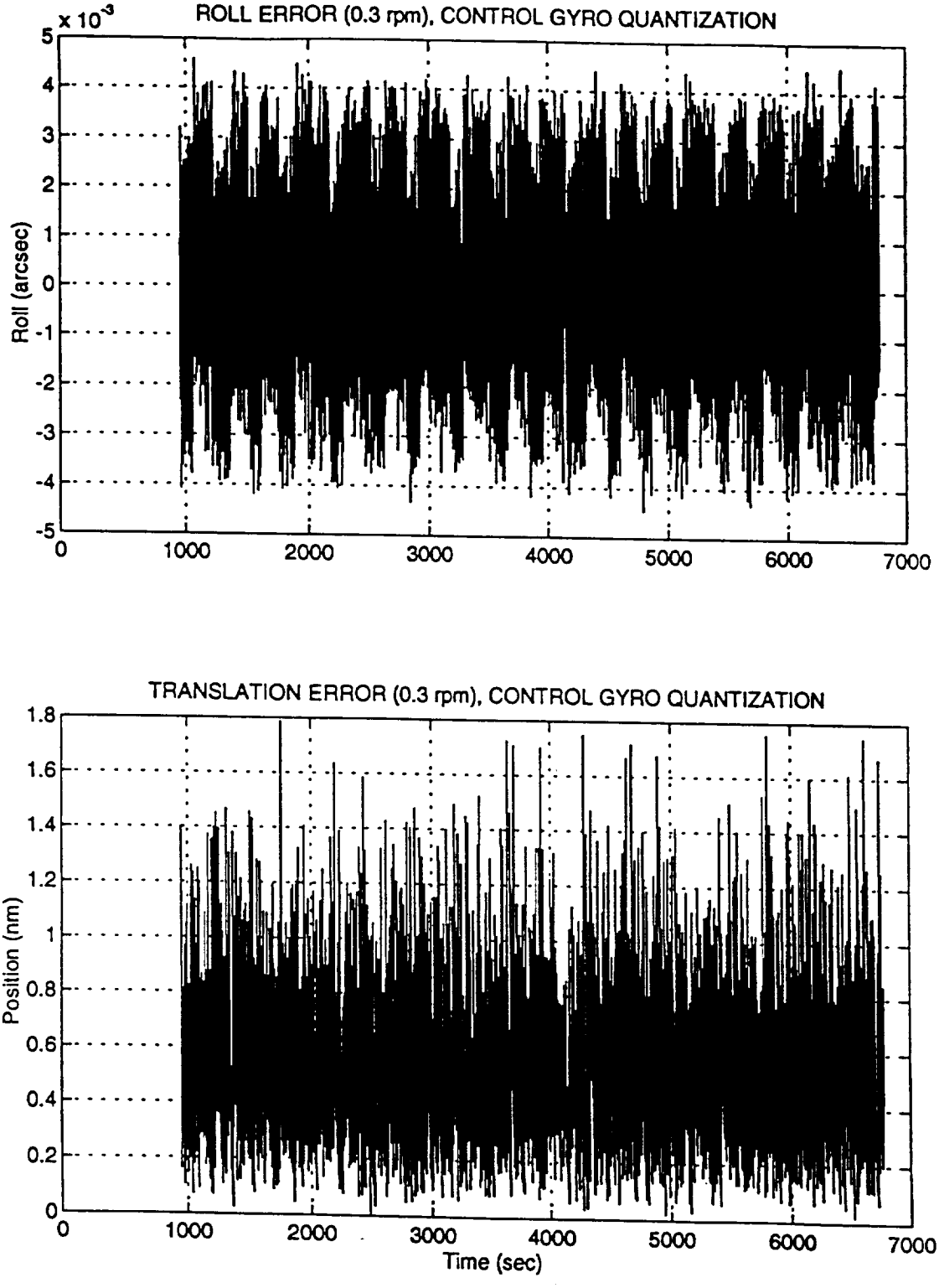

Figure 3-15 LOS Error (.3 rpm, GSV and GSI, Drag Free Sensor Noise)

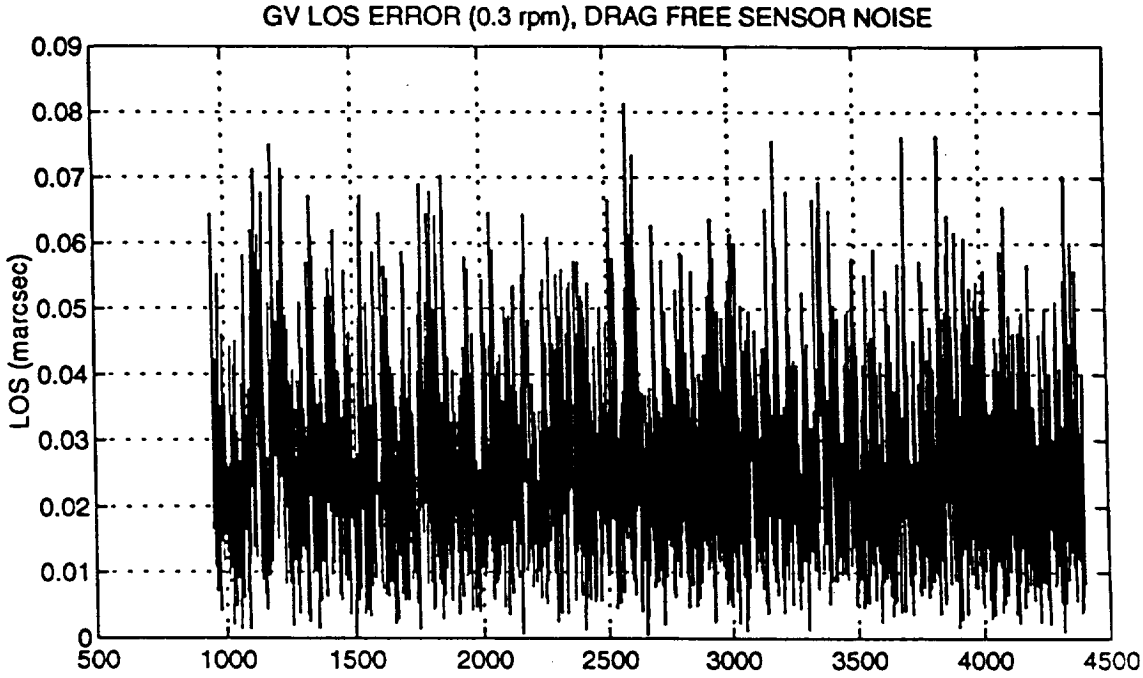

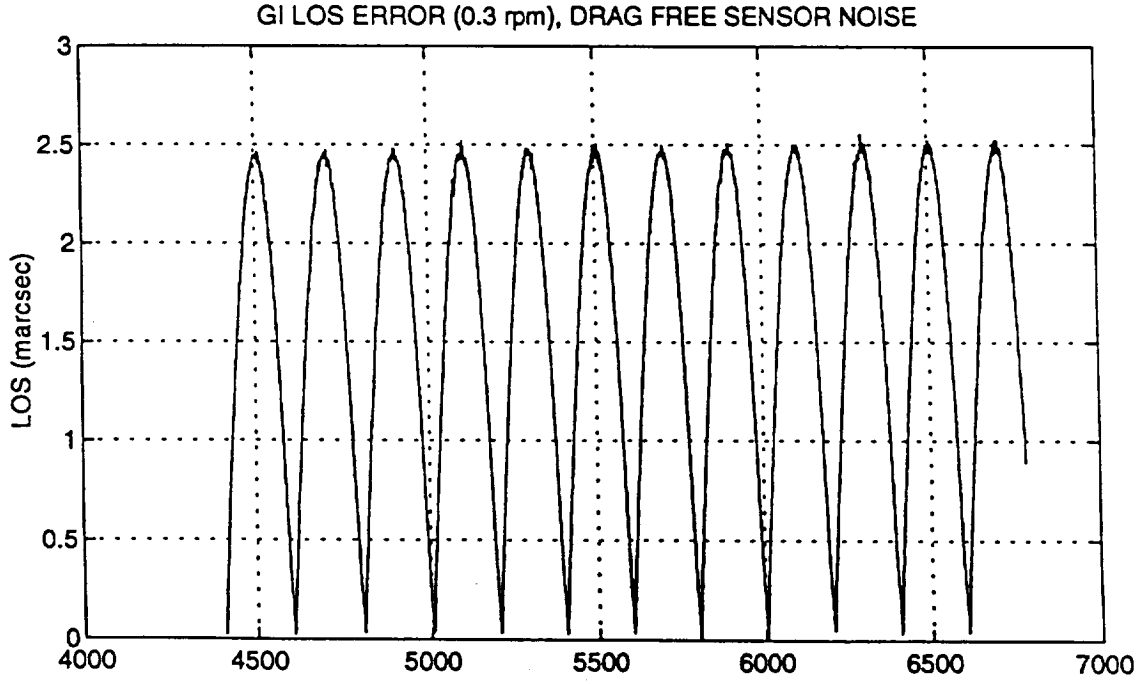

Figure 3-16 Roll and Translational Error (.3 rpm, Drag Free Sensor Noise)

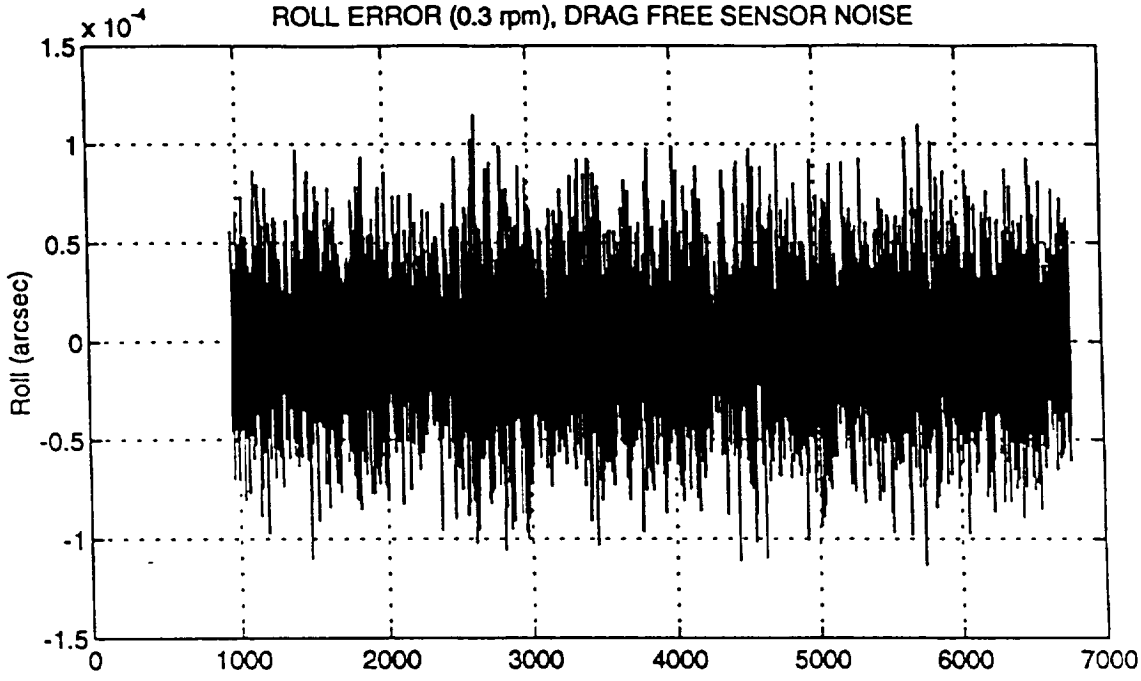

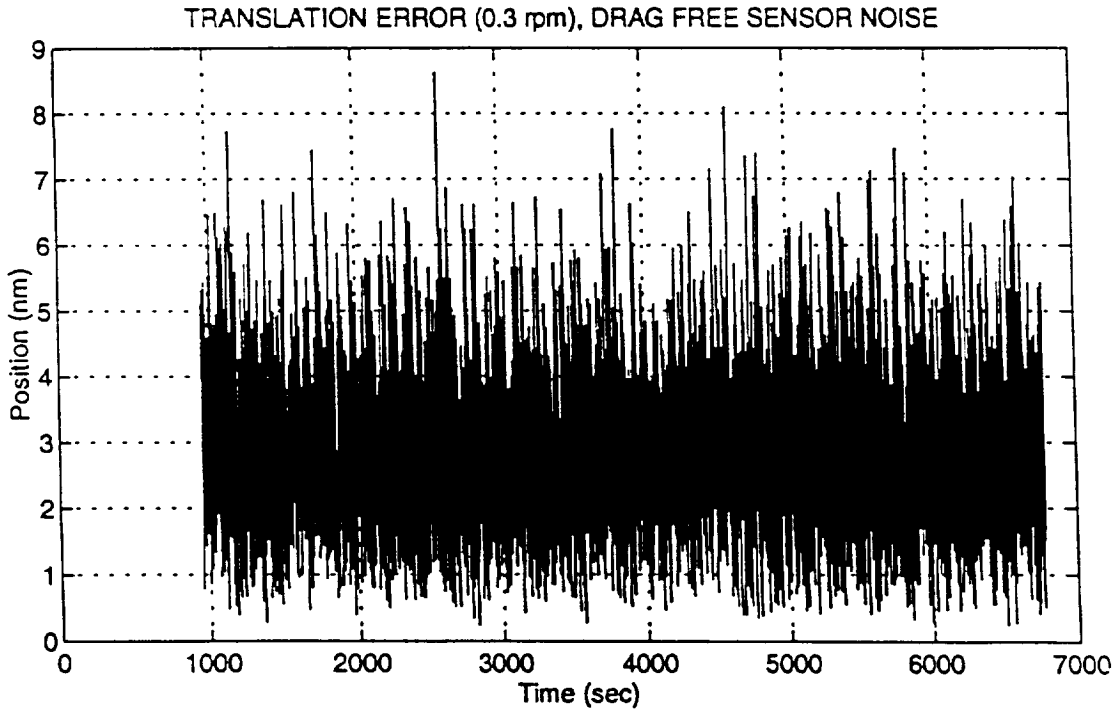

Figure 3-17 LOS Error (.3 rpm, GSV and GSI, Drag Free Sensor Quantization)

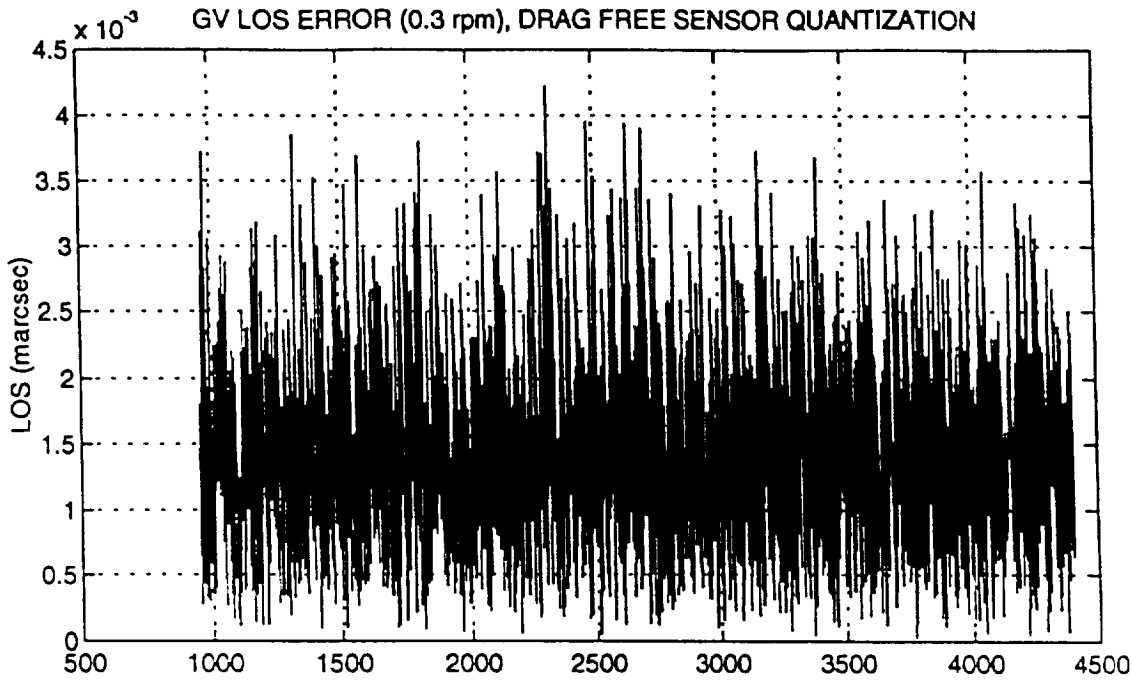

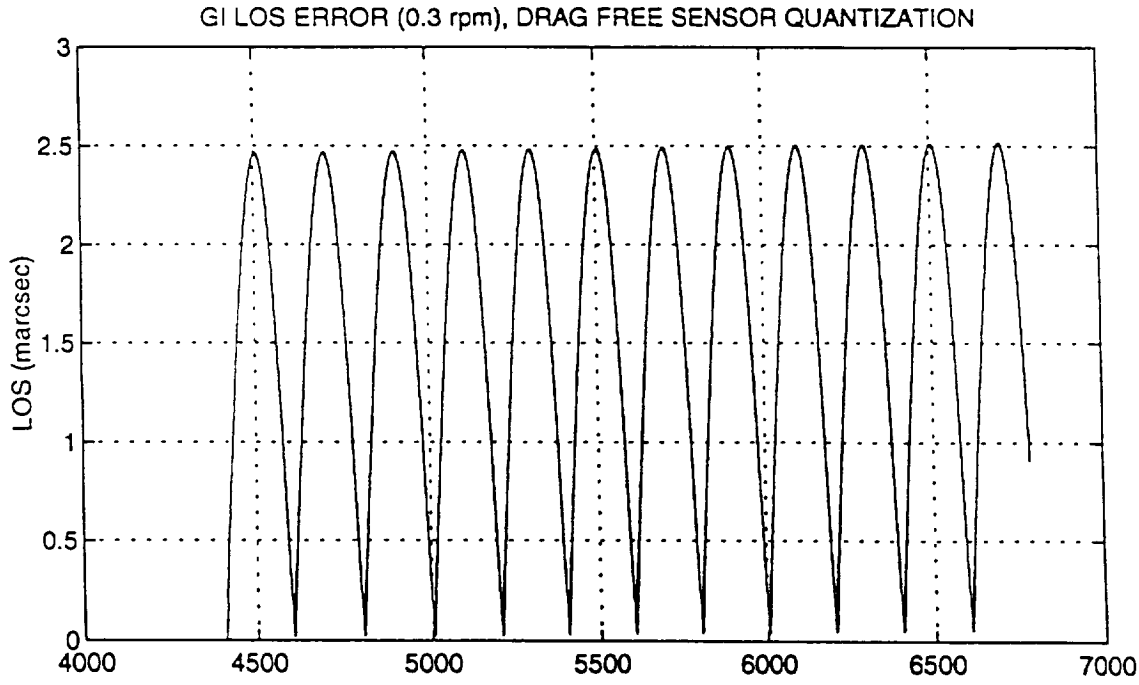

Figure 3-18 Roll and Translational Error (.3 rpm, Drag Free Sensor Quantization)

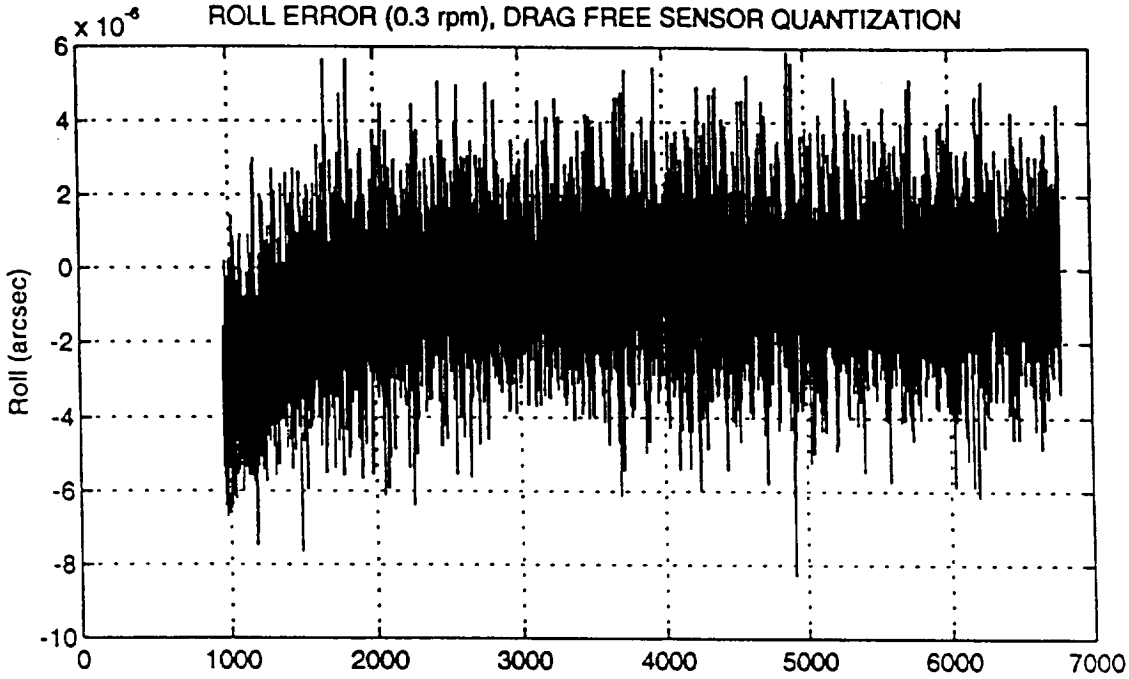

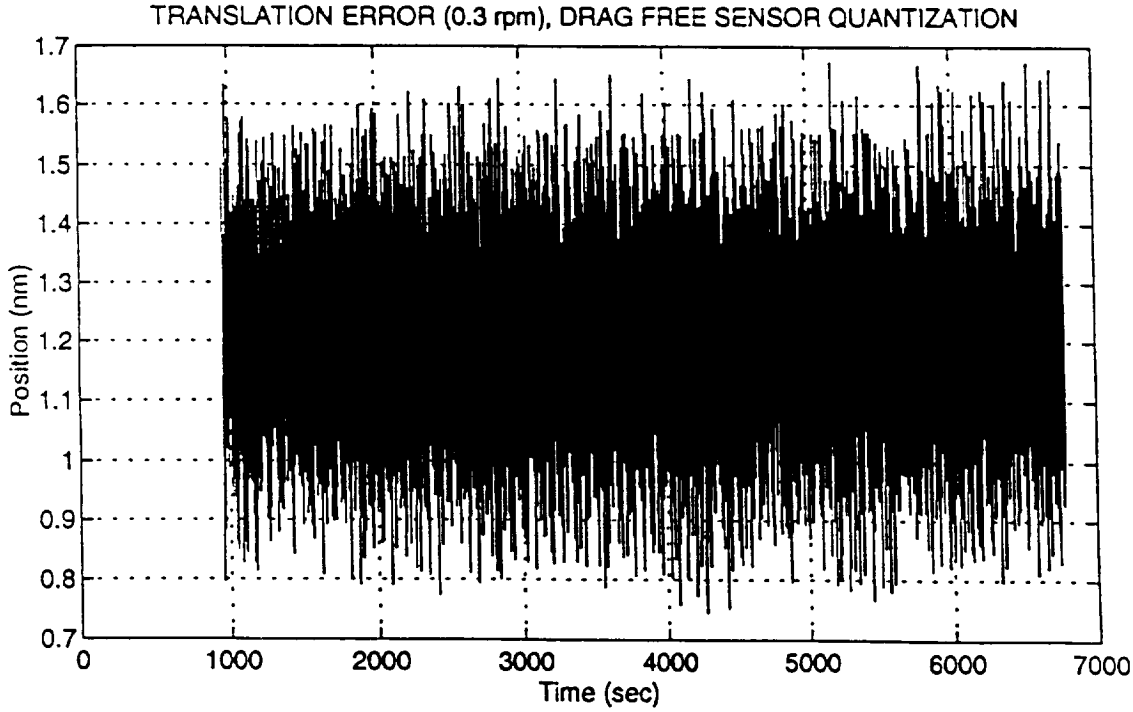

Figure 3-19 LOS Error (.3 rpm, GSV and GSI, All Disturbances and Errors)

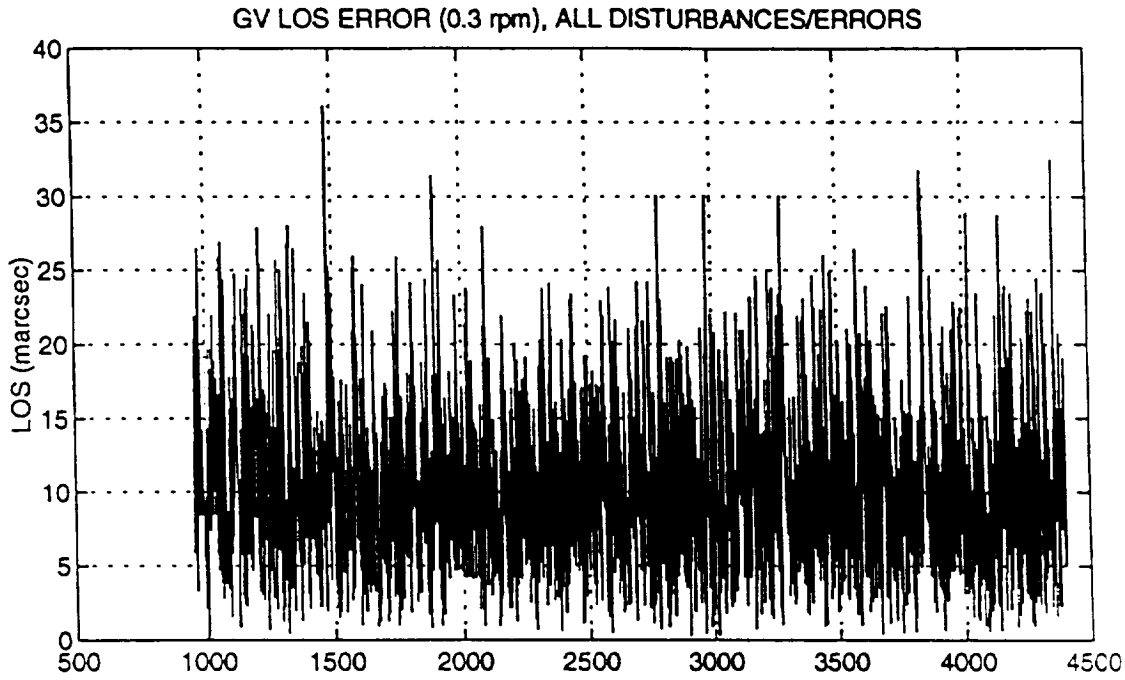

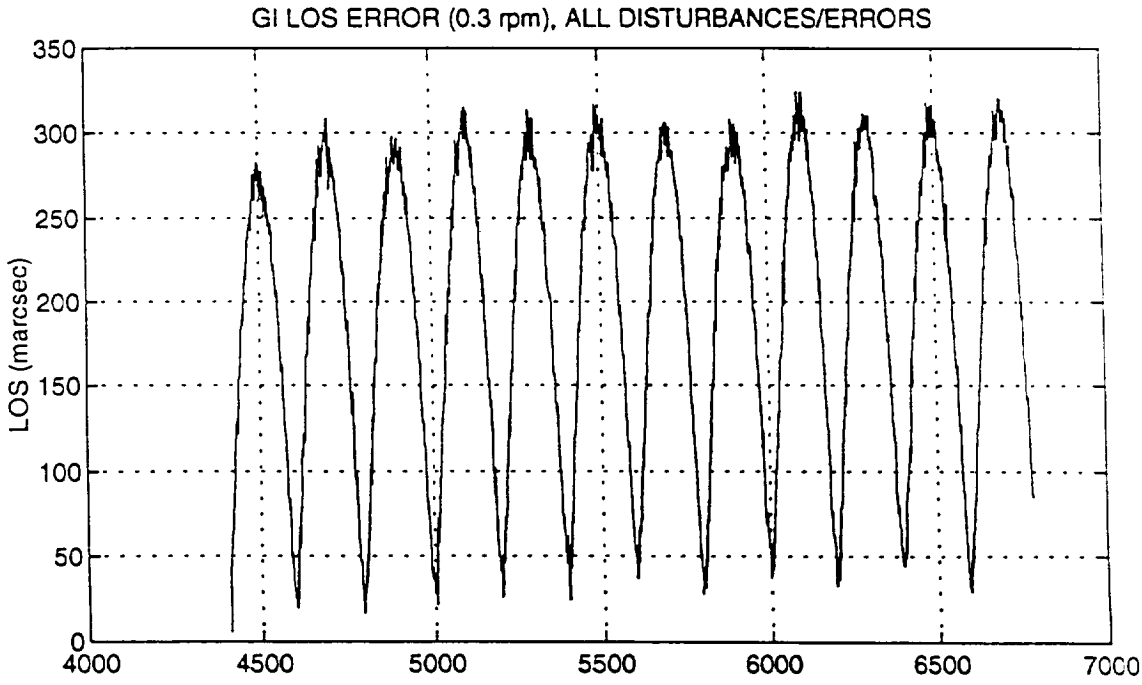

Figure 3-20 Roll and Translational Error (.3 rpm, All Disturbances and Errors)

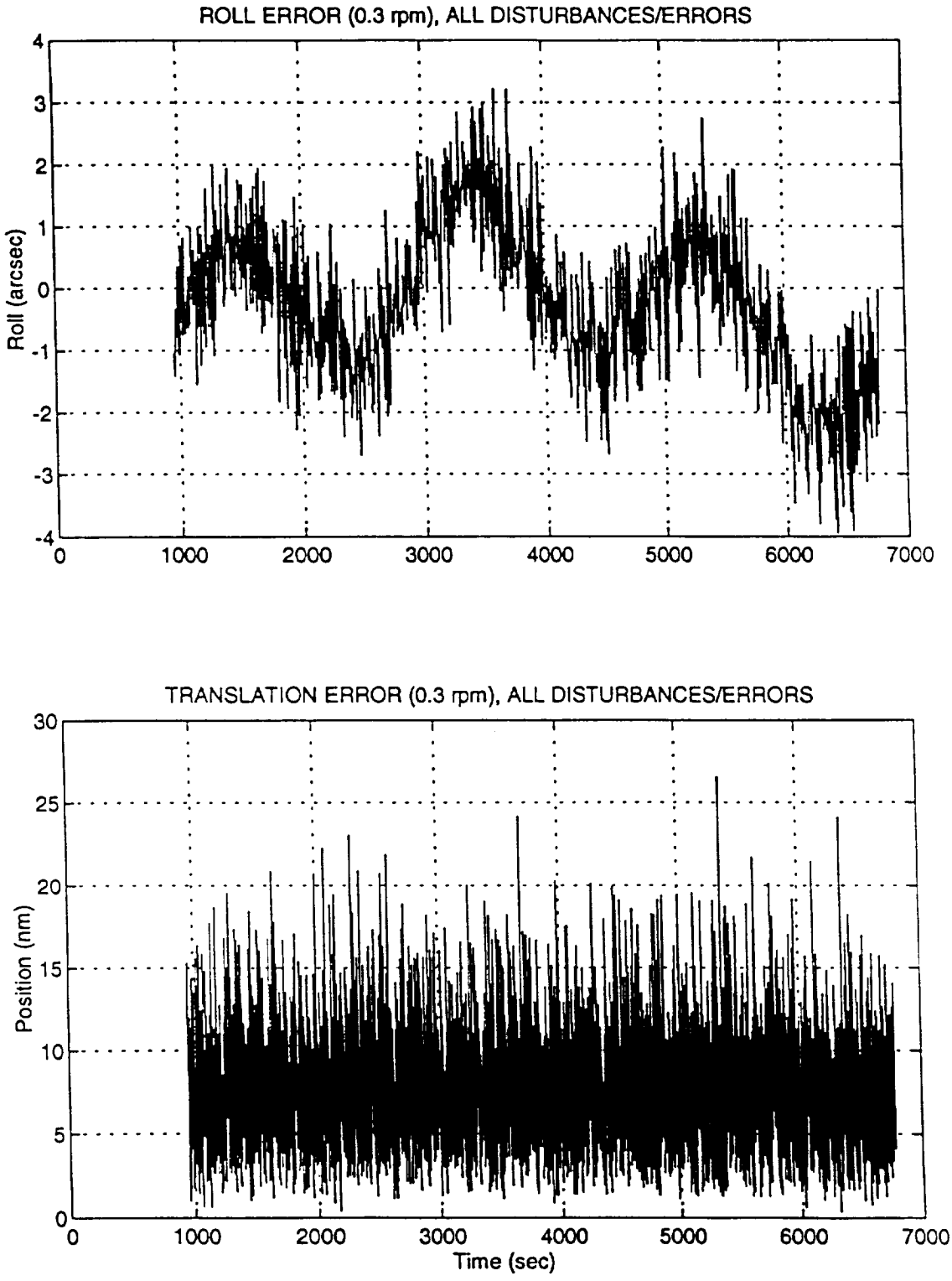

Figure 3-21 LOS Error (.5 rpm, GSV and GSI, Environmental Dist Only)

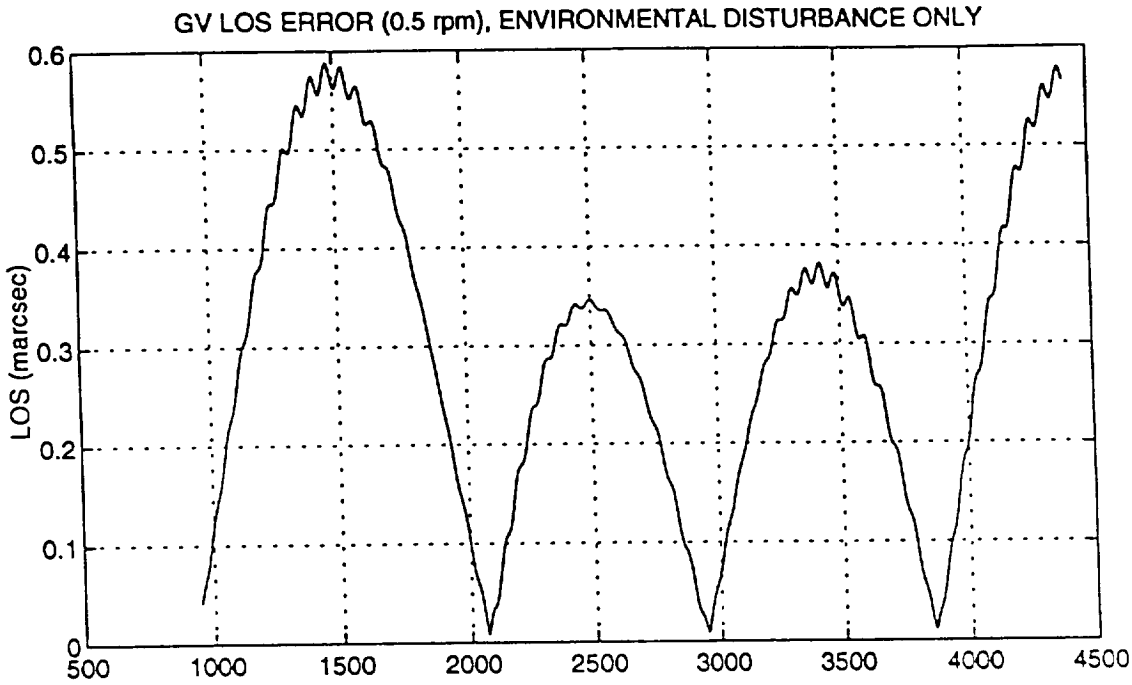

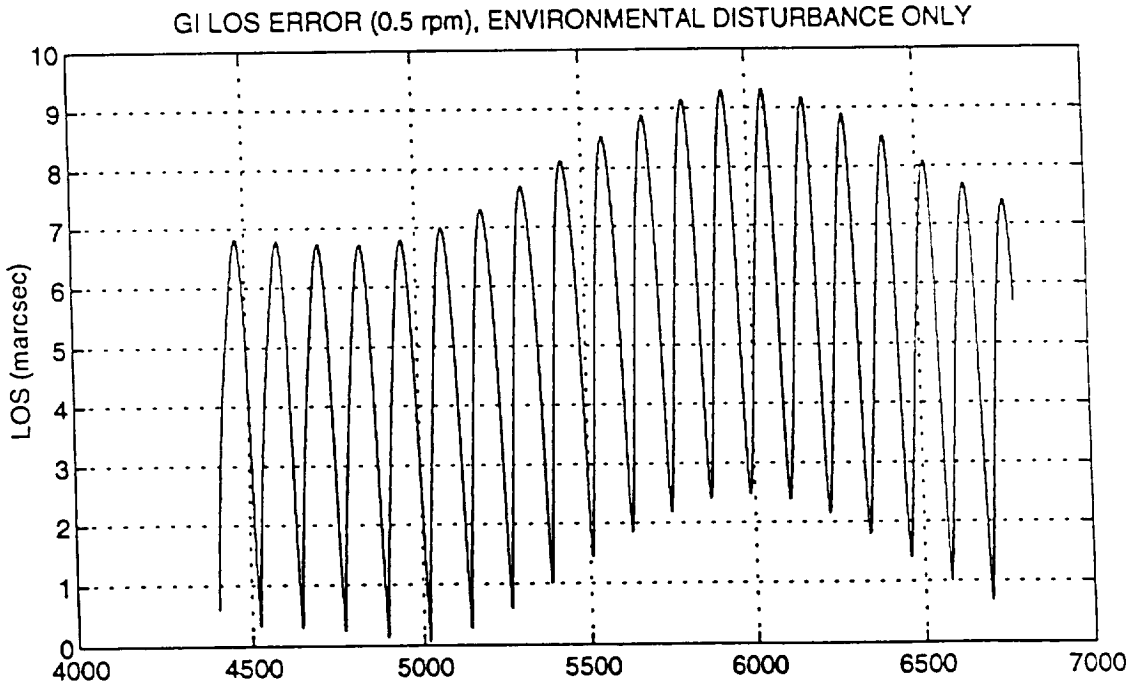

Figure 3-22 Roll and Translational Error (.5 rpm, Environmental Dist Only)

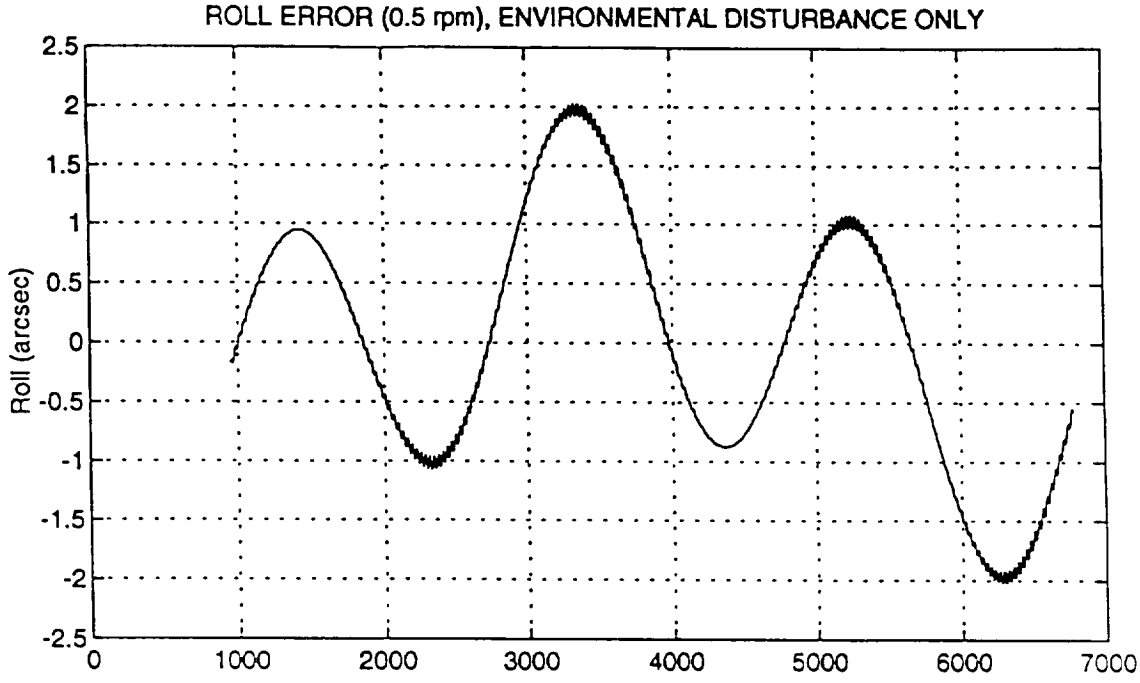

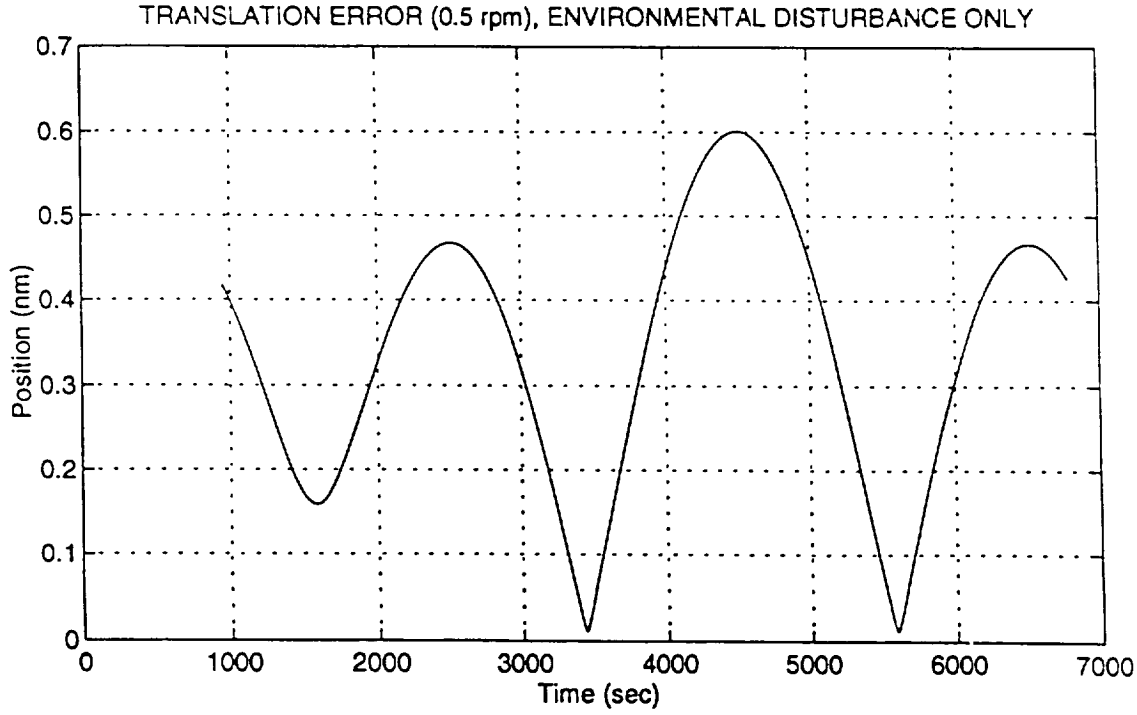

Figure 3-23 LOS Error (.5 rpm, GSV and GSI, Thruster Errors)

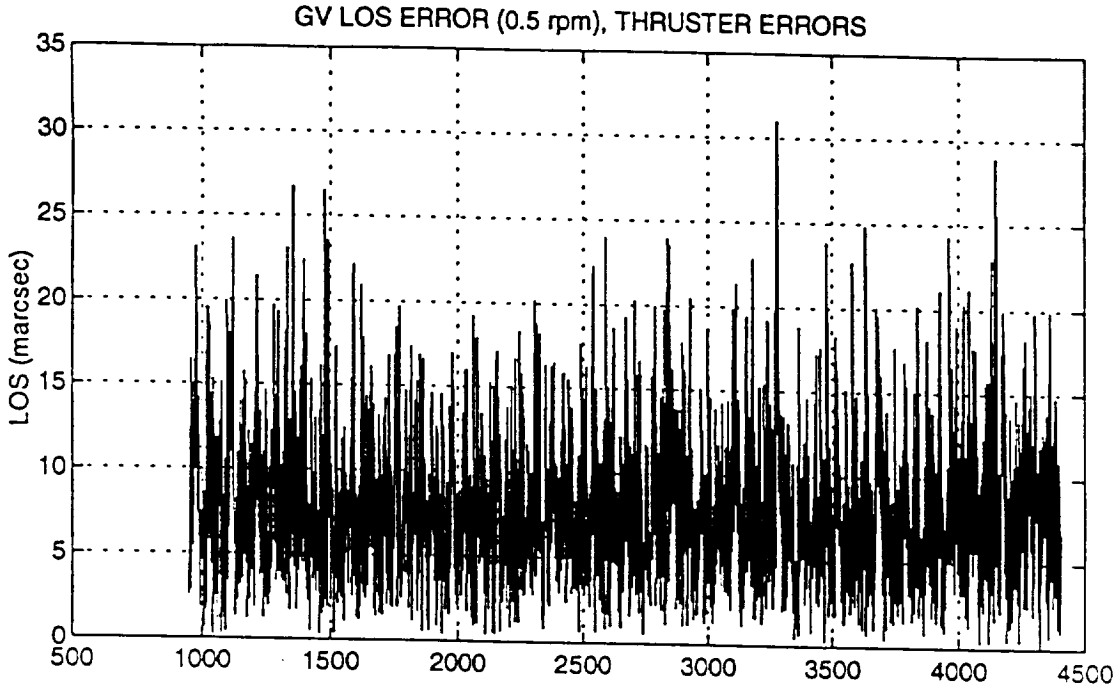

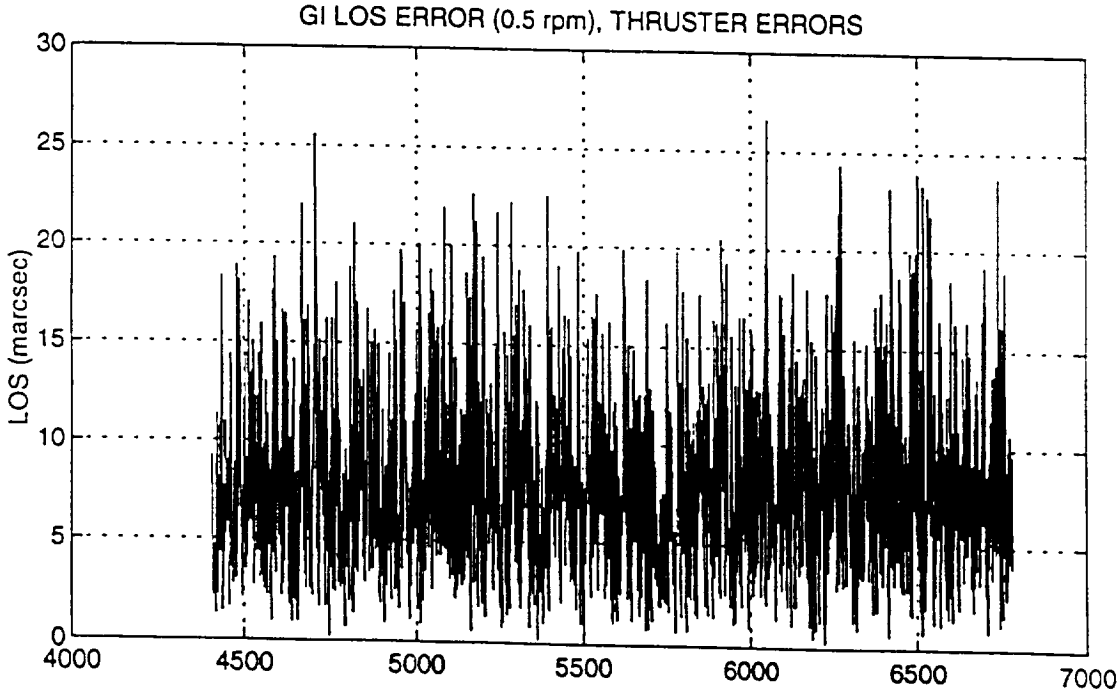

Figure 3-24 Roll and Translational Error (.5 rpm, Thruster Errors)

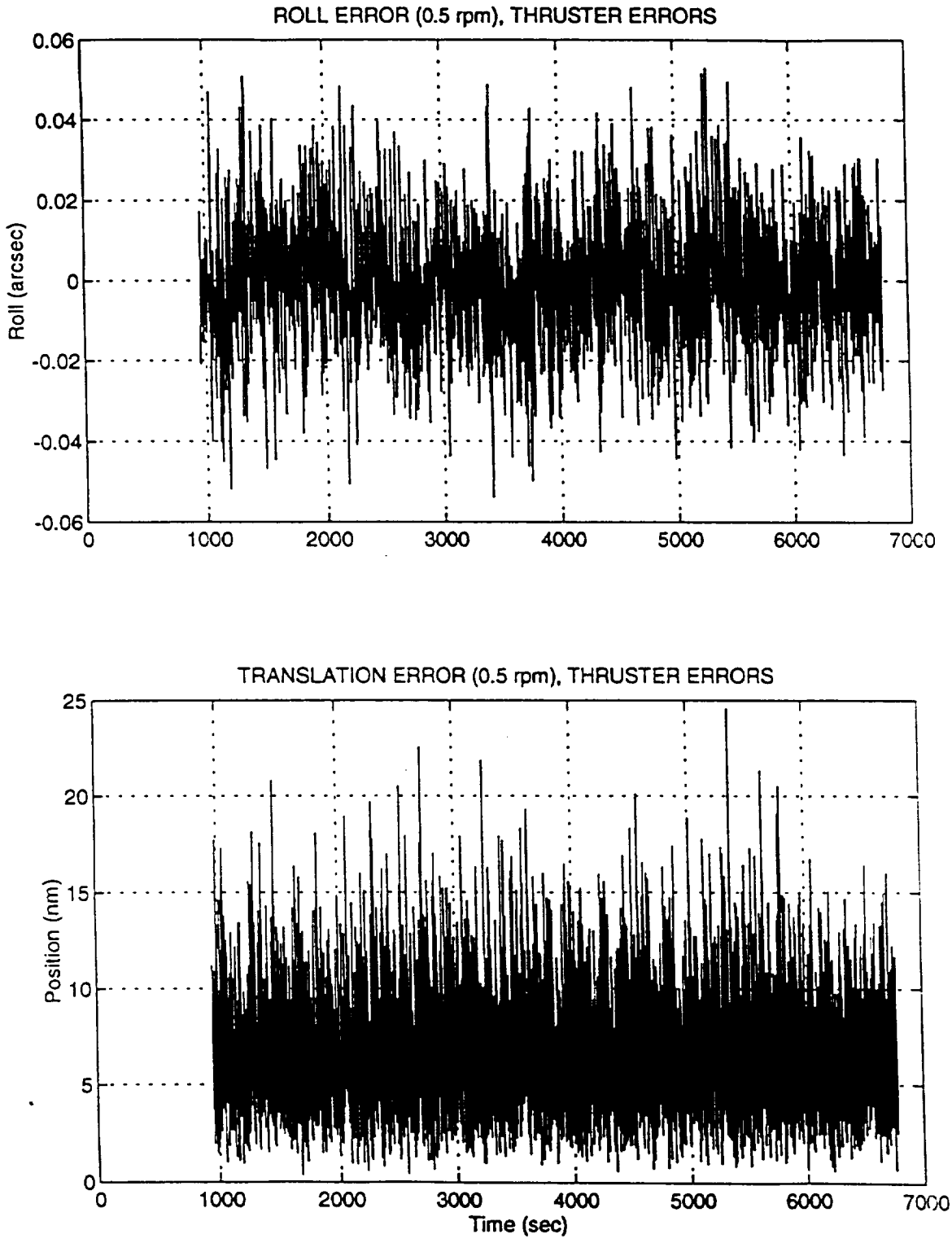

Figure 3-25 LOS Error (.5 rpm, GSV and GSI, Roll Star Tracker Noise/Quantization)

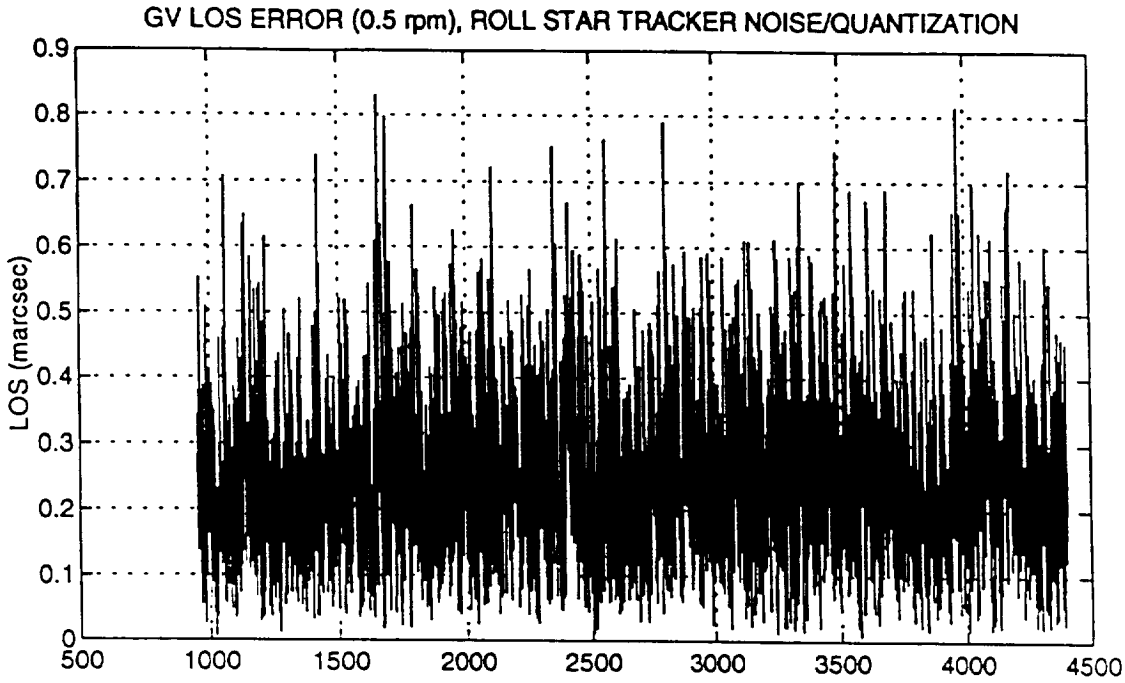

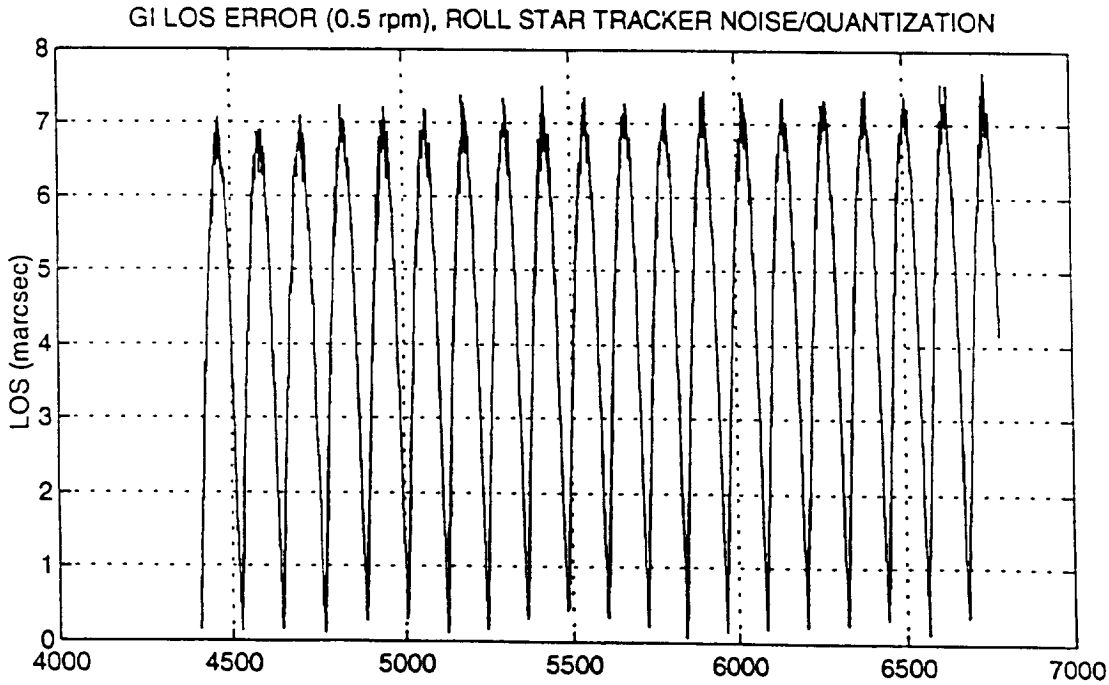

Figure 3-26 Roll and Translational Error (.5 rpm, Roll Star Tracker Noise/Quantization)

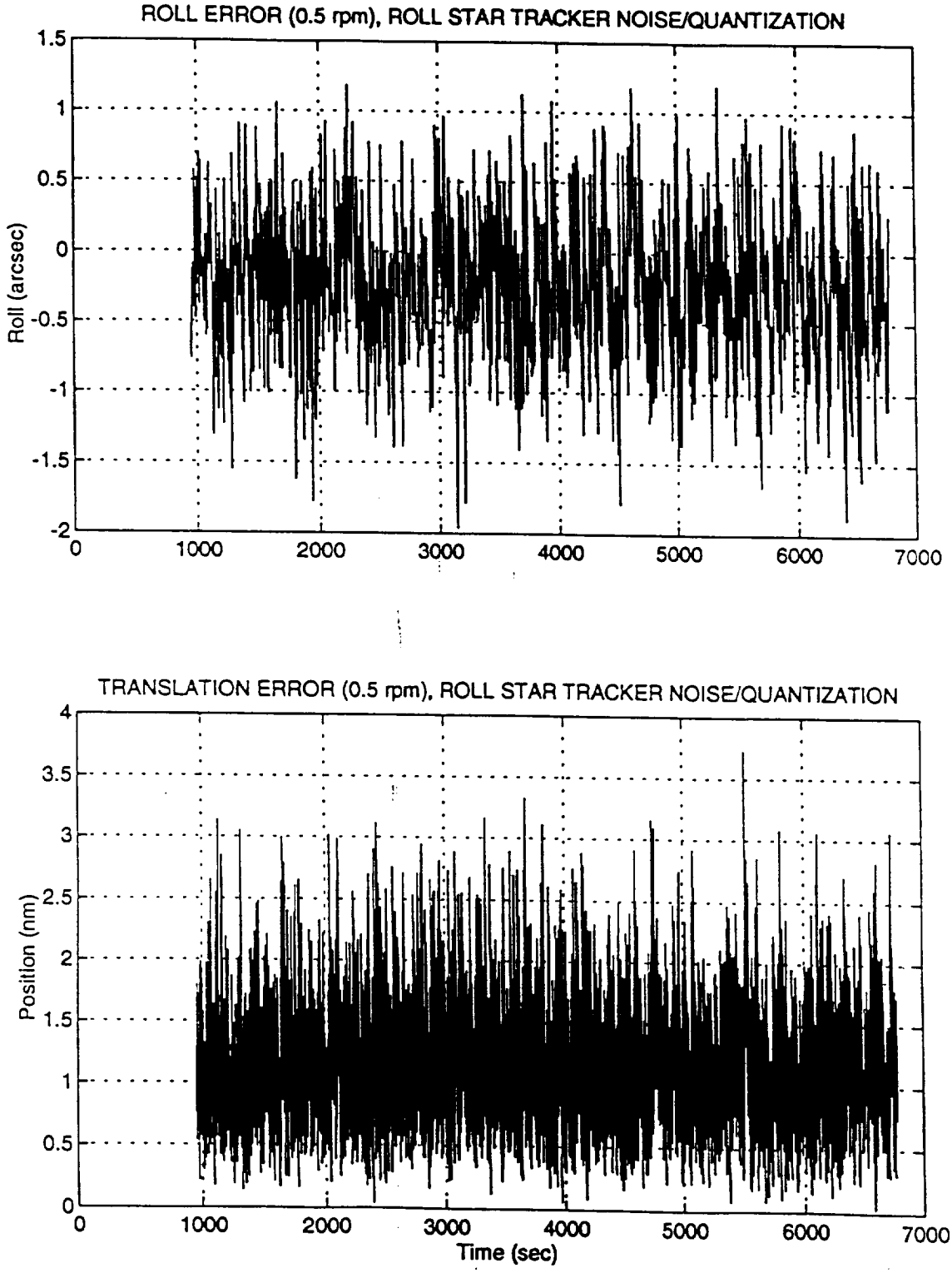

Figure 3-27 LOS Error (.5 rpm, GSV and GSI, Science Telescope Noise/Quantization)

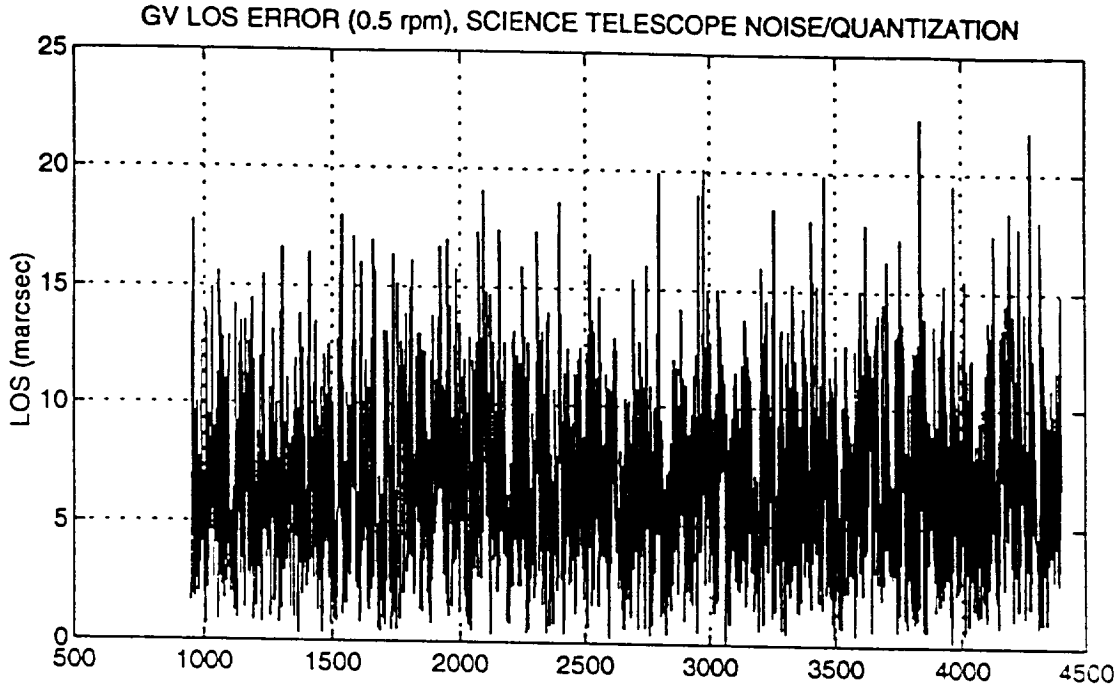

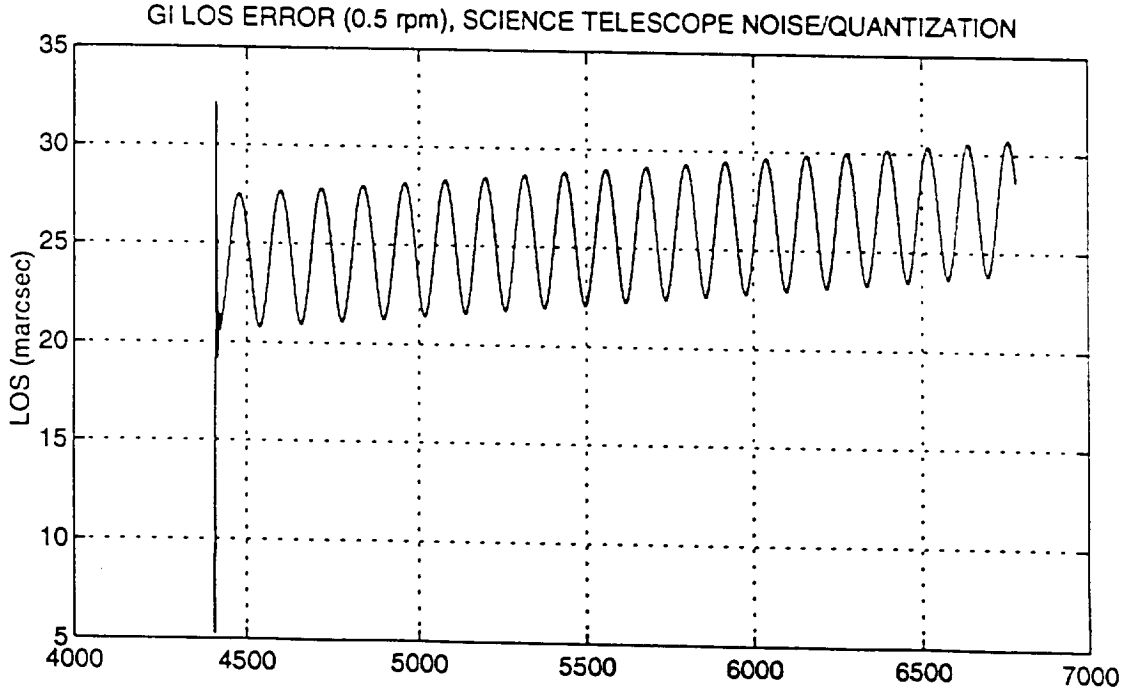

Figure 3-28 Roll and Translational Error (.5 rpm, Science Telescope Noise/Quantization)

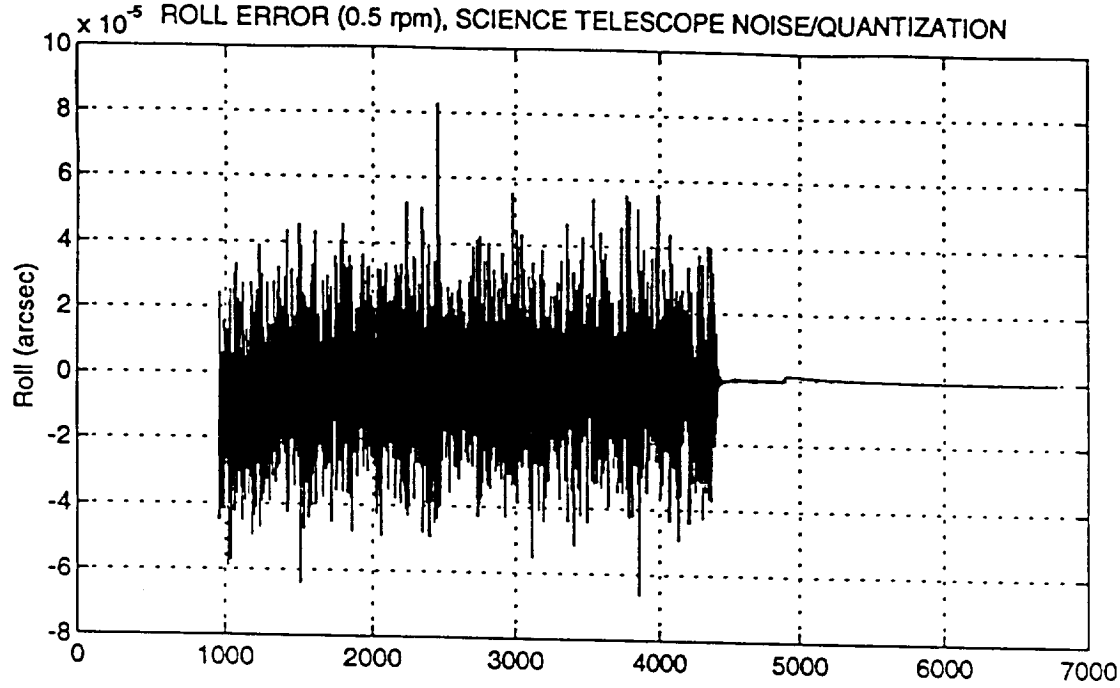

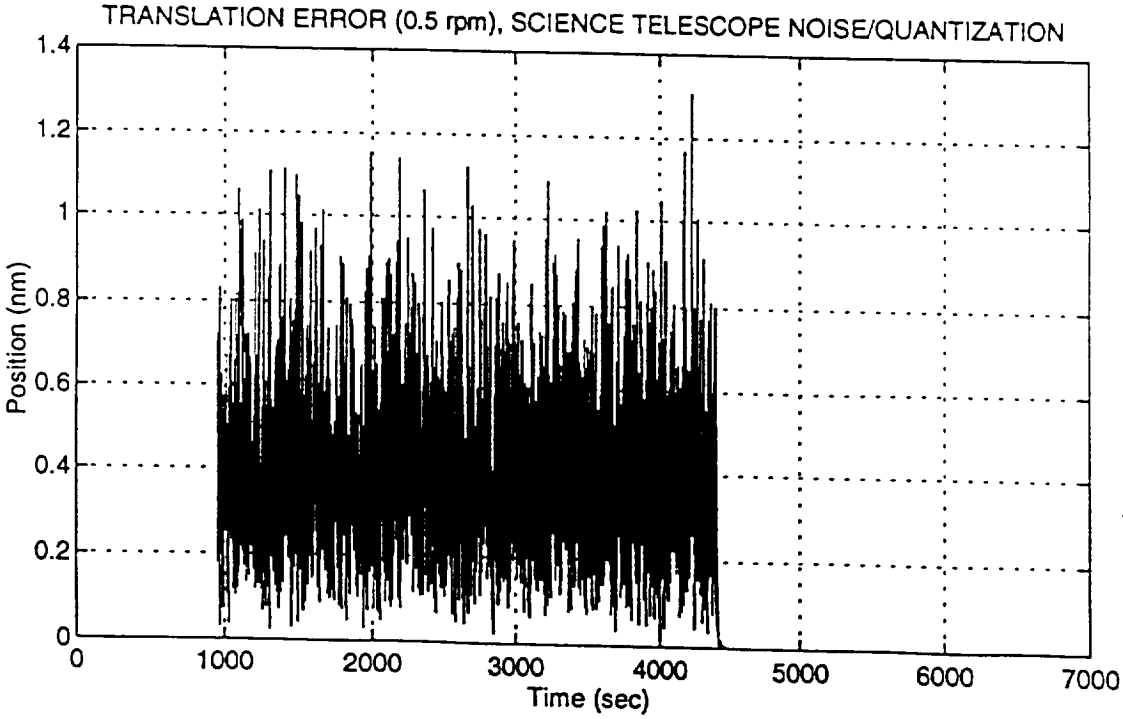

Figure 3-29 LOS Error (.5 rpm, GSV and GSI, Control Gyro Drift)

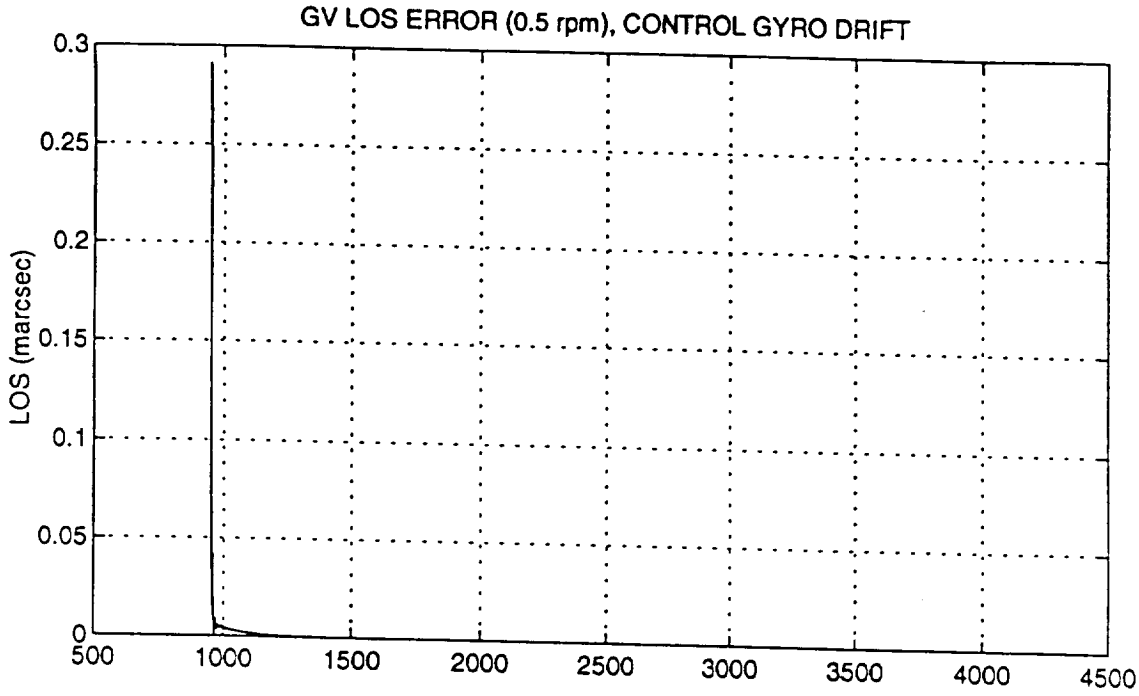

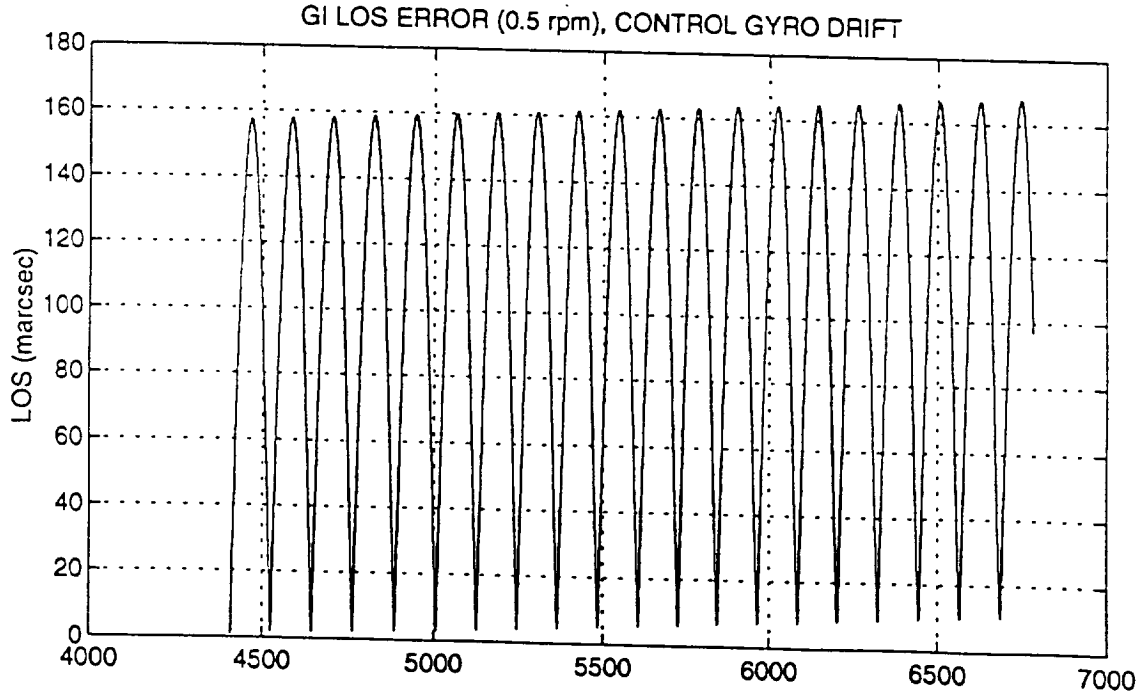

Figure 3-30 Roll and Translational Error (.5 rpm, Control Gyro Drift)

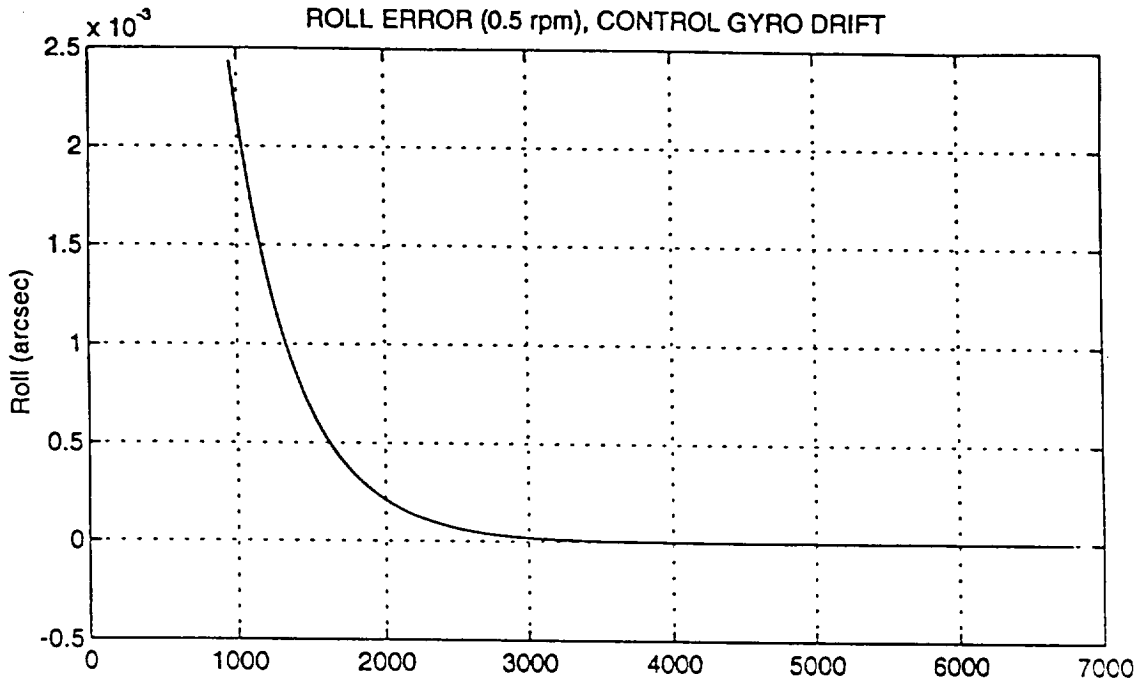

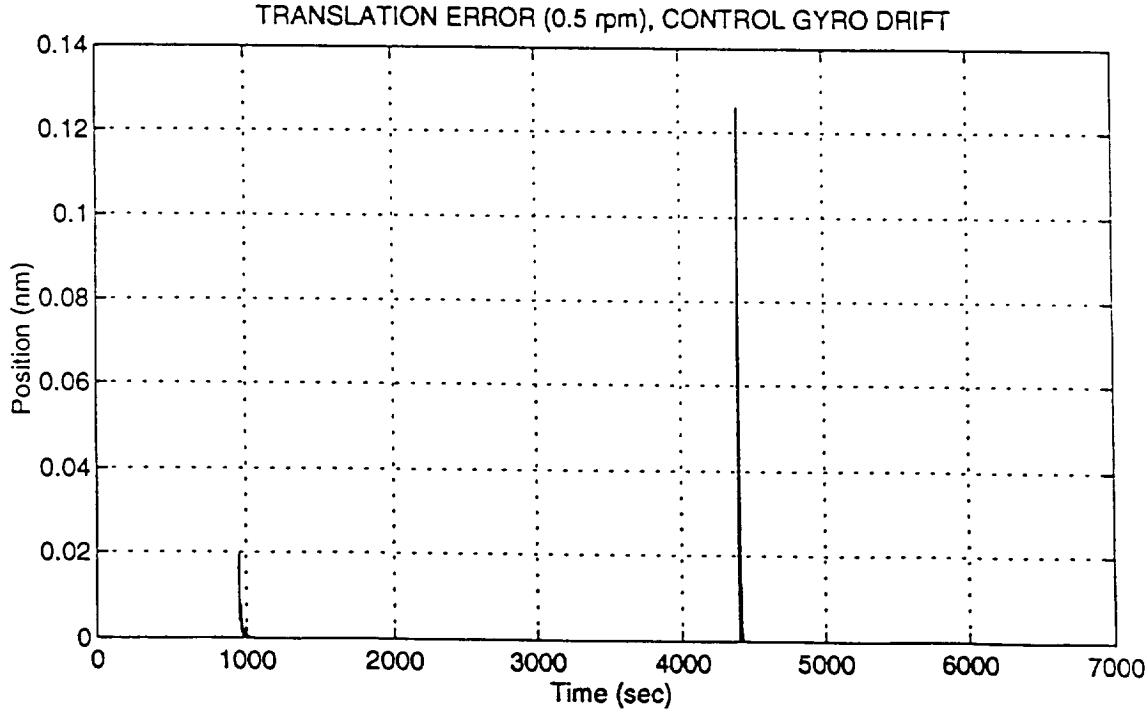

Figure 3-31 LOS Error (.5 rpm, GSV and GSI, Control Gyro Noise)

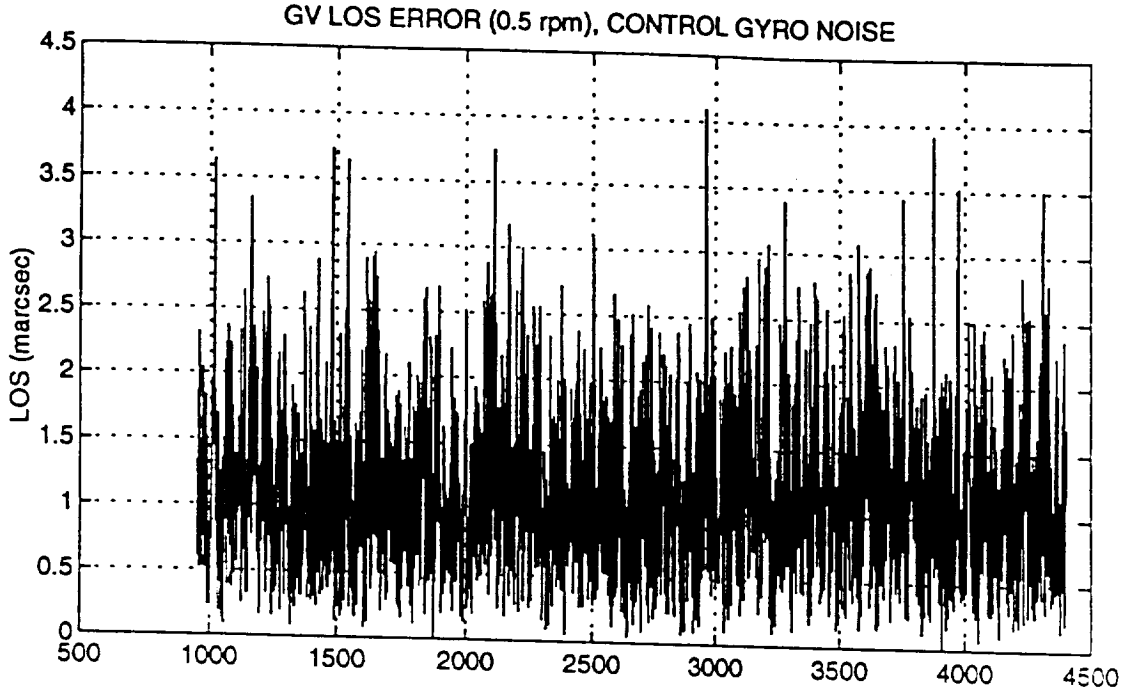

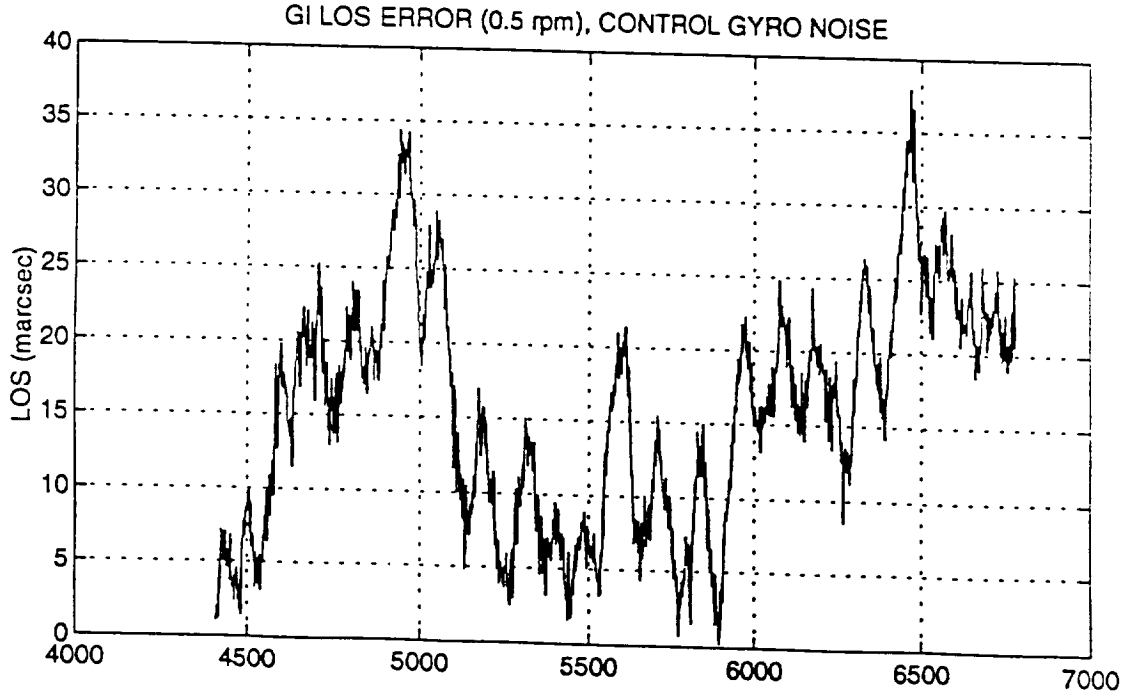

Figure 3-32 Roll and Translational Error (.5 rpm, Control Gyro Noise)

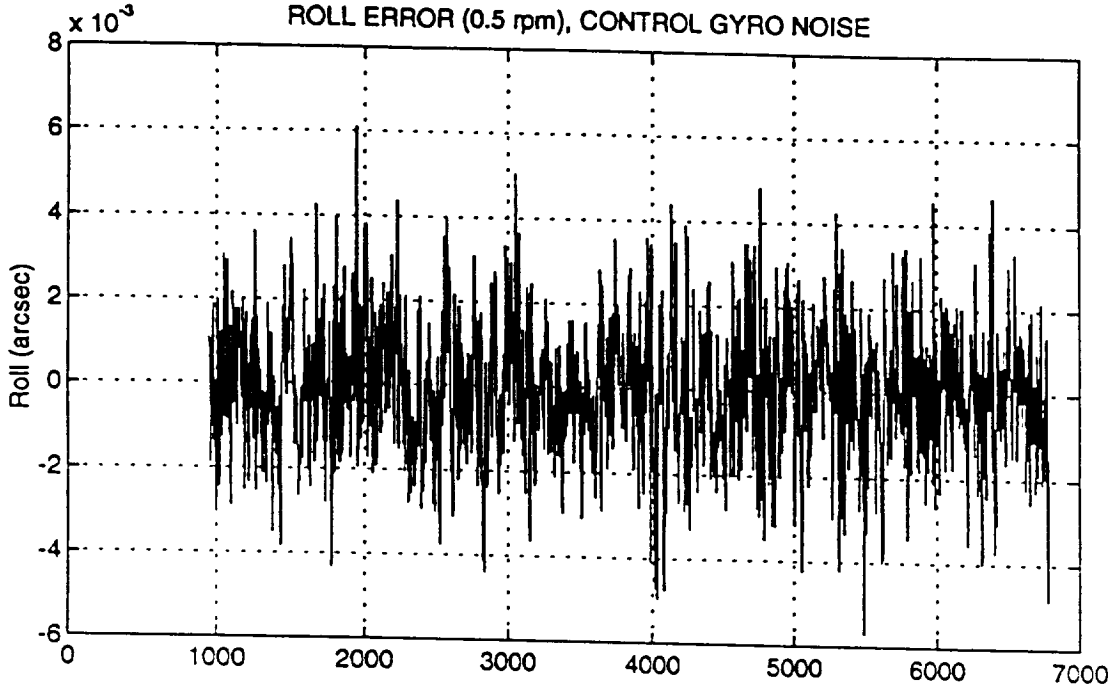

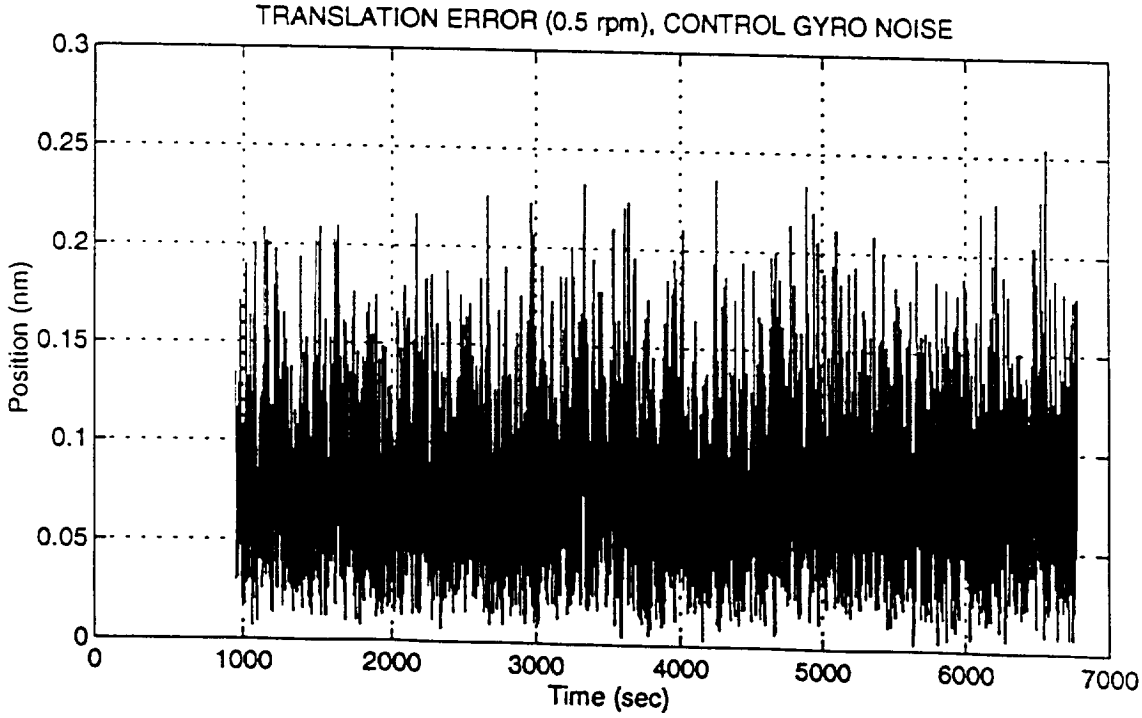

Figure 3-33 LOS Error (.5 rpm, GSV and GSI, Control Gyro Quantization)

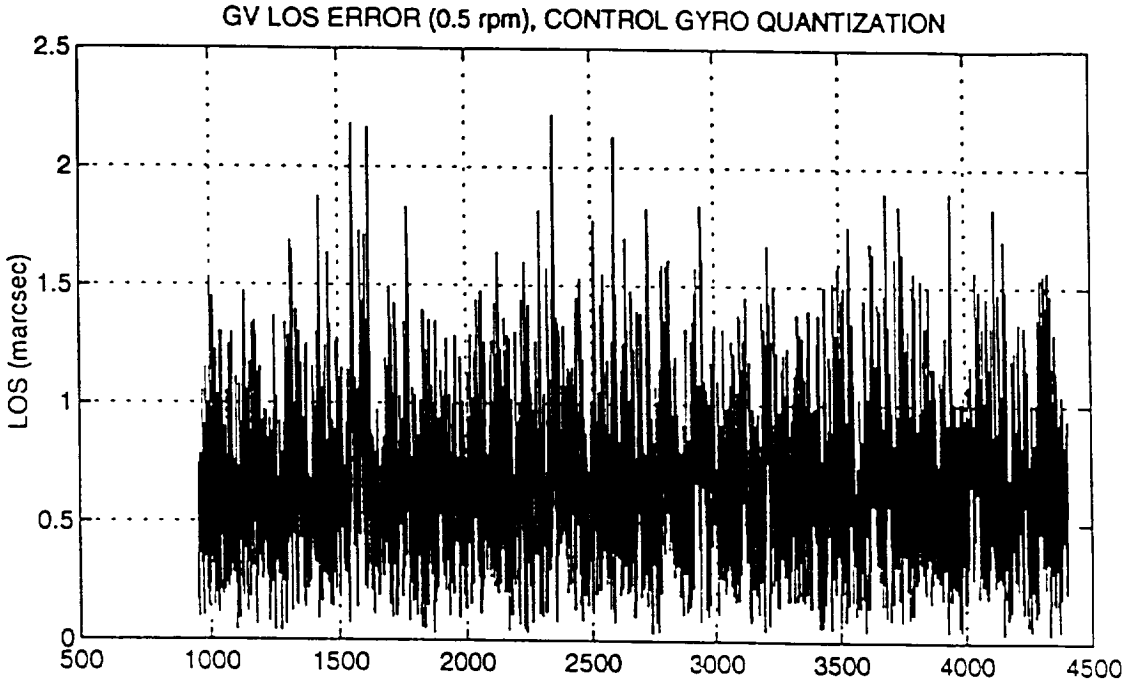

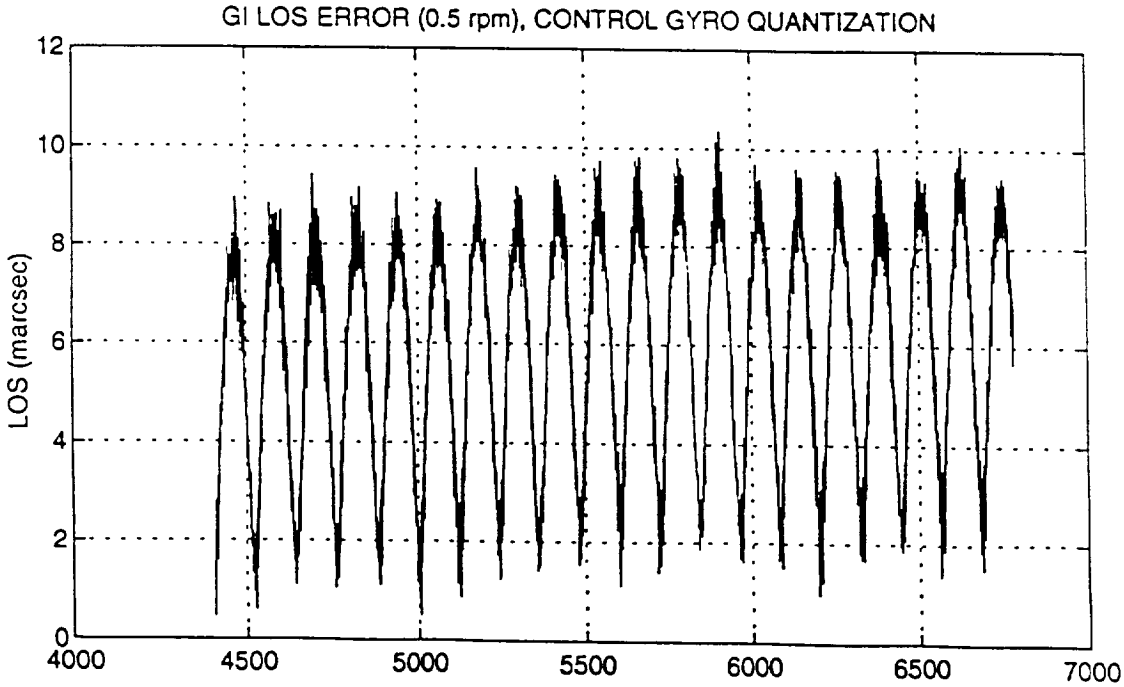

Figure 3-34 Roll and Translational Error (.5 rpm, Control Gyro Quantization)

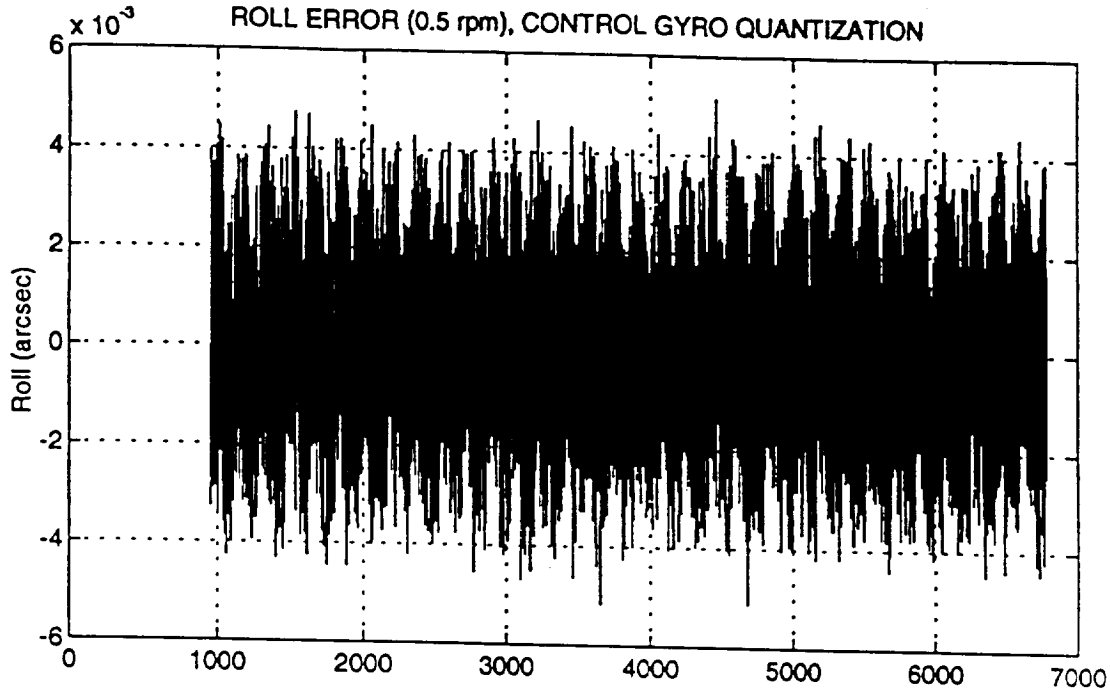

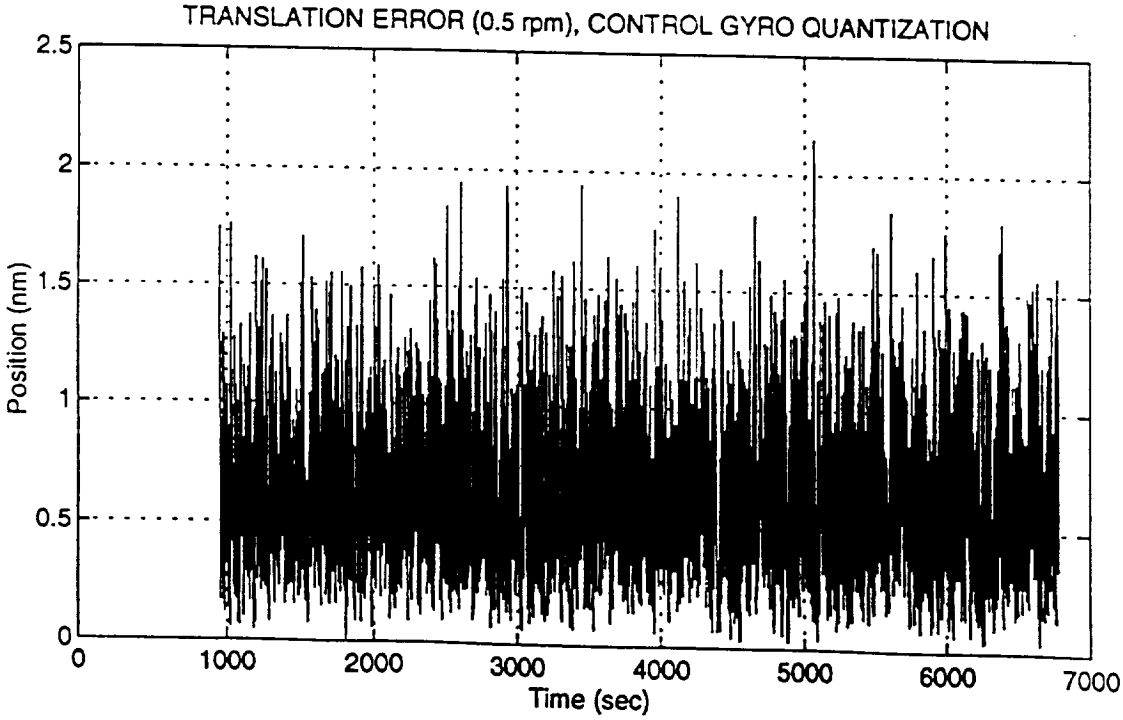

Figure 3-35 LOS Error (.5 rpm, GSV and GSI, Drag Free Sensor Noise)

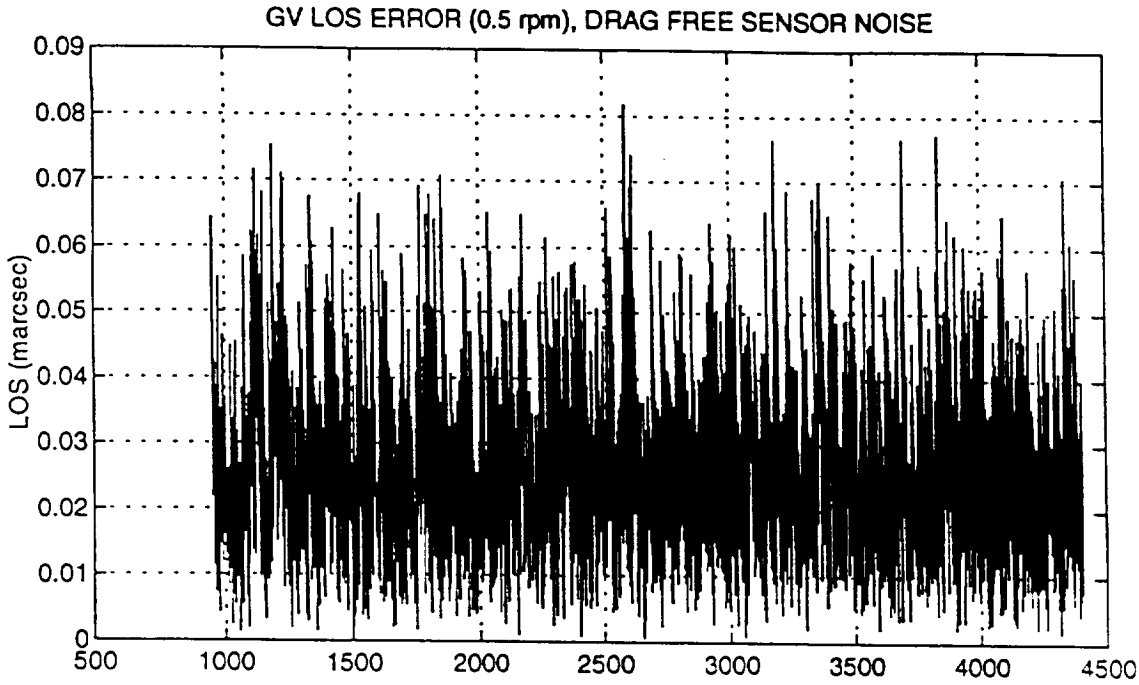

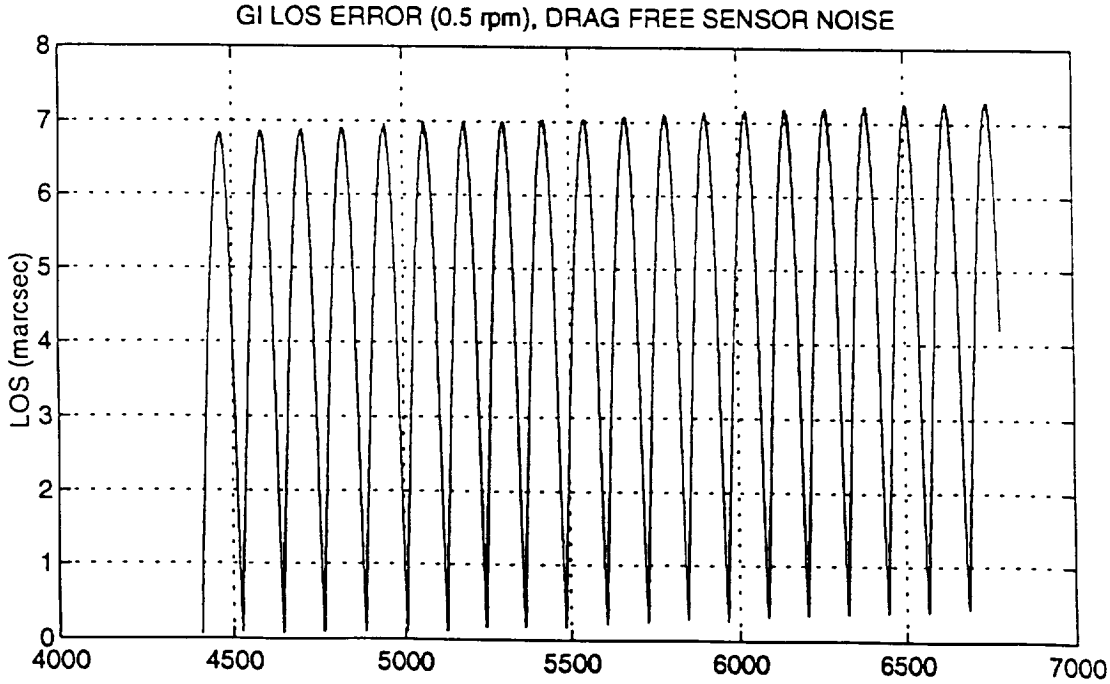

Figure 3-36 Roll and Translational Error (.5 rpm, Drag Free Sensor Noise)

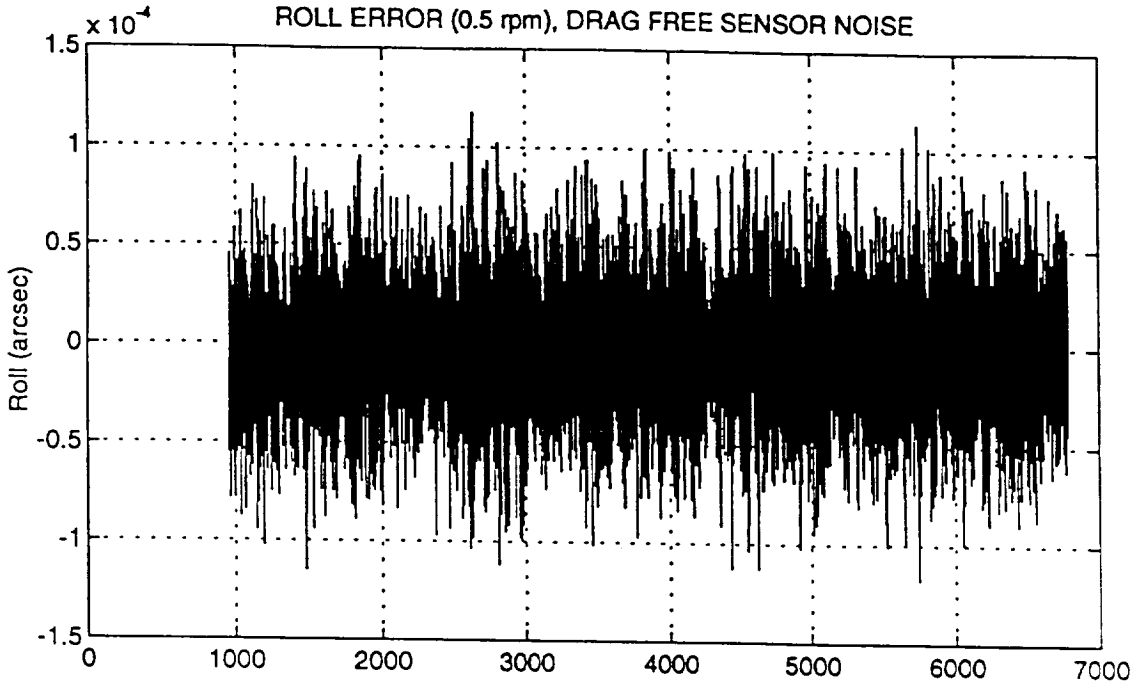

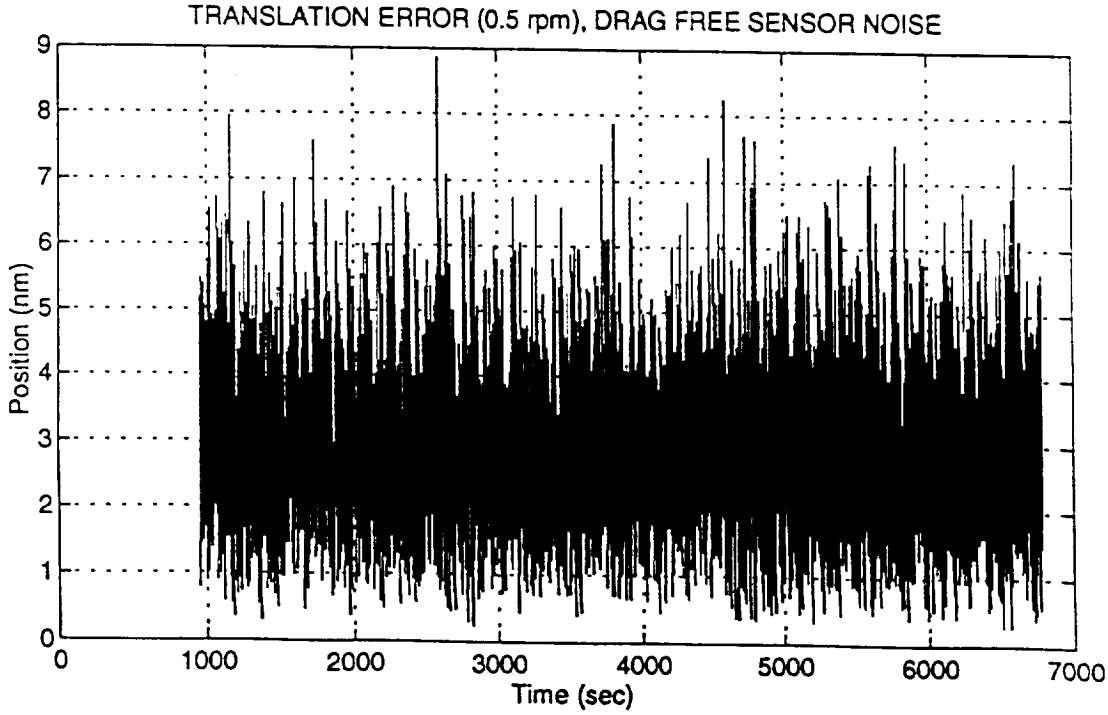

Figure 3-37 LOS Error (.5 rpm, GSV and GSI, Drag Free Sensor Quantization)

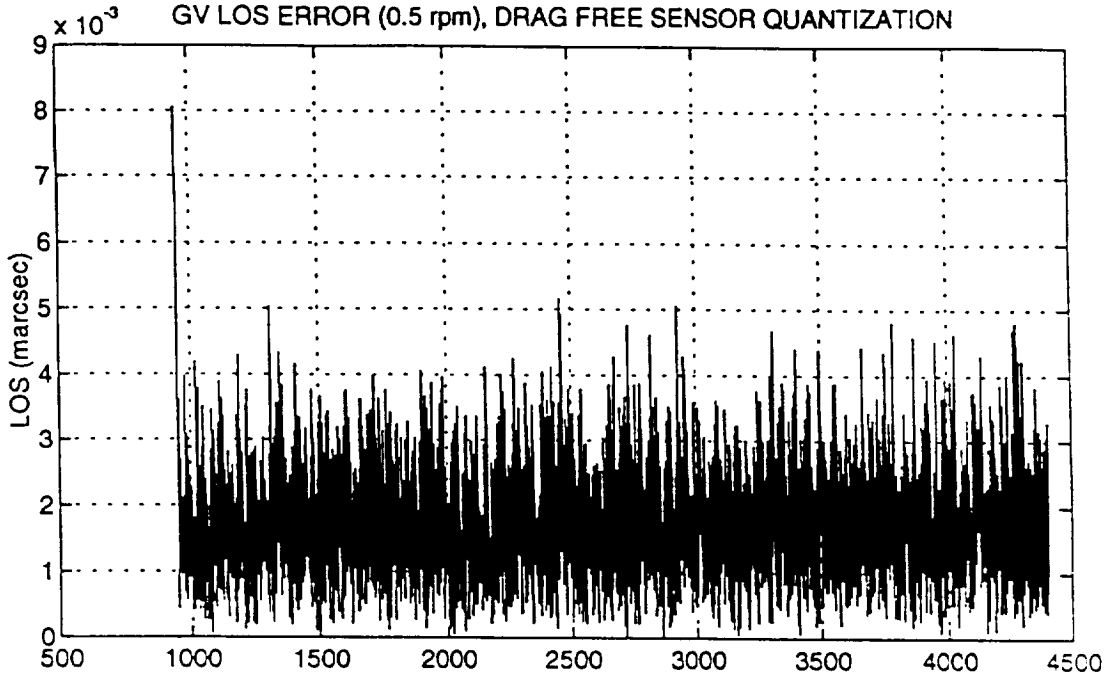

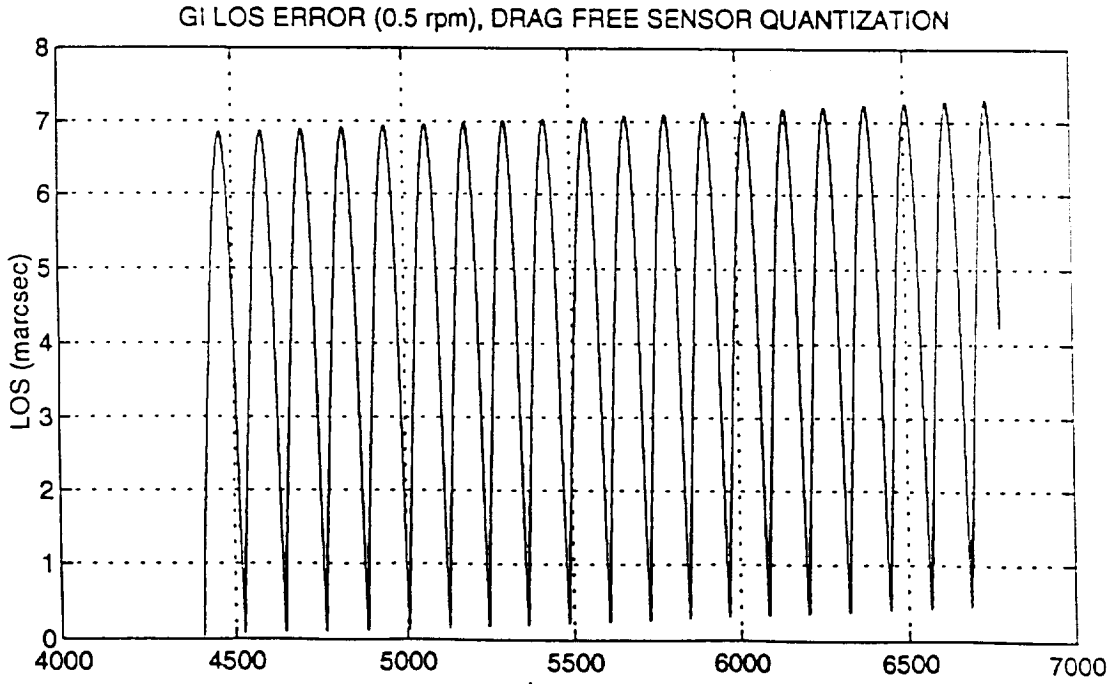

Figure 3-38 Roll and Translational Error (.5 rpm, Drag Free Sensor Quantization)

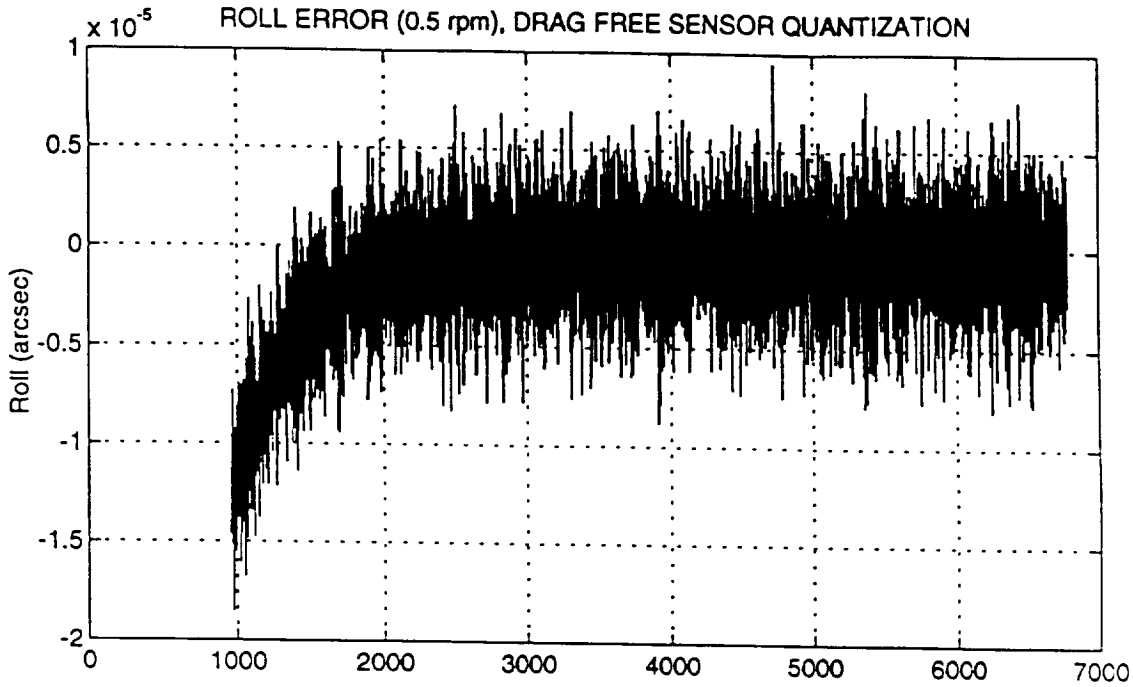

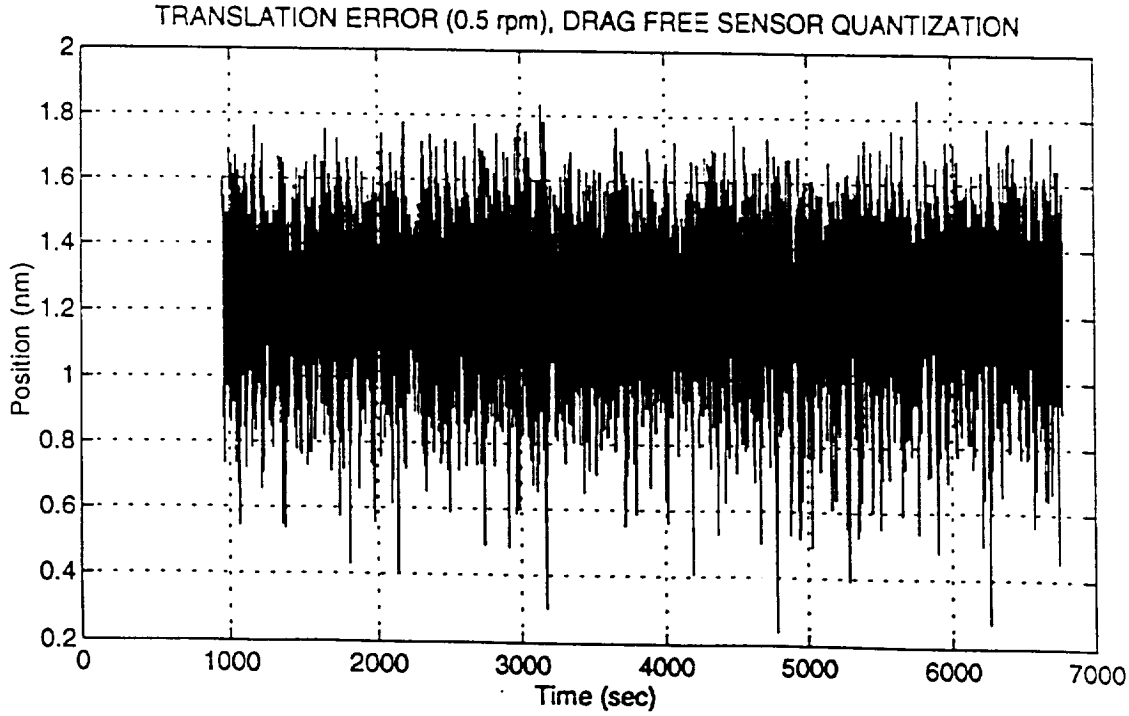

3.1. Thrust Requirements

The total thrust / flow requirements were examined for each of the sensor and actuator errors to determine which had a significant effect. In each case, the aerodynamic, gravity gradient and magnetic disturbances were applied. The 2000 second run in each case started during the Guide Star Invalid period and switched to Guide Star Valid phase at approximately 900 seconds. A plot was produced for each case which included total thrust required, control thrust required, and flow (null dump) thrust required. The flow command was a constant 6.5 mg/sec (8.3 mn thrust) with an I_{sp} of 130 seconds. Figure 3.1-1 shows the thrust command with perfect sensors and actuators. The control thrust command varies between 4 and 7 mn, below the 8.3 mn flow command. Figure 3.1-2 shows the thrust command with a roll star tracker noise whose standard deviation is 5 arcsec. The control thrust command exceeds the 8.3 mn flow command in this case.

Figure 3.1-3 shows the thrust command with a science telescope noise whose standard deviation is 22.36 marcsec. The control thrust command is very nearly the same as the perfect case. Figure 3.1-4 shows the thrust command with a control gyro noise whose standard deviation is 0.002236 arcsec/sec. The control thrust command is also nearly the same as the perfect case. Figure 3.1-5 shows the thrust command with a drag free sensor noise whose standard deviation is 3.354 nm. The control thrust command varies between 4 and 8.4 mn, rarely exceeding the 8.3 mn flow command. Figure 3.1-6 shows the thrust command with a thruster noise whose standard deviation is 0.0559 mn. The control thrust command varies between 4 and 8 mn. Figure 3.1-7 shows the thrust command with a roll star tracker quantization whose least significant bit weight is 0.5 arcsec. The control thrust command is again approximately the same as the perfect case. Figure 3.1-8 shows the thrust command with a science telescope quantization whose least significant bit weight is 0.25 marcsec. The control thrust command is again nearly the same as the perfect case. Figure 3.1-9 shows the thrust command with a pitch/yaw control gyro quantization whose least significant bit weight is 1.3 marcsec. Once again the control thrust command is very nearly the same as the perfect case. Figure 3.1-10 shows the thrust command with a high range roll control gyro quantization whose least significant bit weight is 375 marcsec. The control thrust command exceeds the 8.3 mn flow command in this case. Figure 3.1-11 shows the thrust command with a low range roll control gyro quantization whose least significant bit weight is 37.5 marcsec. The control thrust command varies between 4 and 8.4 mn, rarely exceeding the 8.3 mn flow command. Figure 3.1-12 shows the thrust command with a drag free sensor quantization whose least significant bit weight is 1.0 nm. The control thrust command is again nearly the same as the perfect case. Figure 3.1-13 shows the thrust command with a thruster quantization whose least significant bit weight is 0.0025 mn. Once again little deviation from the perfect case is observed. Figures 3.1-14 through 3.1-16 show the thrust command with thruster hysteresis of 0.100, 0.010, and 0.005 mn, respectively. The control thrust command in Figure 3.1-14

for 0.100 mn thruster hysteresis exceeds the 8.3 mn flow command, while the lower two hysteresis cases in Figures 3.1-15 and 3.1-16 are similar to the perfect case. Figure 3.1-17 shows the thrust command with a control gyro drift of 0.003 arcsec/sec. The control thrust command again deviates little from the perfect case.

These results indicate the potential sensor errors that can result in excessive thruster flow. These are the roll star tracker noise, roll control gyro quantization, particularly in the high range, and large thruster hysteresis, such as 0.10 mn.

Figure 3.1-1 Thrust Command For Perfect Actuators and Sensors

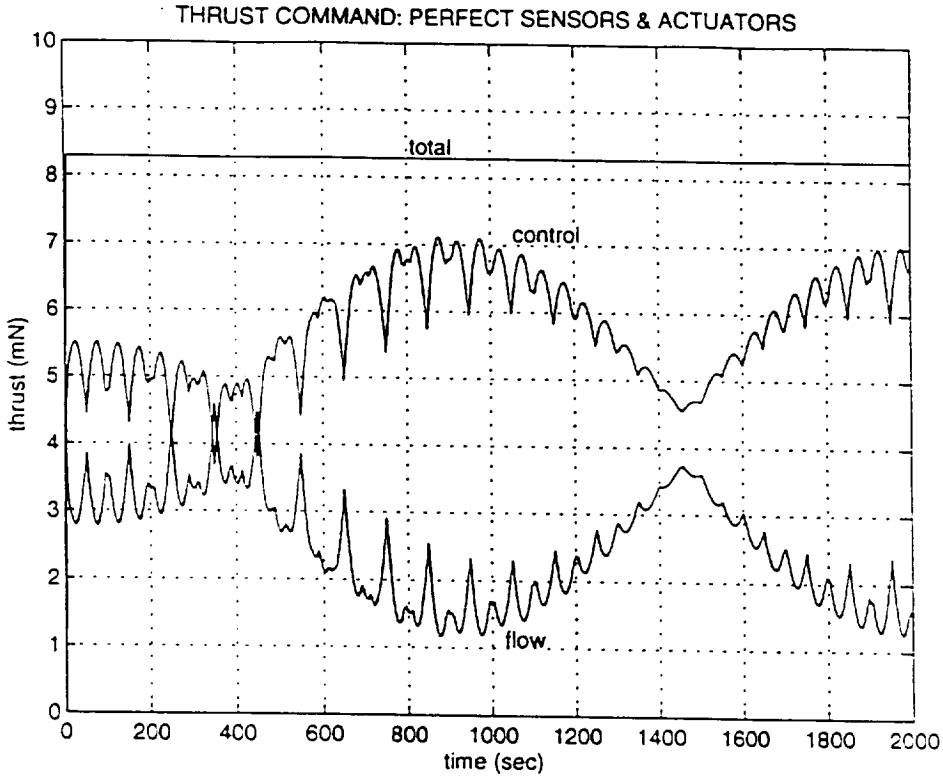

Figure 3.1-2 Thrust Command For Roll Star Tracker Noise

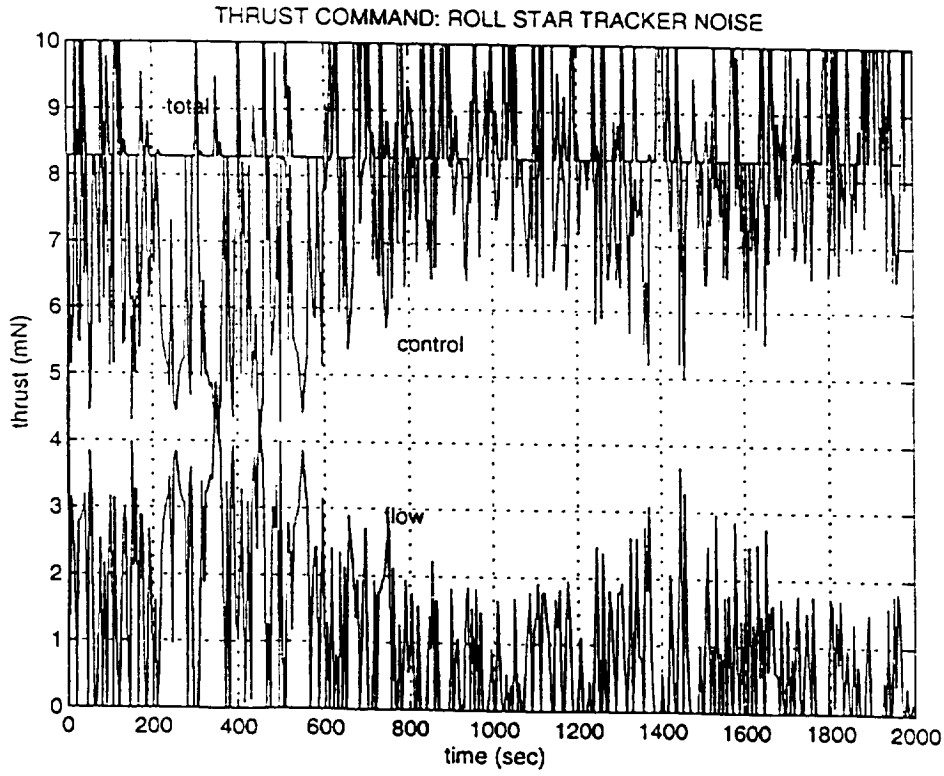

Figure 3.1-3 Thrust Command For Science Telescope Noise

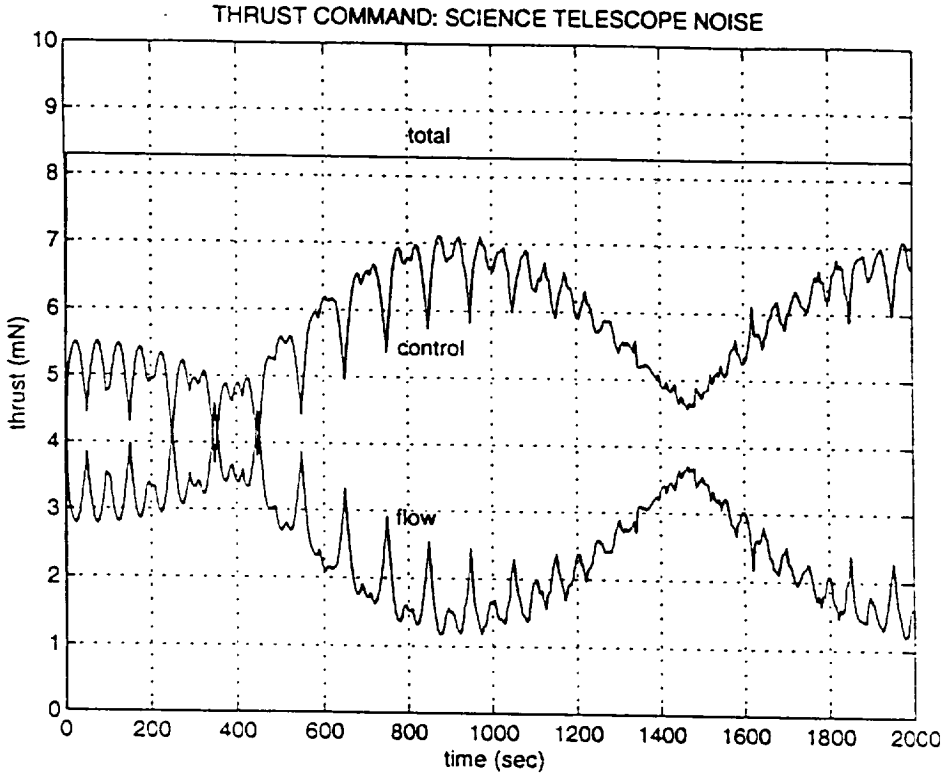

Figure 3.1-4 Thrust Command For Control Gyro Noise

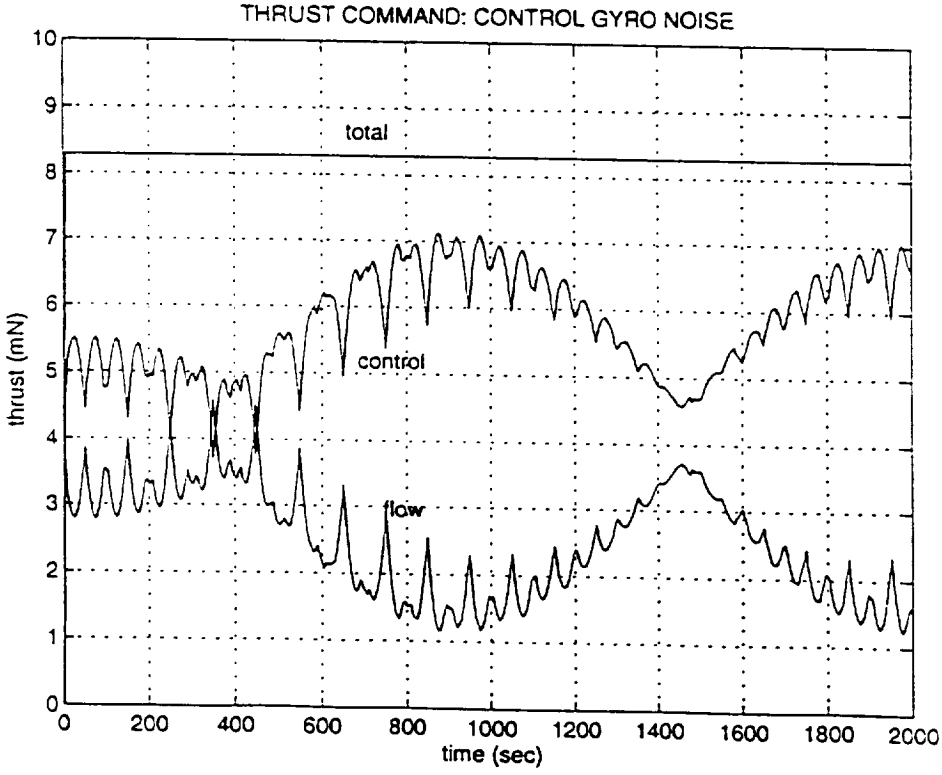

Figure 3.1-5 Thrust Command For Drag Free Sensor Noise

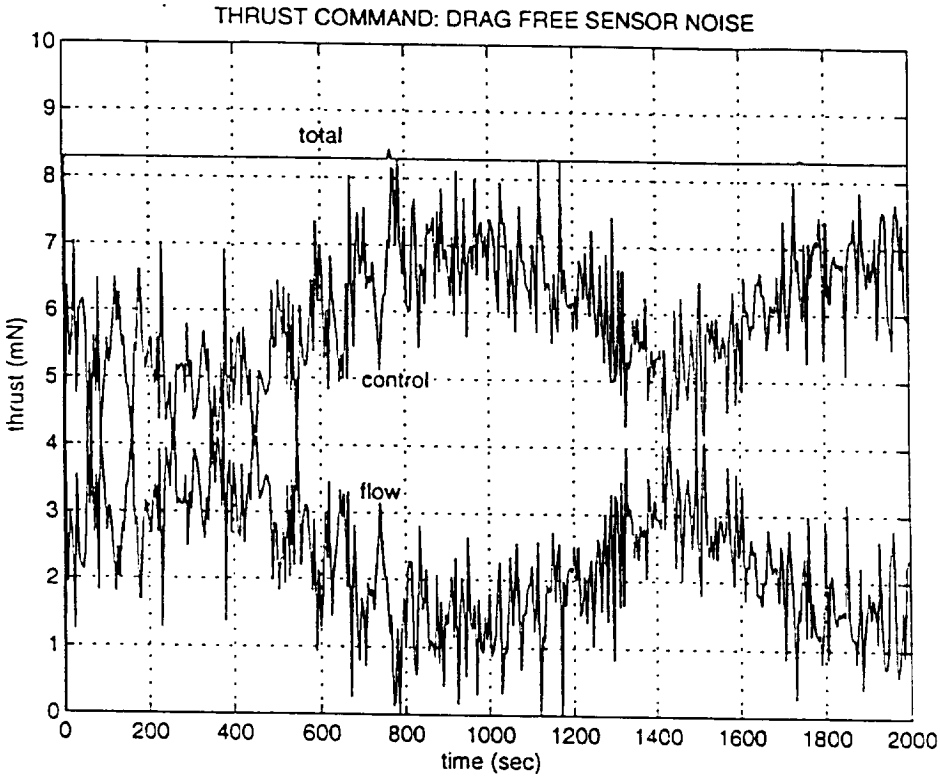

Figure 3.1-6 Thrust Command For Thruster Noise

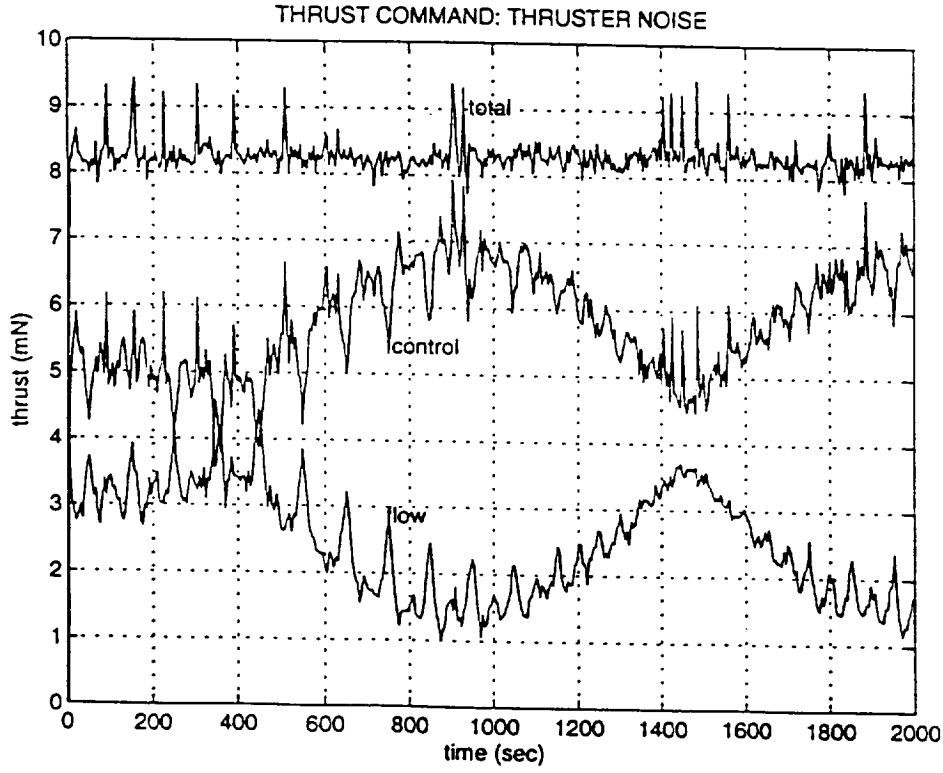

Figure 3.1-7 Thrust Command For Roll Star Tracker Quantization

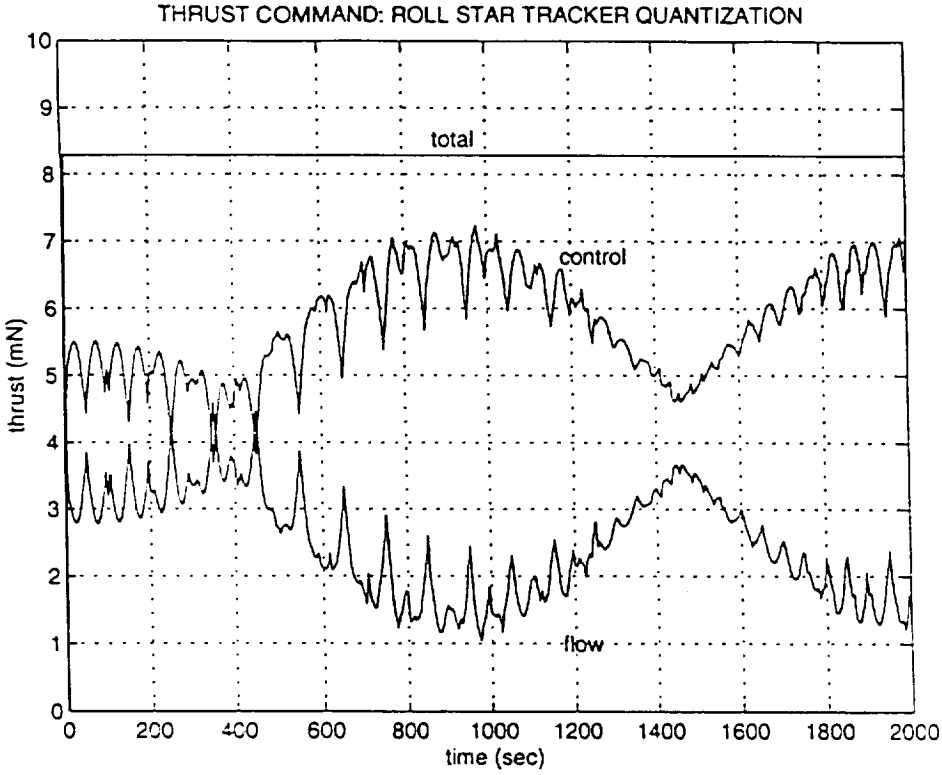

Figure 3.1-8 Thrust Command For Science Telescope Quantization

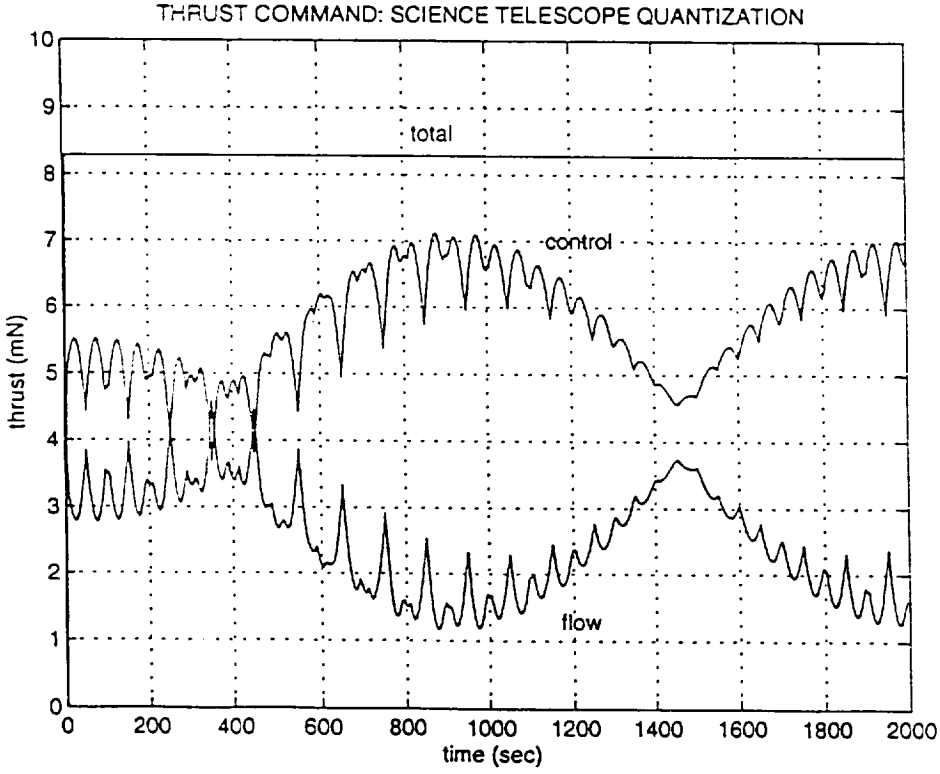

Figure 3.1-9 Thrust Command For Pitch/Yaw Control Gyro Quantization

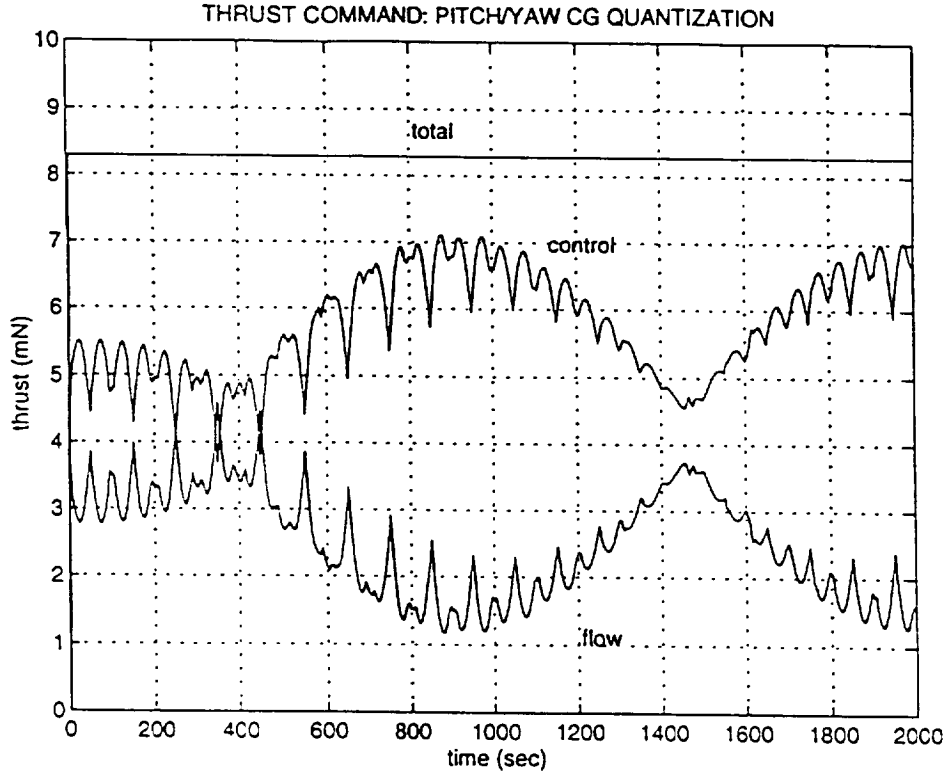

Figure 3.1-10 Thrust Command for High Range Roll Control Gyro Quantization

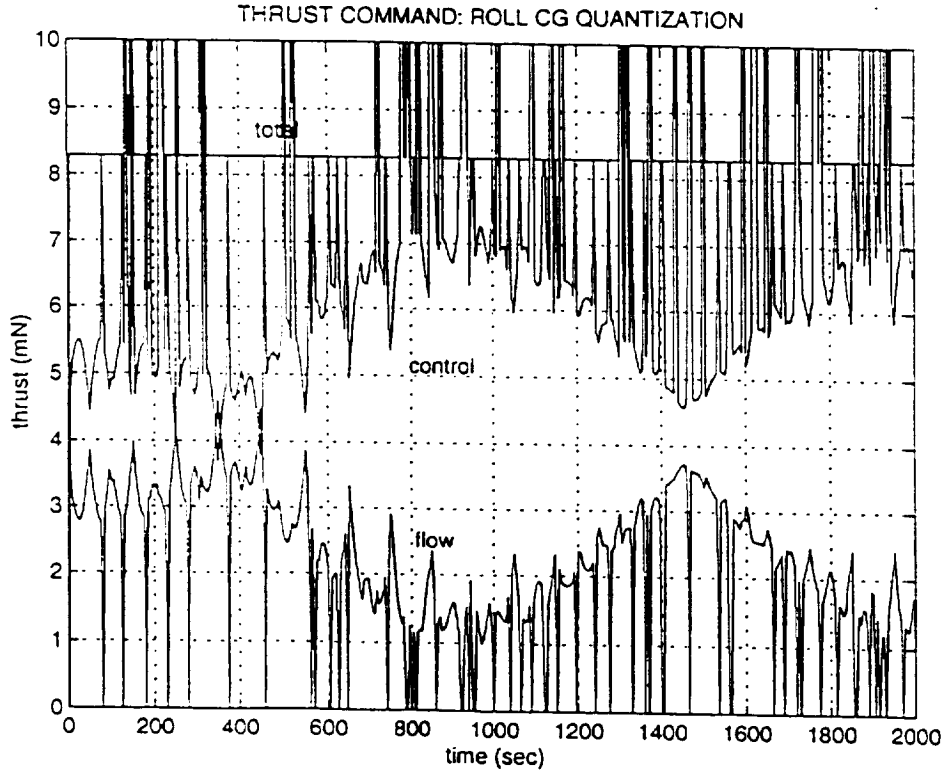

Figure 3.1-11 Thrust Command for Low Range Roll Control Gyro Quantization

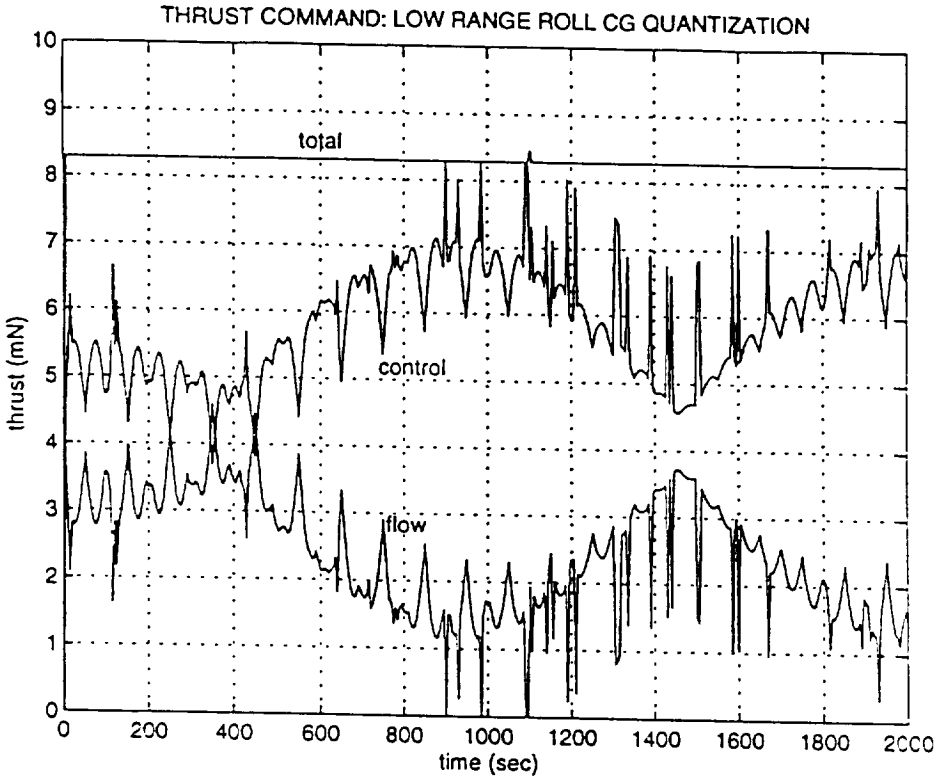

Figure 3.1-12 Thrust Command For Drag Free Sensor Quantization

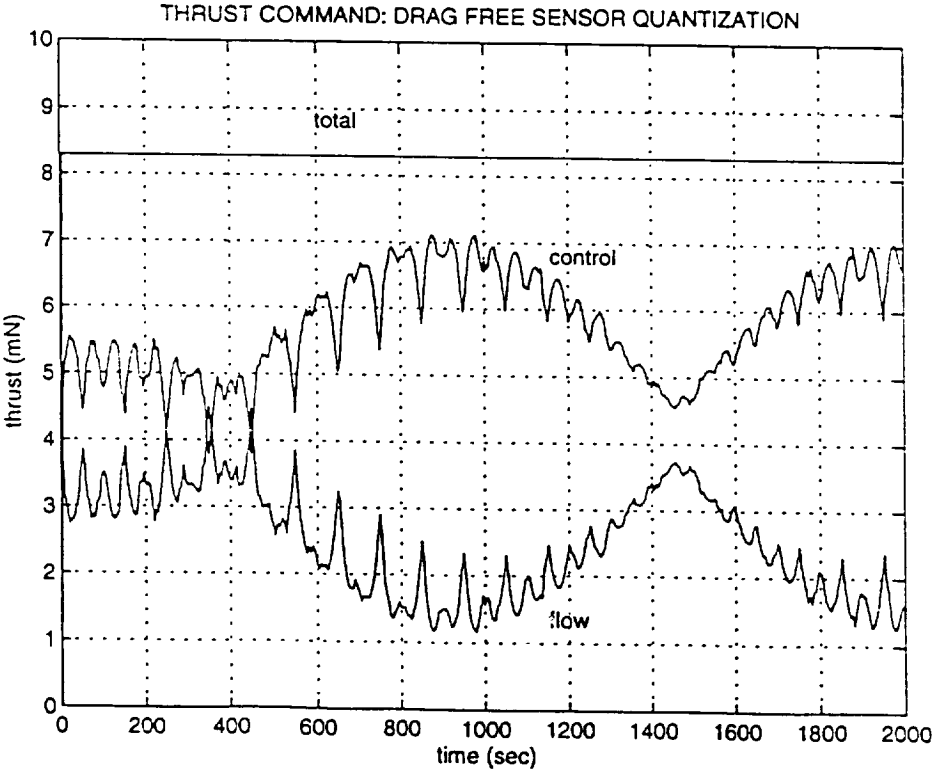

Figure 3.1-13 Thrust Command For Thruster Quantization

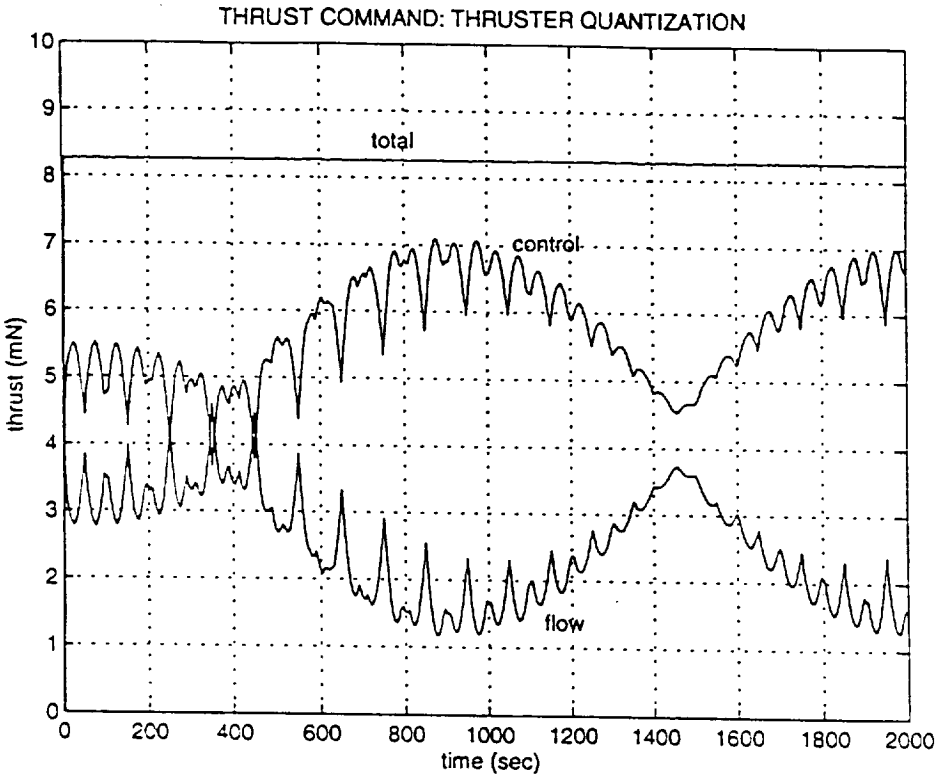

Figure 3.1-14 Thrust Command For Thruster Hysteresis Of 0.10 mn

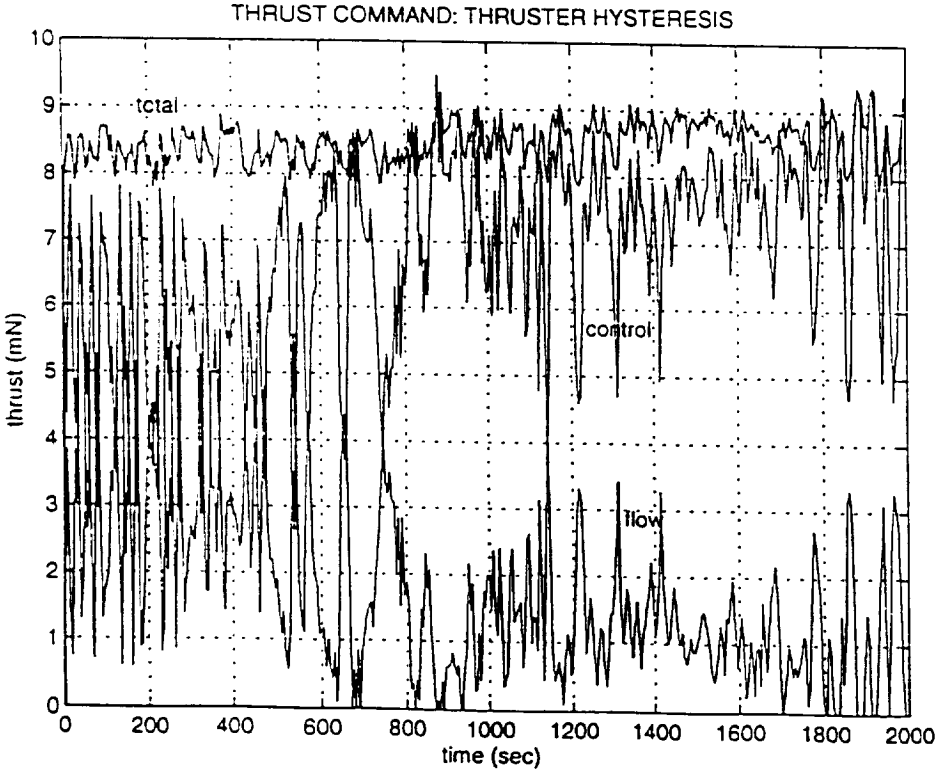

Figure 3.1-15 Thrust Command For Thruster Hysteresis Of 0.01 mn

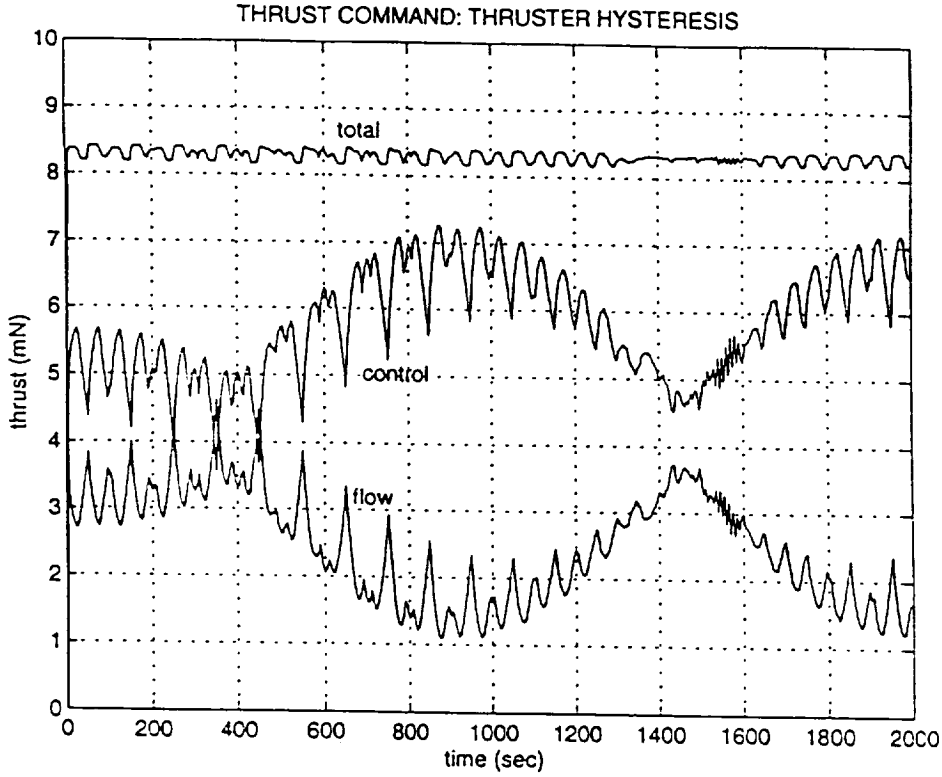

Figure 3.1-16 Thrust Command For Thruster Hysteresis OF 0.005 mn

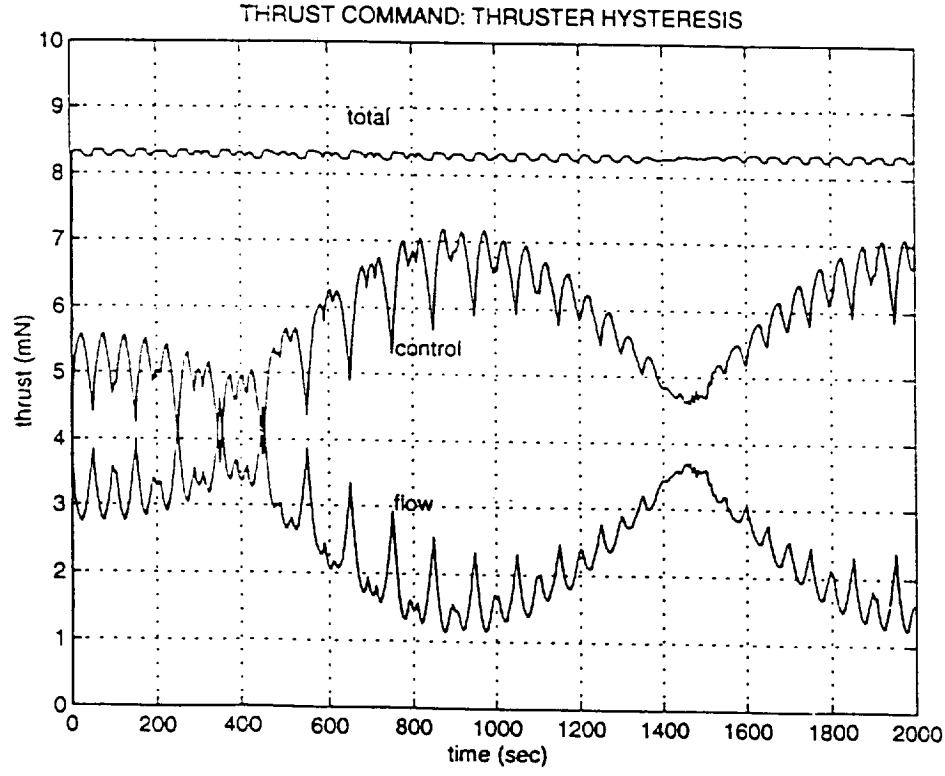

Figure 3.1-17 Thrust Command For Control Gyro Drift

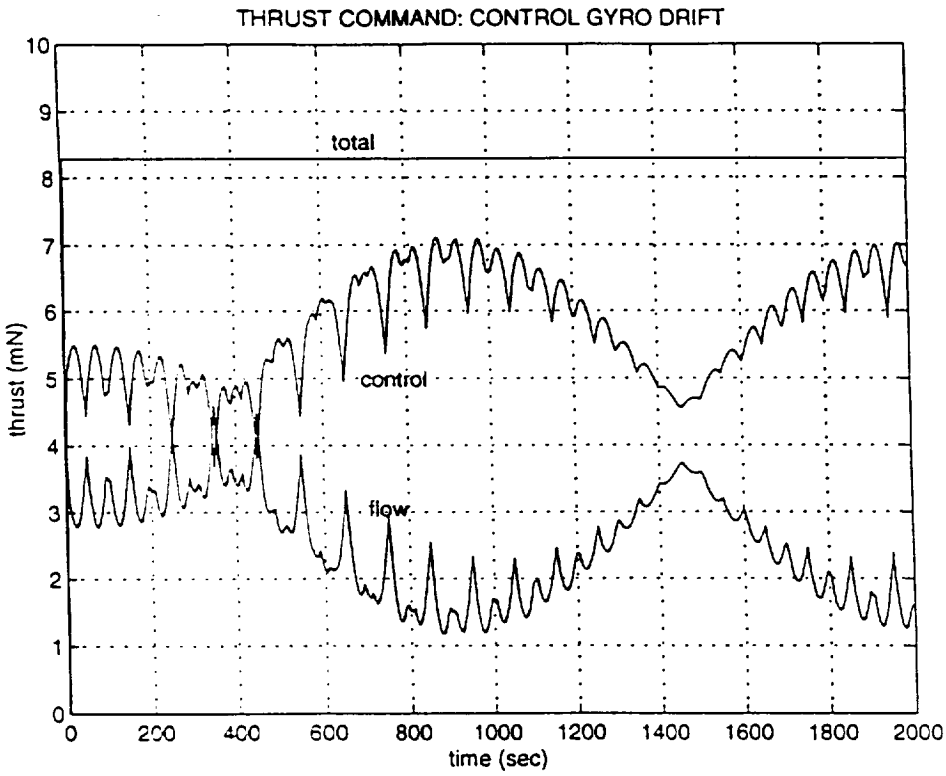

4. GPB Error Budget Evaluation Results

The GPB error budget evaluation results from the GPB TREETOPS simulation are broken down into the Lockheed specified budget components. Table 4-1 shows the fine pointing, pitch/yaw, Guide Star Valid error budget components. Table 4-2 shows the fine pointing, pitch/yaw, Guide Star Invalid error budget components. Table 4-3 shows the roll error budget components. Table 4-4 shows the translation error budget components. The short and long term errors as shown in the Lockheed error budget document[5] are combined in these tables. The errors not addressed in this study are left blank. The simulation errors quoted in the DETERMINATION, CONTROL, and summary blocks are taken from a simulation run where all of the subordinate errors are active. The number in parenthesis in each of these blocks is the RSS combination of the errors noted in the lower level blocks. Notice that the RSS totals and the composite simulation runs show approximately the same errors, indicating that the errors are essentially uncorrelated in producing control error. The Table 4-5 compares the observed control errors with the top level GPB control requirements and with the Lockheed budgeted allocations. Notice that the control errors predicted by the TREETOPS simulation are less than both the requirements and the Lockheed budgeted values.

Table 4-1 Fine Pointing Guide Star Valid Error Budget

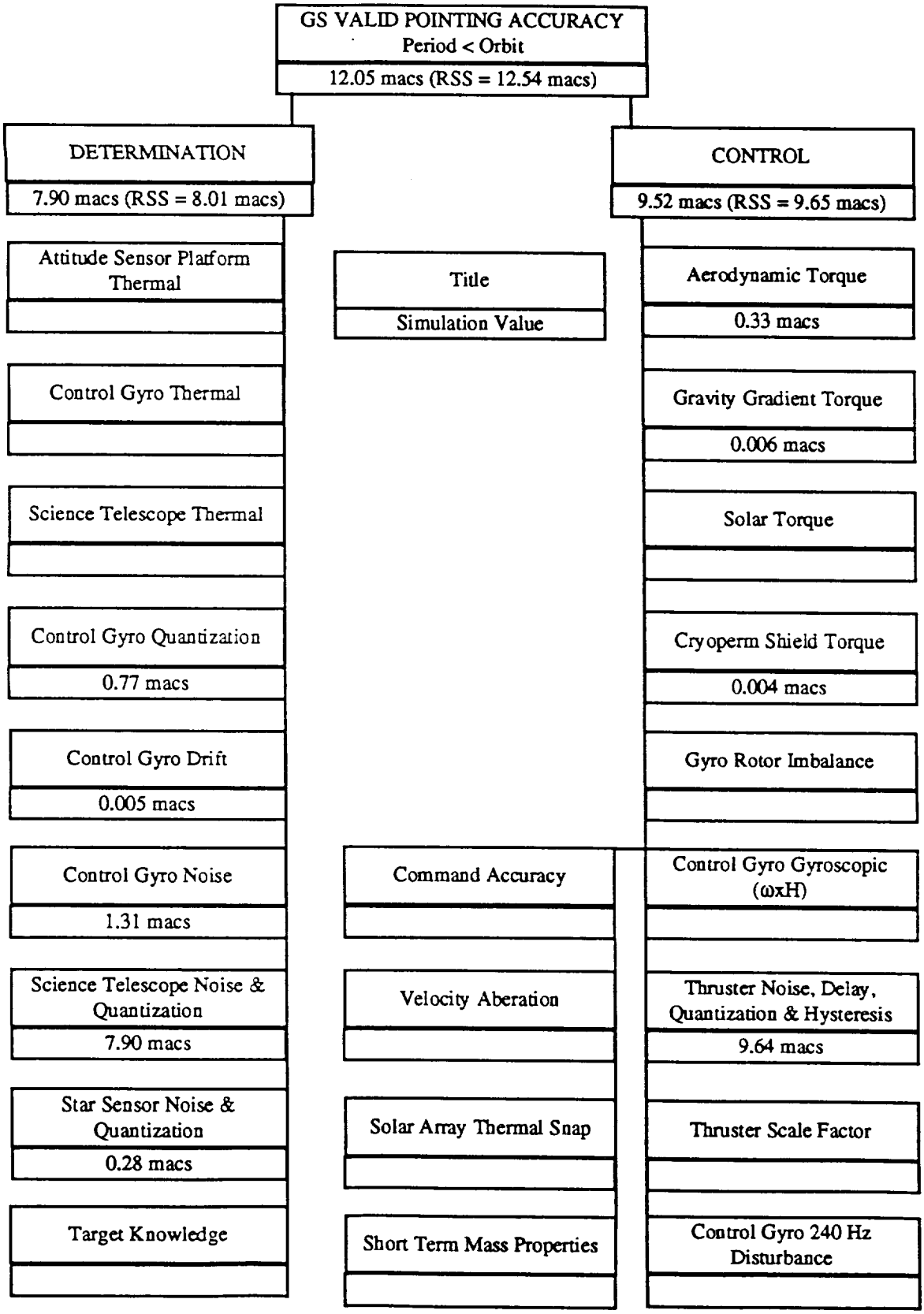

Table 4-2 Fine Pointing Guide Star Invalid Error Budget

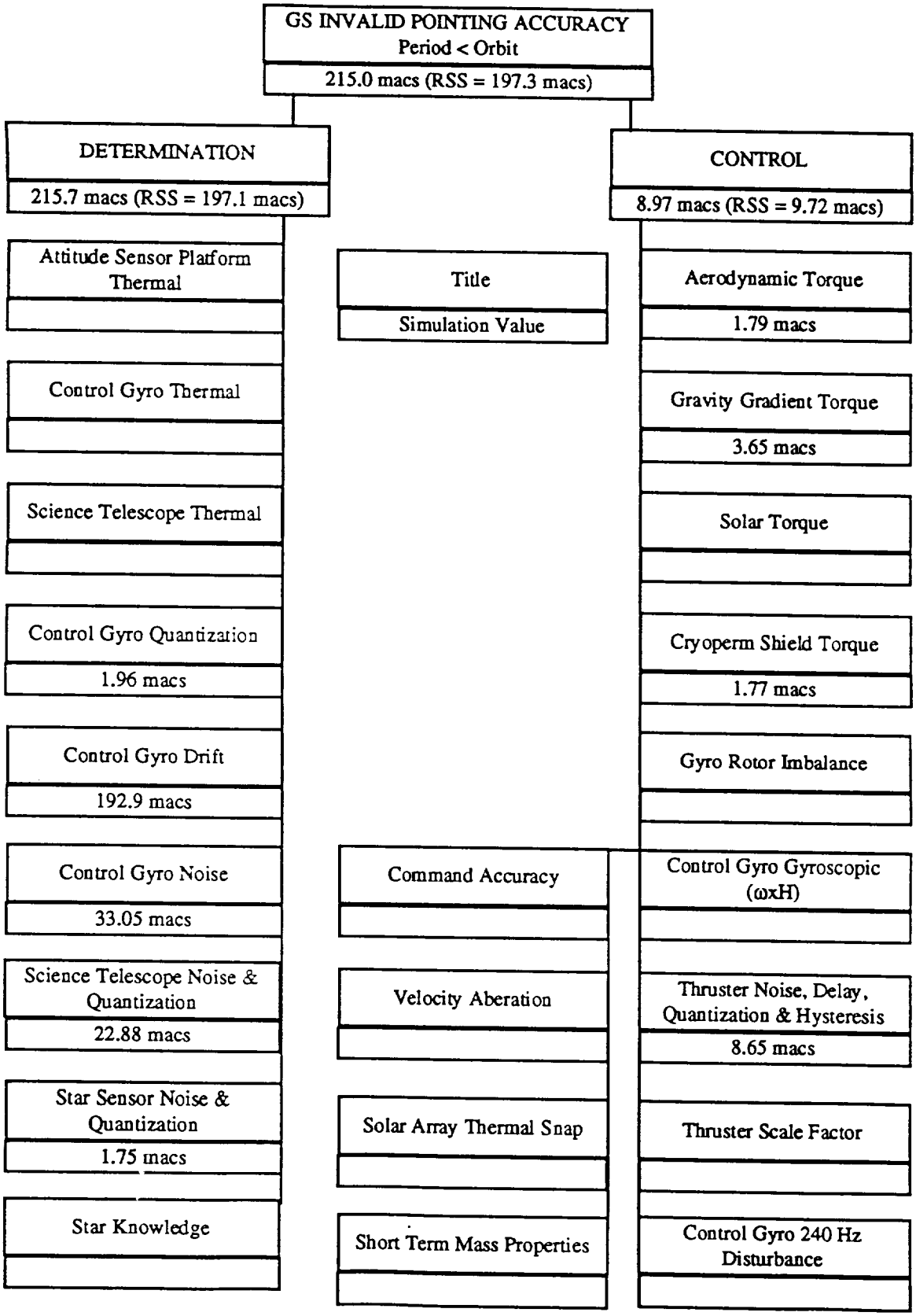

Table 4-3 ROLL Error Budget

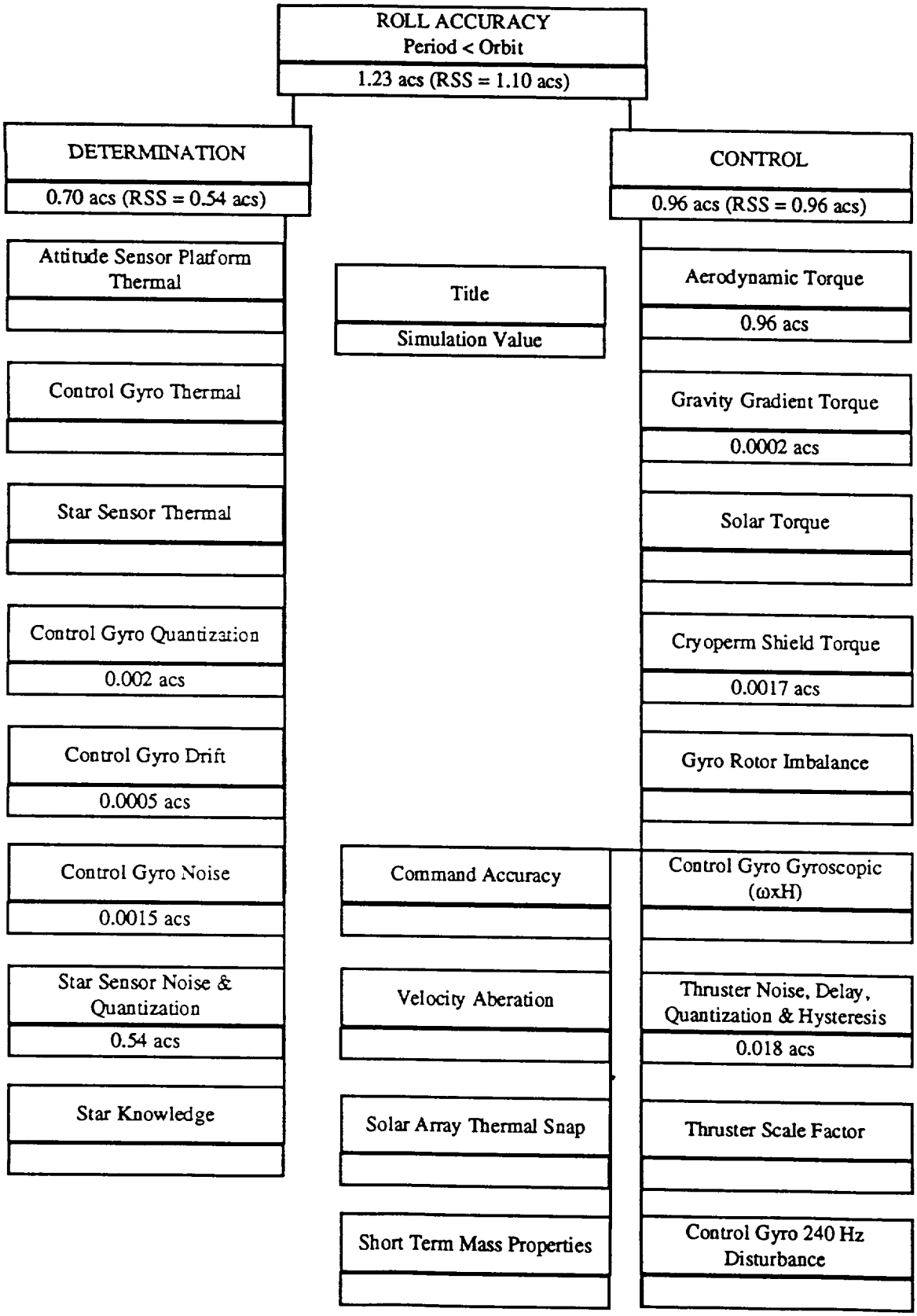

Table 4-4 Translation Error Budget

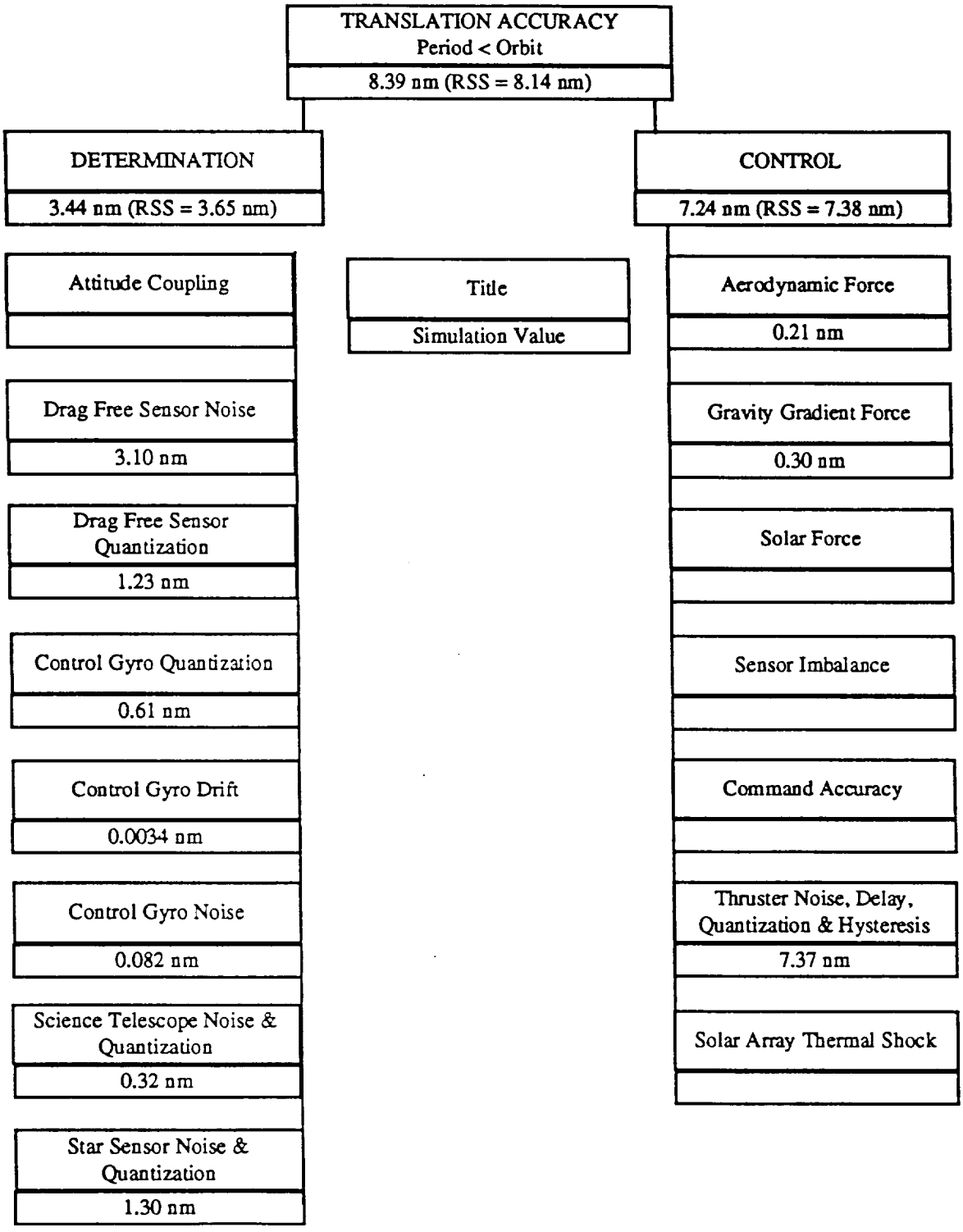

Table 4-5 GPB Simulation / Control Requirements Comparison

	Requirement	Lockheed Budget	Maximum Observed Error
LOS Error - GSV	20 mas (1 σ)	19.9 mas (1 σ)	12.05 mas (1 σ)
LOS Error - GSI	2000 mas (1 σ)	56.9 mas (1 σ)	215 mas (1 σ)
Roll Error	10 arcsec (1 σ)	10 arcsec (1 σ)	1.23 arcsec (1 σ)
Translational Error	100 nm (1 σ)	21 nm (1 σ)	8.39 nm (1 σ)

5. Conclusions

Models of fluid slosh and spacecraft flexibility were developed and added to the standard rigid body GPB simulation using the TREETOPS simulation package. Detailed slosh data was used to model the liquid center of mass motion produced by the liquid helium. A detailed flexible body model of the GPB spacecraft was obtained from Lockheed, processed, and integrated into the TREETOPS simulation structure.

Performance results from the TREETOPS GPB simulation indicate that during quiescent periods of spacecraft activity, flexible body and slosh effects add only a small amount of additional control error over the standard rigid body response. The sloshing elements and flexible spacecraft components do not respond significantly to the spacecraft disturbances. It was discovered, however, that thruster flow limits are sensitive to specific sensor errors, such as roll star tracker noise, roll control gyro quantization, particularly in the high range, and large thruster hysteresis. If these errors are not filtered or held below specific values overcommanding of the thrusters is possible.

A control error budget analysis was conducted and showed that all control requirements of the GPB program are met by the current configuration with significant margin.

6. References

[1] Hung, R.J., Long, Y.T., and Zu, G.J., "Coupling of Aerodynamics, Magnetic, and Gravity Gradient Torques-Driven Sloshing with Spacecraft Dynamics", University of Alabama in Huntsville

[2] Lockheed Missiles and Space Company, "GPB System Design and Documentation, Control System Error Budgets and Capability, SE-04, Part 5", March 10, 1995

[3] Lockheed Missiles and Space Company, "Relativity Mission Thruster Critical Design Review", 27 September 1994

[4] Lockheed Missiles and Space Company, "GPB System Design and Documentation, Attitude and Translation Control Subsystem Description, SE-04, Part 2", March 10, 1995

[5] Skinner, Michael, "Universal File: On-Orbit Structural Dynamics Model", Engineering Memorandum No. SMS 227, Lockheed Martin, January 19, 1996.

[6] Kasdin, N. Jeremy, and Gauthier, Christian, "Gravity Gradient Gyroscope Drifts in the NASA Gravity Probe B Experiment", submitted for publication in the Journal of the Astronautical Sciences,

NASA **Report Documentation Page**

1. Report No.	2. Government Accession No.	3. Recipient's Catalog No.
Final Report		

4. Title and Subtitle	5. Report Date
Performance Evaluation Gravity Probe B Design	April 5, 1996

7. Author(s)	6. Performing Organization Code
Mr. Ronnie Francis Dr. Eugene M. Wells	8. Performing Organization Report No.

9. Performing Organization Name and Address	10. Work Unit No.
Control Dynamics, A Division of bd Systems, Inc. 600 Boulevard South, Suite 304 Huntsville, Alabama 35802	11. Contract or Grant No. NAS8-40618

12. Sponsoring Agency Name and Address	13. Type of Report and Period Covered
National Aeronautics and Space Administration George C. Marshall Space Flight Center Marshall Space Flight Center, Alabama 35812	Final Report 25 September 1995 - 5 April 1996
	14. Sponsoring Agency Code NASA/MSFC - GP22-H

15. Supplementary Notes

16. Abstract

This final report documents the work done to develop a 6 degree-of-freedom simulation of the Lockheed Martin Gravity Probe B (GPB) Spacecraft. This simulation includes the effects of vehicle flexibility and propellant slosh. The simulation was used to investigate the control performance of the spacecraft when subjected to realistic on orbit disturbances.

17. Key Words (Suggested by Author(s))	18. Distribution Statement
1. Gravity Probe B 2. Performance	

19. Security Classif. (of this report)	20. Security Classif. (of this Page)	21. No. of pages	22. Price
Unclassified	Unclassified	88	